WISSENSCHAFTSZENTRUM WEIHENSTEPHAN FÜR ERNÄHRUNG, LANDNUTZUNG UND UMWELT

TECHNISCHE UNIVERSITÄT MÜNCHEN

Tree and stand structure and implications for functions and services – New evidence by novel terrestrial laser scanning (TLS) methodologies

Dominik Bayer

Vollständiger Abdruck der von der Fakultät Wissenschaftszentrum Weihenstephan für Ernährung, Landnutzung und Umwelt der Technischen Universität München zur Erlangung des akademischen Grades eines

Doktors der Naturwissenschaften (Dr. rer. nat.)

genehmigten Dissertation.

Vorsitzender: Prof. Dr. Thomas Knoke

Prüfer der Dissertation: 1. Prof. Dr. Dr. h.c. Hans Pretzsch
   2. Prof. Dr. Eric Labelle
   3. Prof. Dr. Stephan Pauleit

Die Dissertation wurde am 20.11.2017 bei der Technischen Universität München eingereicht und durch die Fakultät Wissenschaftszentrum Weihenstephan für Ernährung, Landnutzung und Umwelt am 27.02.2018 angenommen.

"To such an extent does nature delight and abound in variety that among her trees there is not one plant to be found which is exactly like another; and not only among the plants, but among the boughs, the leaves and the fruits, you will not find one which is exactly similar to another."

– Leonardo da Vinci

As the poet said, "Only God can make a tree.", probably because it's so hard to figure out how to get the bark on.

– Woody Allen

Acknowledgments

Contents

Abstract

Structure and function of trees and larger systems such as groups, stands or whole forests undergo constant change. Ongoing functions and processes require and promote changes in structure. Altered structures and thus altered environments on the other hand bring about a changed functioning. This circular feedback between structure, functioning and local environment is an essential aspect to the understanding of tree-dominated ecosystems. Since structure and function are so firmly interwoven, increased knowledge about structure considerably contributes to insights into functions and processes of forest and urban trees. The understanding of dynamics, growth and competition of individual forest trees and even ecosystem functions and benefits of urban trees gains as well.

Spatial explicit structure however, is hard to quantify at levels of detail exceeding what classical dendrometrical methods are able to provide under reasonable efforts. LiDAR measurements in general and in regards to individual tree attributes, terrestrial laser scanning (TLS) in particular, have been increasingly developed and refined during the last decade. Yet, only relatively few studies have utilized the potential of TLS measurements beyond the scope of pure methodology so far. This thesis contains a strong methodological aspect in regards to the advancement of information gain from TLS data as well. Nonetheless, the application of the developed approaches is an integral part as well in order to contribute to the understanding of actual ecological questions.

Besides research paper II of this thesis, which is mainly a demonstration of the potential value of TLS data for tree modeling, in order to investigate a broad range of the many aspects of tree structure, this thesis is based on (i) structural properties of tree crowns and their intra- and interspecific variation, (ii) structural dynamics during the process of gap closing and (iii) tree structure and its implications for ecosystem functions and services in varying urban environments. Over the course of the respective studies, studies on Norway spruce (*Picea abies* [L.] Karst.), European beech (*Fagus sylvatica* L.),

black locust (*Robinia pseudoacacia* L.) and small-leaved lime (*Tilia cordata* Mill.) have been conducted.

Significant variations in structure between species but also between varying environmental conditions such as stand-mixture or the type of urban environment have been found during all involved studies. Norway spruce and European beech showed morphological differences between mixture types which contributes evidence to the understanding of mixing effects on stand growth. Through principal differences of crown shapes and the resulting opportunity to occupy niches in the canopy which would normally already be occupied or at least more heavily contested by trees of the same species, the available space above-ground may be filled by photosynthetic organs more thoroughly. The dynamics of space conquering during the recapture of generated forest gaps revealed further differences between both species and their preferences in short- to mid-term resource allocation. While spruce invested additional above-ground resources mainly into *dbh* growth, beech heavily invested into the fast and sweeping lateral crown extension. Black locust and small-leaved lime as well displayed significantly different morphologies and allometric relations and in regards to some structural attributes showed significant alterations between different urban environments. The detailed information about crown structure assists in understanding urban ecosystem functions and services such as air pollution reduction, temperature regulation or noise mitigation.

Part I.

Cumulative Thesis

This dissertation is based on investigations contained in the following four original articles.

Research Paper I: Bayer, D., Seifert, S., Pretzsch, H. (2013). Structural crown properties of Norway spruce (*Picea abies* (L.) Karst.) and European beech (*Fagus sylvatica* L.) in mixed versus pure stands revealed by terrestrial laser scanning. *Trees* 27:1035-1047

Summary

The development of tree morphology within mixed-species stands is a key factor for the understanding and modeling of mixed-stand dynamics. Most research however, focuses on the morphological variation between different tree species and neglects the variation within members of the same species growing under different competitive circumstances. In contrast, this study addresses structural crown properties of mature Norway spruces (*Picea abies* [L.] Karst.) and European beech (*Fagus sylvatica* L.) regarding their variation within a species depending on intra- and interspecific competition.

   In order to achieve this, individual trees of both species growing in mixed-species as well as pure stands have been scanned using a Riegl LMS-Z420i terrestrial laser scanning device. Through the development and application of a novel skeletonization approach, it was possible to gain detailed information about the inner crown structure. The obtained parameters include branch angles, branch shapes, branch lengths, branch bending, ramification, detailed crown volume and growing space occupation of branches within the crown. Many of these parameters were hardly accessible so far under reasonable efforts in a non-destructive manner. The presented methodologies proved to be suitable to gain detailed information about the morphological traits of tree crowns independently of species. In contrast to automated skeletonization attempts, the applied semi-manual

skeletonization yields robust results independent of species which can be applied in dense environments like forest stands.

Significant differences between trees growing in pure stands and in mixture could be identified. Norway spruce revealed significantly longer branches and larger crown volumes growing in the mixed stand environment when compared to the pure stand. European beech's members of the mixed-species stand featured flatter branch angles, stronger ramification, greater crown volumes and a lower share of an individual branch's space occupation within the total crown volume. The results show, that interspecific competition can significantly influence structural traits of tree crowns.

Author Contributions   Dominik Bayer conducted the scan acquisitions, prepared and preprocessed the raw TLS data. Dominik Bayer conceived, designed, developed and applied the skeletonization procedures including the programming tasks as well as the statistical analysis. Dominik Bayer wrote the manuscript, Stefan Seifert and Hans Pretzsch contributed to the writing.

Research Paper II: Beyer, R., Bayer, D., Letort, V., Pretzsch, H., Cournède, P.-H. (2017). Validation of a functional-structural tree model using terrestrial lidar data. *Ecological Modelling* 357:55–57

Summary

Three-dimensional, individual tree and forest data is more and more attained by terrestrial laser scanning (Leeuwen and Nieuwenhuis 2010; Pretzsch et al. 2011). The increased accessibility of high resolution spatial data enhances the simultaneous development of methodologies allowing for robust and destruction-free acquisition of quantitative structural parameters describing crown shape and even a crown's inner components such as branches as well as their size and shape (Bayer et al. 2013). 3D TLS data is however not yet utilized in the parametrisation and validation of spatially explicit tree models, apart from a few exceptions, e.g. Potapov et al. (2016).

In order to evaluate the tree growth model presented by Beyer et al. (2017c), 3D TLS data was used besides long-term forest inventory and allometric data. Using a Riegl LMS-Z420i terrestrial laser scanning device, the sub plot 3 of the experimental site "Fabrikschleichach" was scanned. At the time the scans were acquired, the stand was comprised of European beech (*Fagus sylvatica* L.) at the age of 180 years. Due to the difficulties caused by occlusion of crown parts covered by neighboring trees and even parts of a tree's own crown, the trees were scanned in leafless state. The scanner's position was optimized in such a way, that the visibility of the desired crowns was as unrestricted as possible. To further maximize the detection of inner crown parts, the scanner's last-target mode and combinations of multiple single scans covering different angles of the crowns were used.

The measured relative twig densities and the simulated relative leaf density were found to be structurally similar concerning shape and size. Applying an appropriate metric, they proved to be reasonably close, illustrating how LiDAR data can be used to analyze the results of spatial simulations of functional-structural growth models. Considering the future potential, especially in the scope of technical advancements of LiDAR devices, tree growth modelers may benefit from close collaboration with LiDAR practitioners.

Author Contributions   Dominik Bayer and Robert Beyer are joint first authors. Dominik Bayer designed and conducted the TLS scan acquisition. Dominik Bayer prepared and preprocessed the raw TLS data. Robert Beyer designed and conducted the comparison to Beyer et al. (2017c). Robert Beyer, Dominik Bayer, Véronique Letort, Hans Pretzsch and Paul-Henry Cournède contributed to the writing of the manuscript.

Research Paper III: Bayer, D., Pretzsch, H. (2017). Reactions to gap emergence: Norway spruce (*Picea abies* (L.) Karst.) increases growth while European beech (*Fagus sylvatica* L.) features horizontal space occupation – evidence by repeated 3D TLS measurements. *Silva Fennica*. 51:5, article id 7748, doi.org/10.14214/sf.7748

Summary

One of the main driving factors of species-specific competition and productivity within forest stands lies in the dynamics of forest gap emergence and closure. Tree mortality caused by competition, storm damage, bark beetle attacks, thinning and various other kinds of disturbances repeatedly cause openings in the canopy as well as vacancies in the root space. In the past, these forest gaps were mainly of interest regarding the mosaic-cycle concept of natural unmanaged ecosystems. During the course of the ongoing transition from monocultures towards more complex and heterogeneous mixed-species stands however, artificially generated gaps play a fundamental role (Burschel and Huss 1997; Puettmann et al. 2012; Drössler et al. 2016). Yet, classical dendrometric methods are hardly capable of time- and cost-effectively measuring the three-dimensional tree structure, crown dynamics and space occupation non-destructively.

   Three artificially created forest gaps from 2006 to 2012 using a Riegl LMS-Z360 during 2006 and 2008 and a Riegl LMS-Z420i terrestrial laser scanning device during 2010 and 2012 have been observed. The gaps consisted of Norway spruce (*Picea abies* [L.] Karst.) and European beech (*Fagus sylvatica* L.) growing in pure stands and mixed-species stands. The main objectives were to scrutinize (i) the species- and gap type specific effect

of gap emergence on the crown structure and allometric relations on tree level, (ii) the conquering of the newly available above-ground resources and (iii) the development of the crown cover within the gap area concerning space occupation and multi-layering.

The analyzed gap development suggests, that Norway spruce invests freshly available above-ground resources into increased growth of dbh and biomass in general. Spruce displays significantly higher resilience against loss of crown mass induced by mechanical damage as well. European beech reacted differently. Additional above-ground resources are invested primarily into accelerated occupation of new growing space within the canopy. The stand type, meaning pure or mixed-species, had no significant impact on the major observed factors of gap dynamics. It is likely that the sheer abundance of additional light immediately after gap emergence overshadowed the different mechanisms of inter- and interspecific competition during the first years of gap closure.

Author Contributions   Dominik Bayer conducted the laser scan acquisition. Dominik Bayer conceived, designed and implemented the methodologies as well as the statistical analysis. Dominik Bayer and Hans Pretzsch wrote the manuscript.

Research Paper IV: Bayer, D., Pretzsch, H., Moser, A., Rötzer, T. (2017). Structural response of black locust (*Robinia pseudoacacia* L.) and small-leaved lime (*Tilia cordata* Mill.) to varying urban environments analyzed by terrestrial laser scanning. Implications for ecological functions and services. *Urban Forestry & Urban Greening*. under review

Summary

Urban planners face many environmental challenges affecting human health and well-being. The features and benefits of urban trees might be exploited in order to address these challenges. A considerable share of urban trees' benefits and services is directly or indirectly related to stand or individual tree structure which has hardly been elucidated so far. Structural variations may not only occur between differing species but also between individuals of a certain species under varying environmental conditions.

In order to quantify structural traits, TLS data sets of 52 small-leaved limes (*Tilia cordata* Mill.) and 41 black locust (*Robinia pseudoacacia* L.) trees within the city of Munich, growing at the three rather different growing location types town square, street canyon and park have been scrutinized. Non-destructive measurements of the inner crown's skeleton as well as advanced volume and surface related parameters have been conceived, computed and analyzed. Skeletonization was achieved in analogously to research paper I (Bayer et al. 2013). Methodological advancements in the analysis of α-shape based crown volume and surface properties facilitated the localization of the spatial explicit, point-density independent crown centers as well as size-independent measurements of the crown's fractal-like surface complexity. By combining α-shape

and voxel-space techniques, the radial density distribution of crown matter has been attempted to be determined. Further research is required to enhance the methods robustness, however.

Significant differences not only between species but also between growing locations could be observed. The height-diameter relation of the sample trees for example, was significantly influenced by species as well as growing location. Black locust proved its morphological variability by location dependent variations of stem inclination, crown center displacement, and crown surface complexity. The results are discussed in regards to urban ecosystem services and benefits and how increased knowledge about spatially explicit tree structures may contribute to a target oriented planting of urban trees in order to enhance human health and well-being.

Author Contributions   Dominik Bayer conceived, designed and implemented the methodological aspects, including all programming tasks, data preparation and preprocessing as well as the statistical analysis. Dominik Bayer wrote the manuscript. Hans Pretzsch, Astrid Moser and Thomas Rötzer gave valuable input and advice.

Co-authorships

1. Barbeito, I., Dassot, M., Bayer, D., Collet, C., Drössler, L., Löf, M., Rio, M. del, Ruiz-Peinado, R., Forrester, D. I., Bravo-Oviedo, A. and Pretzsch, H. (2017). Terrestrial laser scanning reveals differences in crown structure of *Fagus sylvatica* in mixed vs. pure European forests. Forest Ecology and Management 405:381–390.

2. Beyer, R., Letort, V., Bayer, D., Pretzsch, H. and Cournède, P.-H. (2017c). Leaf density-based modelling of phototropic crown dynamics and long-term predictive application to European beech. Ecol Modell 347:63–71.

3. Beyer, R., Bayer, D., Pretzsch, H. and Cournède, P.-H. (2017b). Reconstructing minimal length tree branch systems from leaf positions. Ecological Informatics 42:61–66.

Part II.

Thesis: Tree and stand structure and implications for functions and services – New evidence by novel TLS-methodologies

1. Introduction

The physiology, phenology and structure of plants indicate the environmental conditions they grow under (Walter 1931; Assmann 1970). Therefore, morphology and foliation are commonly used to assess tree vitality (Oldeman 1990; Roloff 2001). The size, shape and inner structure of tree crowns result from local resource supply and local environmental factors. In forest stands, these are mainly determined by inter- or intraspecific competition within the neighboring stand. While the structure of a tree's crown in pure stands is essential in the feedback mechanisms between functioning, structure and environment (Hari 1985), it may play an even more important role in mixed-species stands because here, different species demonstrate their specific abilities to capture or deny contested resources more efficiently by altering their structures (Pretzsch and Schütze (2009), Figure 1).

The relevance of crown structure and plasticity for mixed-species stands is widely recognized and discussed. However, especially in mature stands, it is hardly elucidated because crown structure is hard to quantify (Pretzsch 2003; Price et al. 2010; Richards et al. 2010). In forest science, Burger (1939) and Badoux (1946) were among the first who initiated the paradigm shift from stand towards individual tree level thinking and modeling. Methods for terrestrial measurement (Röhle and Huber 1985), quantification (Assmann 1970) and modeling (Pretzsch 1992; Pretzsch 2009) of tree crowns have been
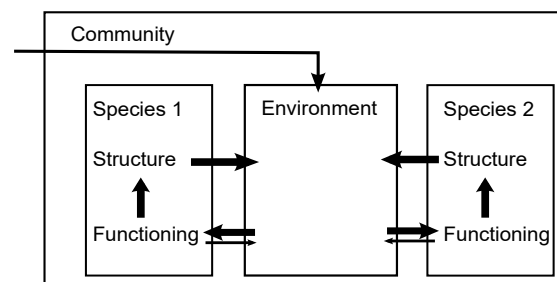

Figure 1.: Feedback between the structure of the stand, functioning and the environment inside a two-species mixed forest stand (Bayer et al. 2013).

12

continuously improved and refined. Based on empirical relationships between growing space of the tree, crown size and stem volume growth, the main objective was to comprehend, predict and maximize tree growth (Assmann 1970; Pretzsch 2006). Another consideration was the effect of silviculture on crown structure and wood quality (Zobel and Van Buijtenen 1989; Wilhelmsson et al. 2002; Seifert 2003; Pretzsch and Rais 2016). Further motivation came from the field of tree allometry (Niklas 1994) and especially from the promising synthesis, scaling approaches and models for the functioning and structure of plants from organ to ecosystem level of the metabolic scaling theory (MST) (Enquist et al. 1998; West et al. 2009). In order to understand and model tree growth in mixture, tracing of the causes of over- or underyielding from stand to the tree or even organ level is required. In mixed-species stands, branch angle, branch length, branch number, ramification and other principle factors determining space-filling within the crown may differ from pure stands and indicate changed resource supply, resource capture, or resource use efficiency (Binkley et al. 2004). These space filling principles and the according morphological patterns caused by interspecific competition can hardly be revealed by classical crown measurement, for example by determining crown length and cross section area in order to estimate the extension of the convex hull (Röhle and Huber 1985). Branches, crown excentricity, leaning and straightness are hardly measurable by optical plummet or hypsometer but determine wood quality (Pretzsch and Rais 2016).

Various kinds of disturbances, for example tree mortality due to competition, storm damage, bark beetle attacks or thinning repeatedly cause openings in the canopy as well as in the root space. These forest gaps and the involved dynamics of gap emergence, contest and space occupation were originally mainly of interest in regard to the mosaic-cycle concept of natural unmanaged ecosystems (Mueller-Dombois 1991; Remmert 1991; Lertzmann et al. 2015). The transition from rather homogeneous monocultures towards more heterogeneous mixed-species stands is one of the major trends in modern forestry. As a part of that, silviculturally generated gaps play an increasingly important role (Burschel and Huss 1997; Puettmann et al. 2012; Drössler et al. 2016). To promote structural and habitat diversity, to initiate natural regeneration, promote light demanding underplanting or to prepare the establishment of light demanding species, gaps are cut into forest stands of middle or advanced age (Pretzsch et al. 2015). Silvicultural concepts which result in openings in the canopy such as selection cutting or femel coupe gain importance. The trend towards gap rich stand structures has also been promoted by

the concept of the emulation of natural disturbance in forest management (Buddle et al. 2006; Kuuluvainen and Grenfell 2012). By the anticipation of the natural death and the timing of the harvest in such a way, that the wood is still of merchantable value, forest management nowadays partly emulates the natural stand development regime (Kuuluvainen and Grenfell 2012).

Although forests are more and more dominated by gaps and border trees and it is evident that the competition for canopy space and its associated resources is a major driver of forest dynamics (Purves et al. 2007), knowledge of tree and stand dynamics at the borders of gaps is still scarce. Similarly to individual tree measurements, the main reason for this deficit lies in the fact that the spatially explicit establishment, structure and dynamics of gaps and trees at gap borders are difficult to quantify by classical methods (Van der Meer and Bongers 1996). Transparency, layering and crown extension and especially vertical crown shape are difficult to access by hemispherical photography. These parameters however, are important for the understanding and modeling of the light regime within the gap, the velocity of gap closure as well as growth resilience after gap emergence (Dieler and Pretzsch 2013; Seidel et al. 2015). Moreover, knowledge about the roughness of the canopy surface and the borderline of forest gaps are important factors in the susceptibility to wind-throw (Quine and Gardiner 2007), the habitat quality and species diversity (Goetz et al. 2010; Müller et al. 2012).

Forestry is not the only field, where tree structure is of major importance. In urban landscapes as well, planners face numerous challenges affecting human health and well-being, many of which are costly to mitigate (Livesley et al. 2016). Urban planners might, however, exploit ecosystem functions and benefits of urban trees in order to address these challenges. Aesthetic considerations aside, structural traits such as shape, density, surface complexity and transparency of tree crowns are major drivers of ecological features and benefits (Bolund and Hunhammar 1999; Gómez-Baggethun and Barton 2013). A tree's potentials for wind-flow mitigation (Mochida et al. 2008; Mochida and Lun 2008), rain-cover, shade, climate regulation, noise reduction (Aylor 1972; Kragh 1981; Fang and Ling 2003), temperature management (Akbari et al. 2001; Akbari 2005; Bolund and Hunhammar 1999; Hardin and Jensen 2007), air purification (Nowak 1994; Nowak 1996; Escobedo and Nowak 2009), waterflow regulation (Higgens et al. 1997; Villarreal and Bengtsson 2005; Pataki et al. 2011) and habitat functionality (Hinsley et al.

2009; Goetz et al. 2010; Tews et al. 2004; Müller et al. 2012), for example, are directly or indirectly related to its structure.

Individual tree development, gap dynamics as well as functions and services of urban trees all heavily determine and themselves are determined by tree structure on various levels. In order to gather spatially explicit, three-dimensional information, terrestrial laser scanning has a lot of potential. Architecture, engineering and archaeology, for example, are fields of application where terrestrial laser scanning (TLS) is already widely utilized for high precision measurements (Vosselmann and Maas 2010). During the last decade, forest scientist as well, have shown increasing interest in this technology and its potential to measure forest parameters for inventory and even individual tree parameters (Huang and Pretzsch 2010; Pretzsch et al. 2011). Especially during recent years, studies utilizing terrestrial laser scanning have began to outgrow the stage of pure methodological (Bucksch et al. 2010; Côté et al. 2011; Hackenberg et al. 2015) development towards contributions to the understanding of ecological questions. Researchers have successfully applied TLS methods to relate a tree's shape (Seidel et al. 2011) or growth (Metz et al. 2013) to its surrounding stand. Further studies have for example dealt with TLS measurements in forest gaps and the impact of gaps on tree diameter increment and crown shape (Seidel et al. 2015; Seidel et al. 2016).

Bayer et al. (2013) conducted one of the first studies investigating relationships between the inner crown structure as well as crown shape and the surrounding stand by the skeletonization of TLS data. Skeletonization is the extraction of a structure description in the form of a collection of connected lines from TLS point clouds. It facilitates detailed analysis of tree morphological traits in a hierarchical fashion. Promising automated skeletonization approaches already exist and continue to be developed (Leeuwen et al. 2011; Bucksch et al. 2010; Bremer et al. 2012; Hackenberg et al. 2015). However, most algorithms are species specific, require several scan positions per tree as well as free-standing test trees and suffer from difficulties dealing with inhomogeneous point densities, data gaps and noise within the dataset (Bucksch 2011; Côté et al. 2011). Especially in the context of forest stands where occlusion is considerably stronger, further research is required until fully automated algorithms may reliably measure crown parameters at branch level. Therefore, the design and development of a semi-manual skeletonization approach (Bayer et al. 2013) was an essential part of this thesis. Furthermore, advanced α-shape and voxel space computations (Bayer and Pretzsch 2017; Bayer et al. 2017)

were developed in order to quantify volume and surface as well as to measure novel parameters such as the fractal-like crown surface complexity.

2. Aims of the Thesis and Research Questions

The main objective of this thesis was the application of terrestrial laser scanning and the design and development of new and innovative procedures for the analysis of urban and forest trees based on TLS point-clouds. While the methodological aspect of this thesis is very strong, it attempts to simultaneously contribute to the discussion and elucidation of currently relevant ecological questions. The following main research questions have been investigated:

- Are structural crown parameters such as branch angles, branch shapes, branch lengths, branch bending, ramification, growing space occupation of branches in the crown and detailed crown volumes derived from α-shapes robustly quantifiable by semi-manual skeletonization? How do these parameters differ between Norway spruce (*Picea abies* [L.] Karst.) and European beech (*Fagus sylvatica* L.) and how does the inter- and intraspecific competition in pure and mixed-species stands influence the structure of both species?

- How do Norway spruce (*Picea abies* [L.] Karst.) and European beech (*Fagus sylvatica* L.) react during the first years after the emergence of a forest gap? Which influence do pure and mixed stand types have? How do the specific structures, dynamics and mechanisms of space occupation develop during the gap closure period?

- How do black locust (*Robinia pseudoacacia* L.) and small-leaved lime (*Tilia cordata* Mill.) differ in quantifiable structural traits? How do both species structurally respond to varying urban environments? Which conclusions can be drawn from advanced structural parameters and allometric relations for both species' ecosystem functions and services?

3. Material and Methods

The structural analysis was based on several parameters derived by several branches of TLS data processing. Most of these parameters are hardly - and in some cases not at all - accessible by classical dendromentrical measurements. Among the target parameters were branch angles, branch length, ramification, branch bending and shape, branch growing space occupation, stem inclination, spatially explicit crown center displacement, surface, surface complexity, crown volume, crown projection area, spherical crown radius and inner crown point density distribution measurements. More detailed explanations are given in the following sections, especially 3.3 - 3.6.

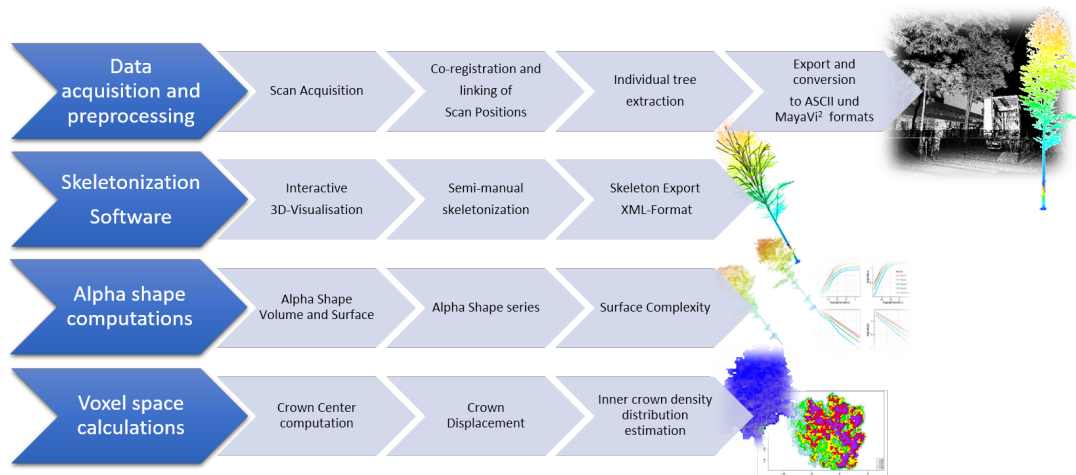**Figure 2.:** Basic overview of the procedures and steps involved in the data analysis.

3.1. Experimental Sites and Sample Trees

The structural traits of spruce and beech analyzed in Bayer et al. (2013) and their differences in pure versus mixed stands have been conducted on sample trees of the age series SON814 (Table 1, west-east spread: 10°28'45''E - 10°31'39''E, north-south spread:

18

Table 1.: Stand characteristics of the experimental plot SON814/3. Volume indicates merchantable wood above 7 cm in diameter at the thinner end. dg: diameter of the median basal area tree.

	Age	dg [cm]	Basal area (m^2/ha)	Volume (m^3/ha)
Norway spruce	128	56.1	36.8	640.6
European beech	143	42.3	19.4	360.0
Total	–	–	56.2	1000.6

47°31′05″N - 47°32′31″N). The experimental plot SON814/3 includes pure and mixed stands of Norway spruce and European beech. The stand is located at 785–800 m above sea level in the ecological region 14.4 ″Schwäbisch-Bayerische Jungmoräne und Molassevorberge. Westliche kalkalpine Jungmoräne″ in Bavaria, Germany. The long-term mean annual temperature amounts to 6.8°C, accompanied by an annual mean precipitation of 1114 mm. During the selection of the sample trees from plot SON814/3, close attention has been payed to individual tree size and competitive situation in order to assure that structural differences were caused by stand mixture itself and not by variations in local stand density or tree size (Bayer et al. 2013).

The sample trees (Table 2) of the gaps observed in Bayer and Pretzsch (2017) are located in the experimental plot FRE813/1 at the ″Kranzberger Forst″ near the city of Freising in Bavaria, Germany. The stands are located at 490 m above sea level in the ecological region 12.8 ″Tertiäres Hügelland. Oberbayerisches Tertiärhüggelland″. Long-term, the averages of air temperature range between 7°C and 8°C. The mean annual precipitation amounts to 750-850 mm. The area is dominated by Norway spruce and European beech. No other tree species are present in proximity to the created gaps. The three analyzed gaps are comprised of spruce and beech in pure as well as mixed species compositions. The area of the gaps has been defined by a polygon which uses the middle of the surrounding gap trees' stem bases as vertices.

In Munich, small-leaved lime (*Tilia cordata*) and black locust (*Robinia pseudoacacia*) (Table 3) were chosen as species for the sample trees (Bayer et al. 2017). Both species differ substantially regarding their ecological features and are a common appearance in Central European cities (Pauleit et al. 2002). The annual long-term precipitation within the city of Munich (48°09′ N, 11°35′ E, 519 m a.s.l.) averages 959 mm while the mean temperature amounts to 9.1°C (DWD 2015). In order to determine quantitative structural parameters for each species as well as their response to varying urban environments,

Table 2.: Individual tree parameters of the gap sample trees at the experimental plot FRE813/1 by species and year.

	Year	dbh (*cm*)	se	h (*m*)	se	CPA (*m²*)	se	h_{CPA}	se
Norway spruce	2006	33.9	2.04	28.3	0.52	14.3	1.49	54.2	0.03
	2008	35.0	2.03	28.6	0.50	15.1	1.24	52.1	0.02
	2010	36.1	2.06	28.8	0.48	15.9	1.05	53.4	0.03
	2012	37.1	2.04	29.0	0.46	17.8	1.12	54.0	0.03
European beech	2006	25.6	1.77	26.6	0.30	19.4	2.75	57.1	0.04
	2008	26.1	1.80	27.0	0.30	26.3	4.12	59.0	0.05
	2010	26.4	1.82	27.3	0.31	22.0	3.22	60.1	0.04
	2012	26.7	1.83	27.6	0.31	24.4	3.62	58.3	0.04

Table 3.: Scanned sample trees within the urban area of Munich.

	N	DBH [*cm*]	se	H [*m*]	se
Tilia cordata					
Park	8	26.7	3.2	12.5	1.2
Place	14	37.9	5.1	12.9	1.1
Street	30	26.5	2.3	11.2	0.7
Robinia pseudoacacia					
Park	7	43.2	10.8	19.3	2.0
Place	11	37.8	4.5	14.3	1.0
Street	23	35.1	4.3	12.4	0.7

such as street canyons (*St*), town squares (*Ts*) and parks (*Pa*), 83 individual trees were scanned. The classification of growing locations was based on the respective tree's environment. Individuals growing in green spaces without surrounding buildings were classified as park trees. The growing location town square has been assigned to free-standing trees in mostly paved places which are readily accessible to the public. Lastly, street trees were defined as trees growing within a street canyon. The initial tree selection was based on adequate visual impression so that damaged, low-forked and pruned trees have not been included. Each tree was scanned a second time, so that data under leaved as well as leafless conditions was available in order to provide the best possible data basis for the respective evaluation procedures.
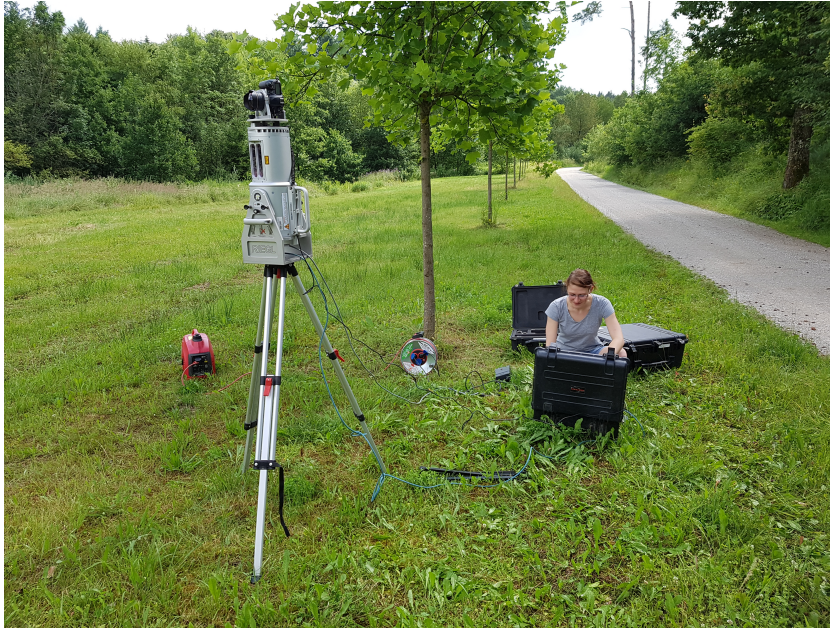
Figure 3.: A student operating the Riegl LMS-Z420i terrestrial laser scanning device via an attached laptop computer.

3.2. Scan Acquisition

Apart from the first two data acquisitions of the Kranzberg gap study (Bayer and Pretzsch 2017) where a Riegl LMS-Z360 terrestrial laser scanning device has been employed, all scans were obtained using the newer Riegl LMS-Z420i follow-up model (Figure 3).

Both devices work according to the time-of-flight principle. Laser impulses are fired towards specific directions at a high rate. For each impulse, the scanner records the time between the emission of the impulse and, depending on the mode, the first or last return of the partial reflections of the beam. The multiplication of the measured time with the speed of light in air yields the double distance to the captured target point. The combination of the many successive measurements' spherical coordinates results in a three-dimensional image of the scanned region.

A problem inherent to every application of laser scanners and optical measurement instruments in general for that matter, to semi-solid bodies or surfaces like tree crowns, is that objects behind obstacles cannot be measured. This may result in sparse point densities in crown regions located further away from the scanner (Hilker et al. 2010). In

order to mitigate this, single scans from different angles of the respective tree or forest gap have been combined. Also very close attention has been paid to the positioning of the laser scanner, in such a way that occlusion from neighboring trees and lower crown parts of the same tree was as minimal as possible. While in the case of urban trees, due to their comparative free-standing nature, occlusion was not very strong, forest trees, especially in mature and dense stands are harder to measure. Therefore scans of forest trees were always acquired outside the vegetation period in order to avoid the occlusive effect of foliage. Urban trees were scanned under leaf-on and leaf-off state in order to provide the optimal data for the respective analysis.

3.3. Data Preparation

Within the scanner manufacturer's software RiSCAN Pro, the data which is originally delivered in spherical coordinates was translated to Cartesian coordinates. After the co-registration and linking of different scan positions covering the same objects from different angles - or in case of the Kranzberg gaps different observation dates as well (Bayer and Pretzsch 2017) - the individual trees of interest were manually isolated from the respective scan's total data set and saved as extra polydata objects (Figure 4). Finally, these individual polydata files were converted to a comma separated ASCII format and exported for further processing.

Where necessary, the exported tree's polydata files were corrected regarding their spacial orientation and positioning by applying the respective scan-specific 4D rotation-translation SOP-matrix (Scanner Position and Orientation) to the data set.

3.4. Skeletonization

In order to achieve the acquisition of hierarchical, spatially explicit data of tree skeletons, software specifically designed for that purpose was developed by Bayer et al. (2013). Utilizing the VTK-based MayaVi visualization library (Ramachandran and Varoquaux 2008), a basis for custom 3D point cloud data measurements with interactive capabilities was established. Through a GUI (Graphical User Interface) particularly designed to identify and define stem and branches including their hierarchical order, the user is able to extract as much of the tree's skeleton as needed for the respective research question at hand (Figure 5). The Program itself is written mainly in the programming
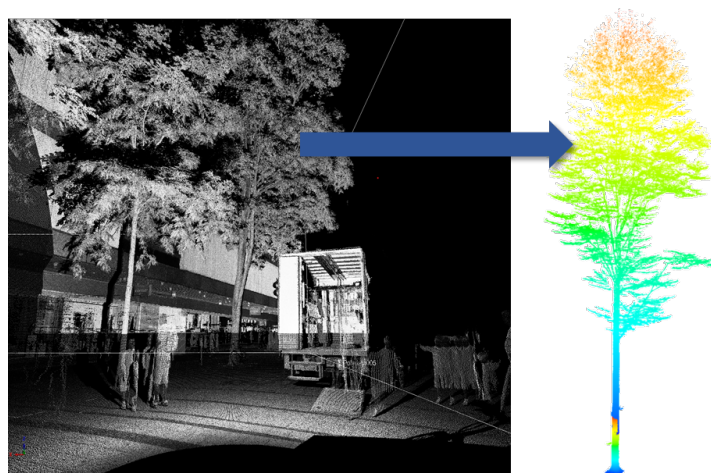
Figure 4.: Schematic illustration of the extraction of an urban tree **(r)** from the total scan position's data set **(l)**. Tree isolation is achieved by manually excluding everything not belonging to the tree such as the truck, passengers or the shopping center in the background.

language Python 2.7, falling back on numerous standard libraries for scientific work and advanced data analysis such as Sklearn, Scikit, Scipy, Numpy, Cython, Pandas, Statsmodels, MayaVi, VTK, Matplotlib and a considerable amount of others. Time critical or computation-heavy parts of the calculations have been optimized using Cython, C/C++ implementations, numerically optimized procedures such as array calculations in place of simple loops or, in many cases, a combination of those. The finished skeletons were stored in a specifically designed .XML format for the extraction and quantification of their structure.

From the finished skeleton, the length l_b of an individual branch was calculated by the summation of its contained segments with $\vec{ss}$ being the start and $\vec{se}$ being the end point of the respective segment. Thus, the curvature of the branch is already taken into account.

$$l_b = \sum_{i=1}^{n} |\vec{ss}_i - \vec{se}_i| \tag{1}$$

By putting l_b in relation to a simpler branch length measurement $l_s = |\vec{b_e} - \vec{b_b}|$, a simple measure of the total crooking of the branch can be determined:

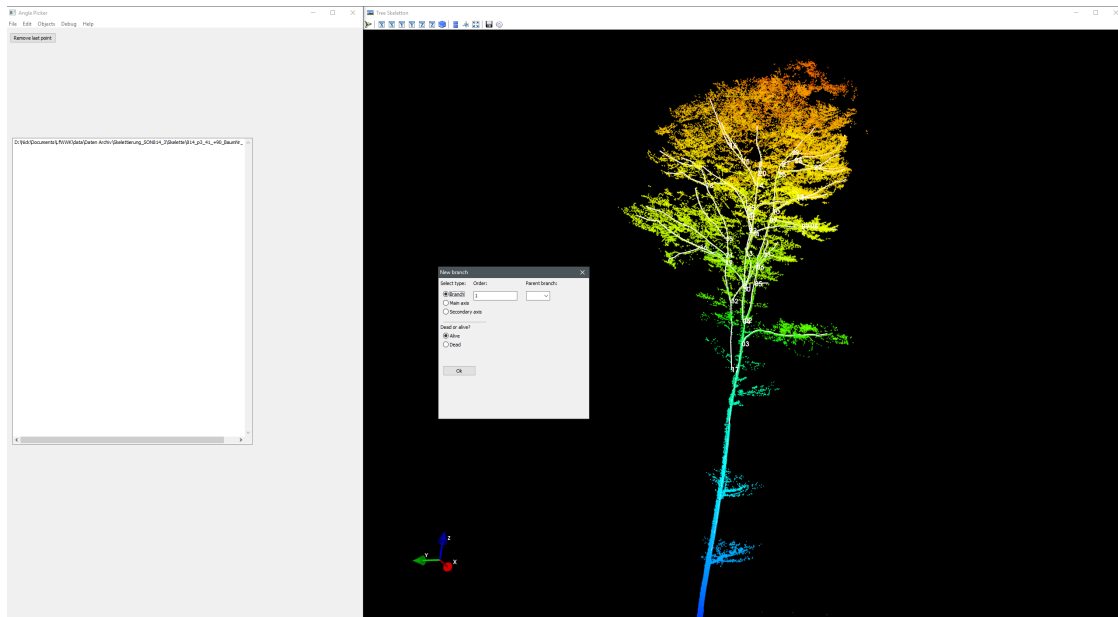$$crook = \frac{l_b}{l_s} \tag{2}$$

Figure 5.: Graphical user interface of the developed skeletonization software during the interactive skeletonization process of an isolated tree. White lines and numbers mark already recorded branch segments.
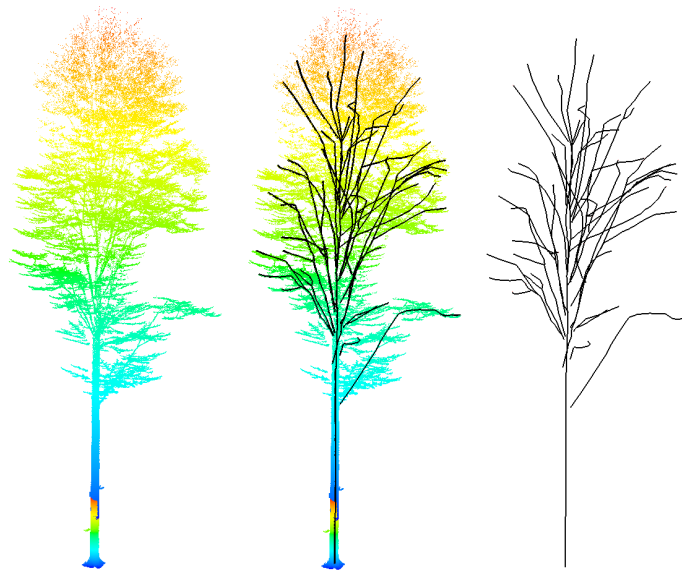

Figure 6.: (l) Original isolated point cloud of an individual tree, **(m)** skeletonized tree and **(r)** isolated skeleton (Bayer et al. 2013).

24

The angles of branches are an important measure for the inner crown structure. However, using a fixed measurement distance (e.g. from branch base 50cm in growing direction) cannot sufficiently describe the whole shape of a branch. Furthermore, fixed values are problematic, since every branch has a different length. Without normalization, measurements would therefore be of limited value beyond basic analysis. To overcome this, in addition to fixed measurement distances, measurement distances relative to an individual branch's size were implemented, making sensible comparisons of shape and structure between different individuals possible. In three dimensional space, in order to compute the unambiguous, smallest angle φ_b between a point on the branch $\vec{s}$ and the gravitational axis $\vec{z}$, the scalar product of both vectors was calculated.

$$\cos(\varphi_b) = \frac{\vec{s} * \vec{z}}{|\vec{s}| * |\vec{z}|}, \tag{3}$$

Since $\vec{s}$ is dependent on the chosen measurement radius r and the shape of the branch in question, $\vec{s}$ must be computed first. If any given branch's $l_s > r$, it penetrates a hypothetical sphere with the measurement radius r and the branch's base as center. The intersection between the first branch segment fulfilling $|\vec{ss} - \vec{b}| < r < |\vec{se} - \vec{b}|$, i.e. penetrating the measurement sphere, is $\vec{s}$.

$$\vec{s} = \vec{p}_1 + \frac{-t_2 + \sqrt{t_2^2 - 4t_1t_3}}{2t_1}(\vec{p}_2 - \vec{p}_1) \tag{4}$$

with

$$t_1 = (x_{p2} - x_{p1})^2 + (y_{p2} - y_{p1})^2 + (z_{p2} - z_{p1})^2 \tag{5}$$

$$t_2 = 2((x_{p2} - x_{p1})(x_{p1} - b_x) + (y_{p2} - y_{p1})(y_{p1} - b_y) + (z_{p2} - z_{p1})(z_{p1} - b_z)) \tag{6}$$

$$t_3 = b_x^2 + b_y^2 + b_z^2 + x_{p1} + y_{p1} + z_{p1} - 2(b_x x_{p1} + b_y y_{p1} + b_z z_{p1}) - r^2 \tag{7}$$

Figure 7 illustrates the involved vectors and measures.

3.5. Alpha Shape Computations

To further describe tree structure, measurements of volume, surface and crown projection were derived from the TLS point clouds. Two- and three-dimensional convex hulls are a simple way to estimate crown volume or projection area. However, much of the

(a)   **(b)**

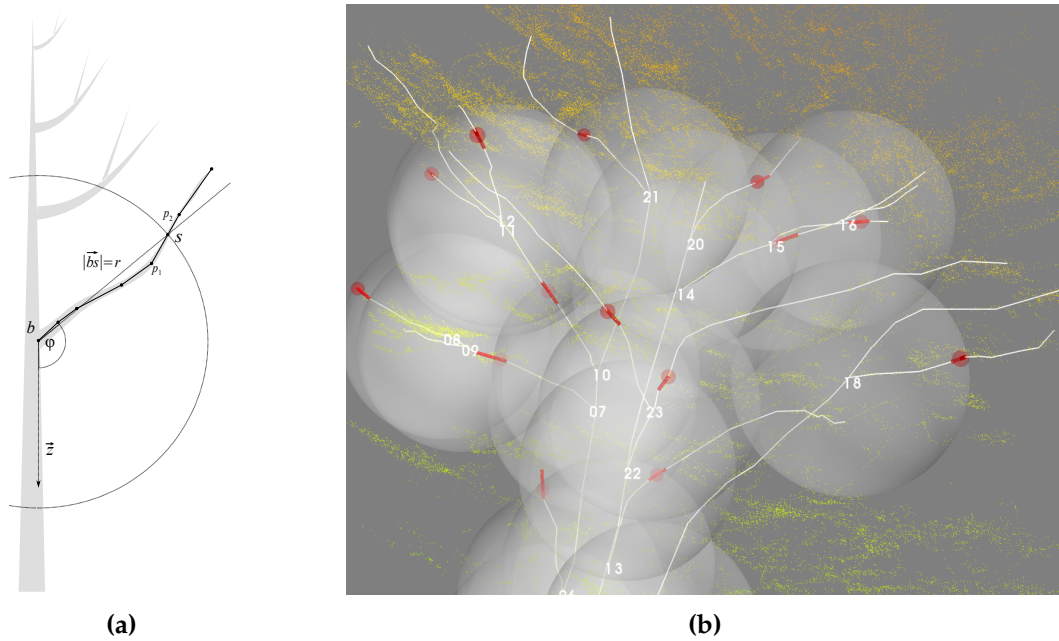**Figure 7.: (a)** Schematic illustration of the branch angle calculation dependent on measurement distance r (Bayer et al. 2013). **(b)** Visual plausibility check of the angle calculations at an early development stage of the skeletonization software's interpretation routines. The grey circles mark the angle measurement radius. Red cylinders mark the calculated branch segment penetrating the measurement sphere.
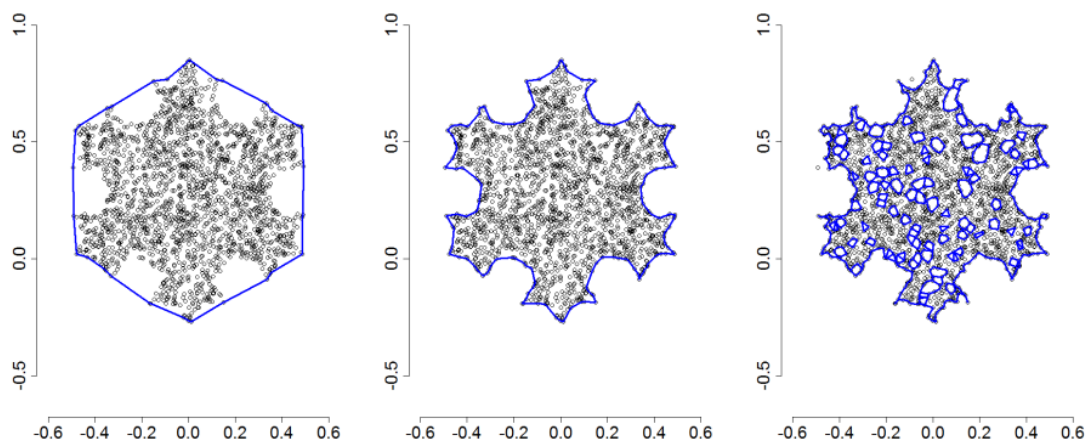
Figure 8.: 2D random point sample of a Koch-Snowflake and derived α-shapes (blue lines) from **(l)** too large where the shape yields only a very coarse, almost purely convex representation of the point cloud, **(m)** sensible where the shape represents the point cloud rather well and **(r)** too small where the shape begins to partially disintegrate because the application radius cannot cover gaps in the dataset anymore. The same principle applies to 3D α-shapes. Image taken from Pateiro-López and Rodríguez-Casal (2010).

precision and measurement detail a TLS device may deliver is lost. Therefore, 2D and 3D α-shapes were applied instead. These shapes are generalizations of the convex hull of a given point set (Edelsbrunner et al. 1983; Edelsbrunner and Mücke 1994). The principle is based on Delauny-triangulation. The benefit of α-shapes is that the α-value may be varied in order to display different levels of detail in the point cloud's surface reconstruction. However, sensible α-values are restricted to a specific range dependent on the resolution and point distribution within the data set. The choice of too large α-values yields coarse representations of the point clouds, suffering substantial loss of detail. Values too small however, may cause the shape to incompletely and incorrectly represent the original object (Figure 8).

In order to objectively choose an appropriate range of α-values, a series of α-shapes, ranging from very detailed ($\alpha = 0.05$ m) to very coarse ($\alpha = 10.0$ m), was calculated. Because of the fractal properties of surfaces, one should expect decreasing values for an object's α-shape volume for decreasing α-values as long as the given data quality and resolution is still capable of producing sufficient detail (Mandelbrot 1967; Mandelbrot 1983). The smallest α-value of a series still fulfilling this law may be considered the smallest sensible α-value.
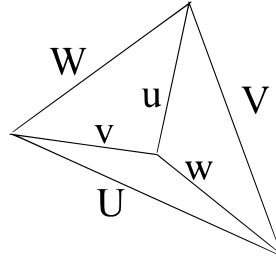
Figure 9.: Tetrahedron edges for the 3D α-shape volume calculation as used in Eq. 8.

The Volume V of a given α-shape, may be computed by the summation of all, mostly irregular, tetrahedrons contained in the shape, since the shape itself is based on Delauny-triangulation. The calculation of the surface area of a 2D α-shape works analogously by accumulating the contained triangles.

$$V = \sum_{i=1}^{n} \sqrt{\frac{1}{288} * det \begin{pmatrix} 0 & u_i^2 & v_i^2 & w_i^2 & 1 \\ u_i^2 & 0 & W_i^2 & V_i^2 & 1 \\ v_i^2 & W_i^2 & 0 & U_i^2 & 1 \\ w_i^2 & V_i^2 & U_i^2 & 0 & 1 \\ 1 & 1 & 1 & 1 & 0 \end{pmatrix}} \tag{8}$$

For each triangle surface defining the border of an α-shape, a normal vector $\vec{N}$ is produced during the computational shape generation. Since the magnitude of $\vec{N}$ is proportional to the triangle surface area A,

$$|\vec{N}_i| \sim A_i, \tag{9}$$

the sum of magnitudes of all $\vec{N}_i$, scaled by a factor C according to measurement unit yields the total surface area S of a given α-shape.

$$S = \sum_{i=1}^{n} |\vec{N}_i| * C \tag{10}$$

Assessing the surface beyond area determination has been achieved by analyzing the α-shape series for each respective point cloud (Figure 10). The surface of an α-shape, like that any given non-theoretical object, has fractal characteristics (Mandelbrot 1983). With smaller scale and higher detail resolution, the measured surface - or circumference in
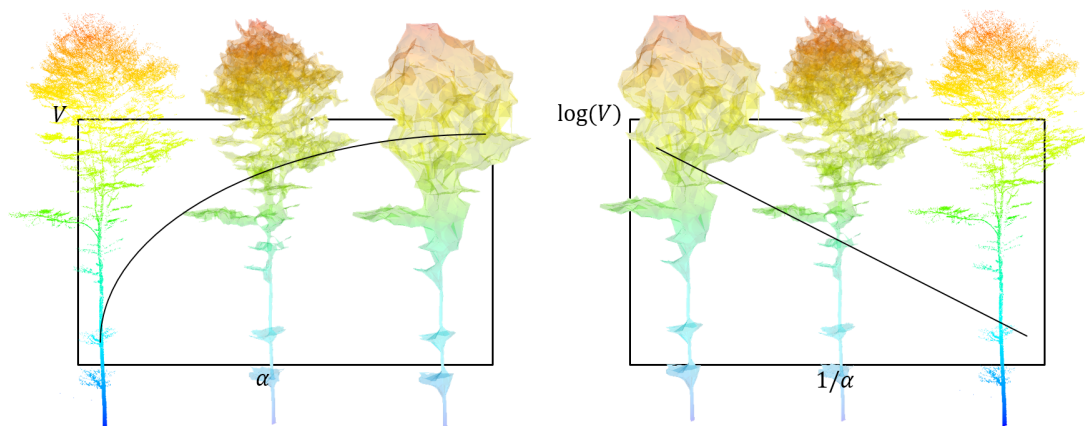
Figure 10.: Schematic illustration of the relationship between applied α-value and the resulting α-shape volume. **(l)** Non-linear relation from small towards large α-values. **(r)** After linearization, the slope of the regression line indicates rate of change of computed volumes. It therefore measures crown complexity. Since the best linearization is achieved by an $1/\alpha$-transformation, more negative slopes mean higher crown surface complexities (Bayer et al. 2017).

case of 2D objects - must increase (Mandelbrot 1967). The rate of the increase indicates the surface's fractal complexity F_s as a function of measurement resolution.

$$F_s = f(\alpha) \tag{11}$$

The linear transformation of the relationship between V and α (Figure 10, Eq. 12),

$$ln(V) = \beta_0 + \beta_1 * \frac{1}{\alpha} \tag{12}$$

with R^2-values of well above 0.95 within measurement groups, proved to be a very robust representation of the expected fractal behavior. β_1-values, representing the linear transformation's slope, indicate the respective surface complexities.

Through a combination of skeleton data and α-shapes, the growing space occupation of a tree's individual branches may be estimated (Figure 11). By generating a higher point density within the actual skeleton branch segments by adding interpolated points with a maximum distances of 10 cm from one another, the total set of skeleton points was translated to a point cloud. Following this, the kd-tree implementation of Manee-wongvatana and Mount (1999) contained in the Scipy.spatial Python library, was applied

29

Figure 11.: (l) Original point cloud and **(r)** individual branch space occupation estimation achieved by combining skeleton data with α-shapes of a kd-tree based nearest-neighbor assignment for a European beech test tree (Bayer et al. 2013).

to conduct a nearest-neighbors search for every point of the TLS point-cloud. However, not the nearest neighbour within the point cloud but within the generated, homogenized skeleton point cloud was calculated, resulting in an assignment of every TLS point to a specific branch of the skeleton.

3.6. Voxel Space Calculations

The spatial crown center is an important structural measure and basis for further analysis. However, the point distribution of a tree crown's TLS data displays gradients depending on crown density and size as well as the scanner's capabilities (first-, last-, multi-return, full-waveform), scan resolution, number of scans and their positions in relation to the tree. Furthermore, tree crowns feature an actual leaf-density distribution which itself can be a desired parameter. Therefore, direct point based crown center estimations such as ordinary least squares calculations usually yield heavily skewed results. In order to overcome this, the crown's point cloud was transformed into a voxel-space

representation. Treating each voxel equally in terms of point content, i.e. declaring the point content as $n = 1$, the crown may be treated like a system of equal particles. In such a system, each particle, or voxel in this case, fulfills

$$\sum_{i=1}^{n} m_i(\vec{v}_i - \vec{c}_m) = 0, \tag{13}$$

where m_i is the hypothetical mass of a voxel, $\vec{v}_i$ represents the positional vector of the respective voxel center and $\vec{c}_m$ is the position of the systems center of gravity. As a consequence, the crown center $\vec{c}_m$,

$$\vec{c_m} = \frac{1}{M} \sum_{i=1}^{n} m_i \vec{v}_i, \tag{14}$$

with M being the hypothetical mass of the system can be determined independently of point density distribution.

After the definition of the crown center, the horizontal crown center displacement CD_h is given by the magnitude of a vector from the xy-projection of the stem base to the xy-projection of the crown center.

$$CD_h = |\vec{b}_{xy} - \vec{c}_{xy}| \tag{15}$$

The relative vertical crown center position CD_v,

$$CD_v = \frac{c_{m_z}}{h}, \tag{16}$$

is defined by the height of c_m in relation to the total tree height h.

After the definition of a spatially explicit crown center, the spherical crown radius r_c was defined by calculating the 95% quantile of all voxel distances d,

$$d = \frac{1}{n} \sum_{i=1}^{n} |\vec{v}_i - \vec{c}_m| \tag{17}$$

from the crown center. Then, voxel quantiles based on point content were calculated (10%, 20%, 30%, ..., 90%). For every one of those quantiles representing a proxy for the
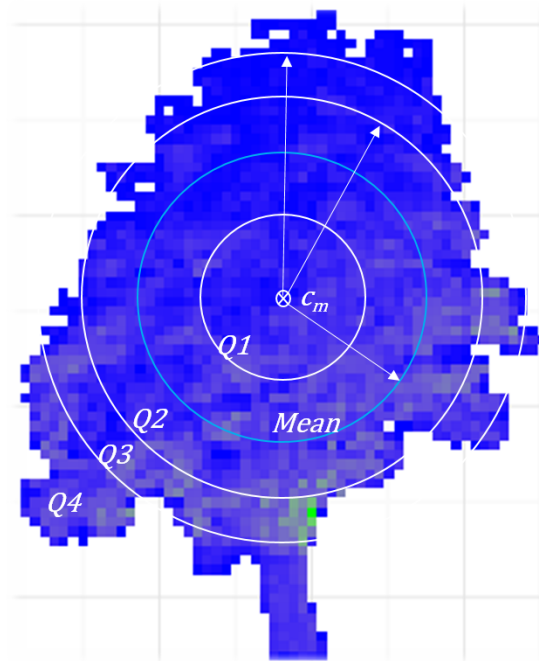
Figure 12.: Illustration of a tree's voxel space representation. Colored squares indicate individual voxels. c_m: crown center of gravity, Q_1-Q_n: mean distances of voxels belonging to a specific density quantile.

inner crown density, the mean distance of voxels belonging to it in relation to the crown radius were computed (Figure 12, Eq. 18, 19).

$$r_\rho = \frac{1}{n} \sum_{i=1}^{n} |\vec{\rho}_i - \vec{c}_m| \qquad (18)$$

$$r_{\rho rel} = \frac{r_\rho}{r_{crown}} \qquad (19)$$

4. Results

4.1. Structural crown characteristics of European beech and Norway spruce in consideration of pure and mixed stands

An overview of the descriptive statistics of Bayer et al. (2013) is given in Table 4. Measured from branch base to branch end, the branch angles were found to be significantly different between pure (138.6°) and mixed stands (128.5°) for European beech (Figure 13a). Furthermore, for beech, the gradient of measured angles over the course of a branch features significantly higher mean angles, staying on a relatively constant level for the pure stand members. Beech's mixed-species stand branch angles however, decline with increasing measurement distance (Figure 13b).

Norway spruce developed significantly longer branches in mixed species stands than in pure stands. Both stand types feature no difference regarding the branch bending. European beech on the other hand displayed no significant difference of branch lengths, however its branches are significantly more bent in mixed stand environments.

In case of Norway spruce, the average number of branches amounted to 20.1 in pure and 26.0 in mixed stands, the difference was not significant however. The branch count

Table 4.: Overview over the descriptive statistics for the analyzed trees in Bayer et al. (2013). N: number of branches per tree, φ: mean branch angle measured from branch base to branch end, l_s: branch length, *crook* bending of branches, SBL: sum of branch lengths, $RLBV$: relative logarithmic branch volume, V: α-shape derived crown volume ($\alpha = 0.25m$).

		Spruce Pure		Mixed			Beech Pure		Mixed		
	Model	*mean*	*se*	*mean*	*se*	*p*	*mean*	*se*	*mean*	*se*	*p*
N	lm	20.1	4.493	26.0	3.092	0.261	18.6	2.663	35.8	3.687	<0.001
φ (°)	lme	89.55	3.175	88.12	4.365	0.747	138.56	2.220	128.52	2.870	0.0022
l_s (m)	lme	2.16	0.210	2.78	0.289	0.0476	4.81	0.209	4.31	0.261	0.0702
crook	lme	95.72e-2	5.631e-3	96.27e-2	7.525e-3	0.475	96.21e-2	4.188e-3	94.39e-2	5.281e-3	0.0024
SBL (m)	lm	45.82	12.536	68.98	8.628	0.0821	89.26	15.560	153.84	10.760	<0.001
$RLBV$ (m^3)	lme	–	–	–	–	–	-3.777	0.121	-4.286	0.160	0.0045
V (m^3)	lm	21.07	7.120	46.23	9.814	0.0202	25.25	5.763	58.97	7.978	<0.001
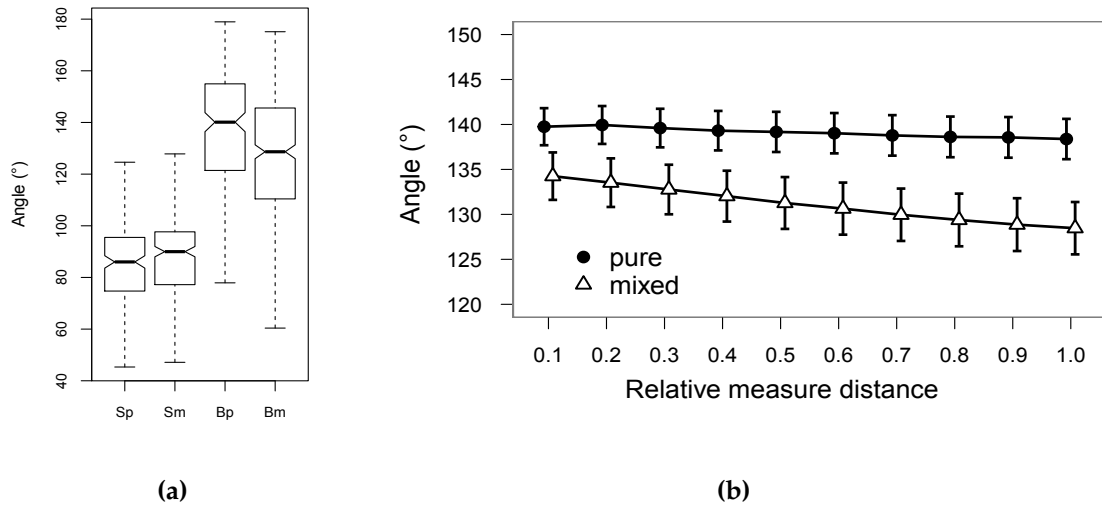
Figure 13.: Branch angle comparison between Norway spruce and European beech from Bayer et al. (2013). **(a)** Absolute branch angles, measured from branch base to branch end for spruce in pure stands (Sp), spruce in mixed stands (Sm), beech in pure (Bp) and beech in mixed stands (Bm). **(b)** Branch angles in relative measurement distances along the course of the respective branch of European beech in pure and mixed-species environments.
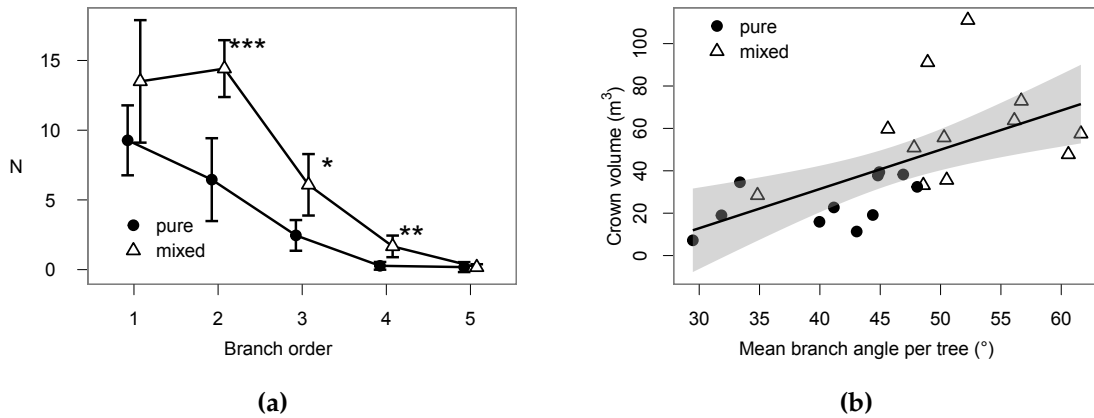
Figure 14.: European beech branches of Bayer et al. (2013): **(a)** Measurable branch count by branch order. **(b)** Relationship between branch angle and crown volume.

of European beech differed significantly in pure and mixed stands. Especially the second, third and fourth branch orders were significantly more abundant (Figure 14a).

Both Norway spruce and European beech developed larger crown volumes in mixed-species stands. The volume increase is mainly related to increased branch lengths in case of Norway spruce in mixed stands. The increased crown volume of European beech is not related to branch length, branch angles however, have a significant influence (Figure 14b).

4.2. Validation of a functional-structural tree model

Figure 15 provides a visual comparison of the empirical, TLS-based densities and the relative leaf densities by the simulations based in the model described by Beyer et al. (2017c) at a stand age of 180 years. Height, radius as well as a distinct concavity for both simulated and empirical data can be noted. Overall, a concentration of the empirical as well as simulated data can be observed and the simulated crown is well within the normal range of crown shapes for the respective age and growth conditions.
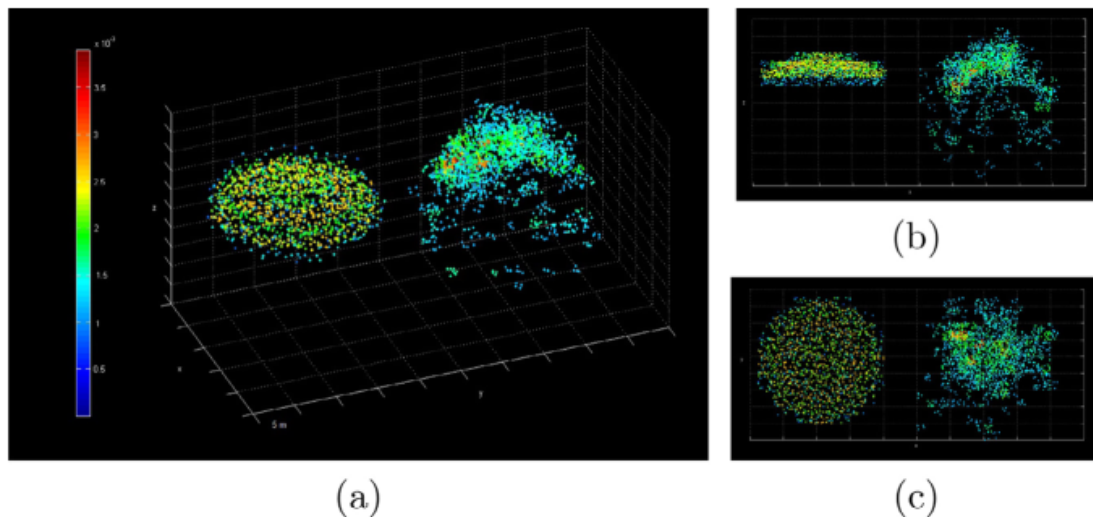

Figure 15.: Emprical (right) and simulated (left) relative twig and leaf-area density in **(a)** oblique, **(b)** side and **(c)** top view (Beyer et al. 2017a).

4.3. Gap closure dynamics of European beech and Norway spruce (Bayer and Pretzsch 2017)

The closure of the forest gaps during the observation period from 2006 to 2012 being subject of Bayer and Pretzsch (2017), is illustrated in Figure 16. In order to close the emerged gap, the crown projection area (CPA) of the border trees has to increase. This increase, while happening in a steady fashion in the case of Norway spruce, proved to be rather erratic in the case of European beech. After an initial thrust in lateral space occupation, the significant crown retreat indicates a heavy loss of crown mass through weather events such as snow, hail and storms. The vertical crown shape, described by the relative height of the maximum CPA of 2D α-shapes of horizontal slices of the point cloud of the respective crown, showed no change for both species as well as all gap types.

The *dbh* growth of spruce was found to be at a significantly higher level immediately after gap emergence and stays at an increased level for the rest of the study. European beech displayed no reaction in terms of *dbh* growth. The temporal allometric crown parameters, describing resource allocation showed no reaction in case of Norway spruce (Figure 17). European beech, in contrast, features a significant peak in the period directly after the creation of the gaps. This suggests resource allocation in favor of lateral crown expansion *dbh*, *h* and biomass growth. Because of the serious reduction of CPA during the period from 2008 to 2010, the investigated crown allometry parameters significantly drop (Figure 17). Norway spruce differentiates itself from beech by displaying overall higher resilience in terms of CPA preservation.

While a statistically significant reaction of the CPA growth increase towards the gap center (CPA_{in}) could not be shown for Norway spruce, European beech displays a rather strong reaction to the emergence of the respective gap (Figure 18). The proportion of the crown being located outside the gap polygon borders, showed considerable weaker reactions for both species.

Regarding the efficiency of space occupation (EOC) over all observations, Norway spruce featured significantly lower values than European beech. Both species followed no well defined trend (Figure 19a, Table 5). In terms of space exploitation (EEX) again, Norway spruce featured significantly higher values than beech over the whole duration of the study (Figure 19b, Table 5). The efficiency of biomass investment (EBI) starts at a similar level, followed by a development resulting in significantly higher values for
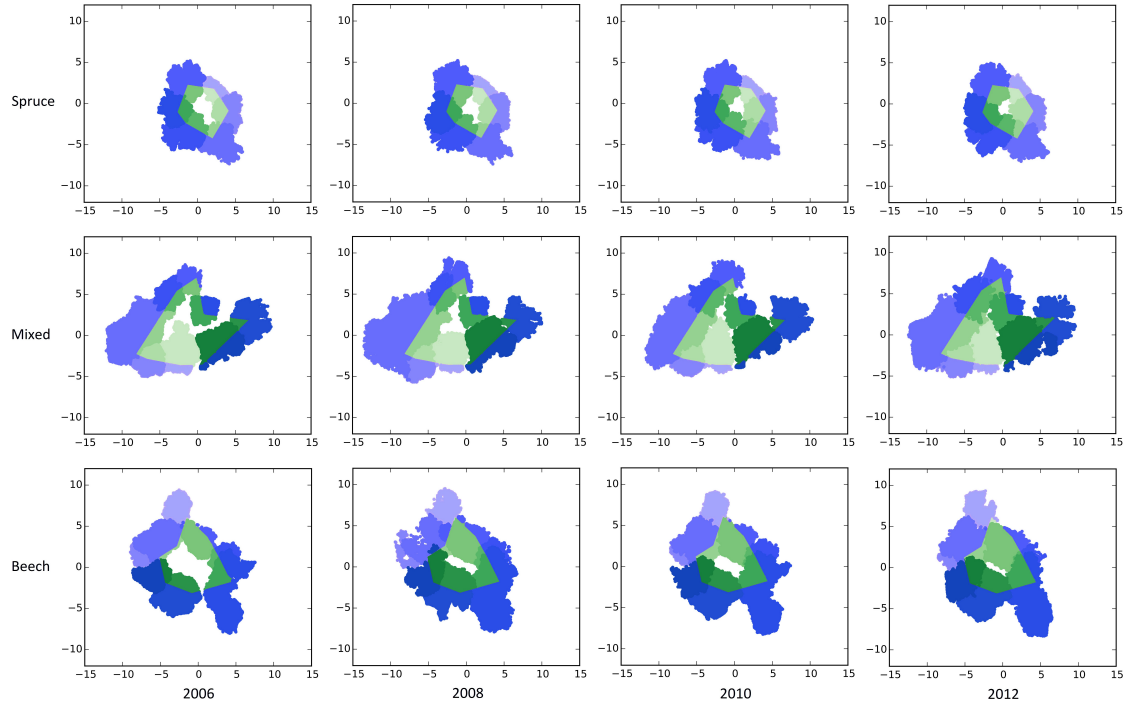
Figure 16.: Bird's eye view of the Kranzberg gap development from 2006 – 2012 generated from TLS data (Bayer and Pretzsch 2017). Observation years are given in columns. (Top row) Pure stand of Norway spruce, (middle row) Norway spruce and European beech in mixture and (bottom row) pure European beech. Green areas mark the gap polygon, shades of green represent the individual border trees. Blue areas mark the gap trees' crown proportions located outside of the gap polygon as well as individual gap trees in different shades.

Table 5.: Space occupation and utilization parameters of Norway spruce and European beech by year (Bayer and Pretzsch 2017).

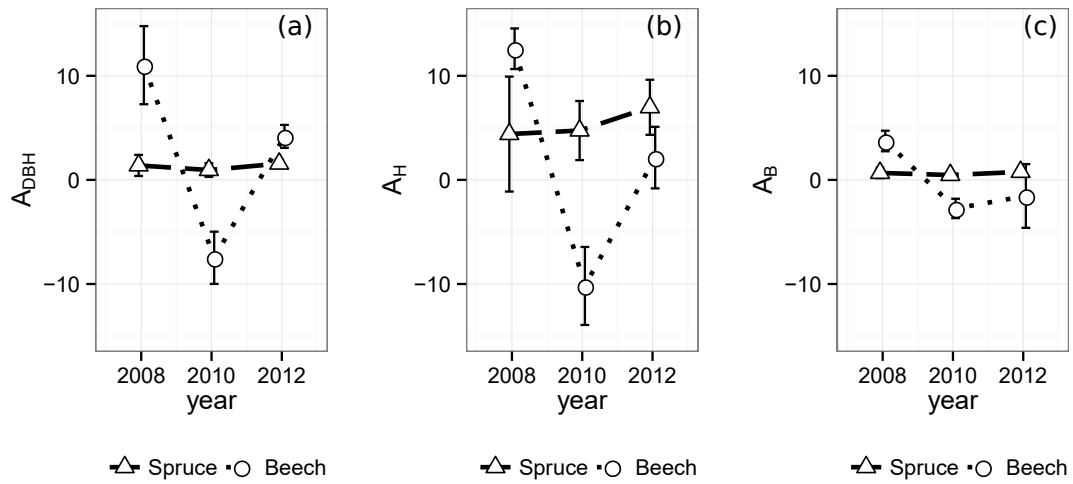|	Year	$CPAG_{in}$ (m^2/m^2)	se	$CPAG_{out}$ (m^2/m^2)	se	EOC (m^2/m^3)	se	EEX $(m^3/a/m^2)$	se	EBI $(m^3/a/m^3)$	se
Norway spruce	2006	–	–	–	–	11.0	1.25	$5.18*10^{-3}$	$9.54*10^{-4}$	$4.98*10^{-2}$	$5.98*10^{-3}$
	2008	0.07	0.07	0.11	0.10	10.8	1.06	$6.48*10^{-3}$	$8.63*10^{-4}$	$6.53*10^{-2}$	$6.71*10^{-3}$
	2010	0.11	0.06	0.03	0.06	10.8	1.00	$6.12*10^{-3}$	$7.41*10^{-4}$	$6.19*10^{-2}$	$5.87*10^{-3}$
	2012	0.26	0.07	0.07	0.05	11.4	1.06	$5.31*10^{-3}$	$7.27*10^{-4}$	$5.83*10^{-2}$	$8.64*10^{-3}$
European beech	2006	–	–	–	–	27.1	4.69	$1.98*10^{-3}$	$2.41*10^{-4}$	$4.38*10^{-2}$	$3.81*10^{-3}$
	2008	1.24	0.42	0.48	0.28	36.4	7.77	$1.50*10^{-3}$	$2.05*10^{-4}$	$4.24*10^{-2}$	$4.61*10^{-3}$
	2010	-0.12	0.08	-0.24	0.06	29.4	6.37	$1.83*10^{-3}$	$3.61*10^{-4}$	$3.89*10^{-2}$	$4.04*10^{-3}$
	2012	0.06	0.05	0.20	0.11	28.7	3.59	$1.38*10^{-3}$	$2.54*10^{-4}$	$3.18*10^{-2}$	$4.21*10^{-3}$

Figure 17.: Temporal crown allometry parameters. Resource allocation towards *CPA* in relation to **(a)** dbh, **(b)** h and **(c)** biomass growth (Bayer and Pretzsch 2017).
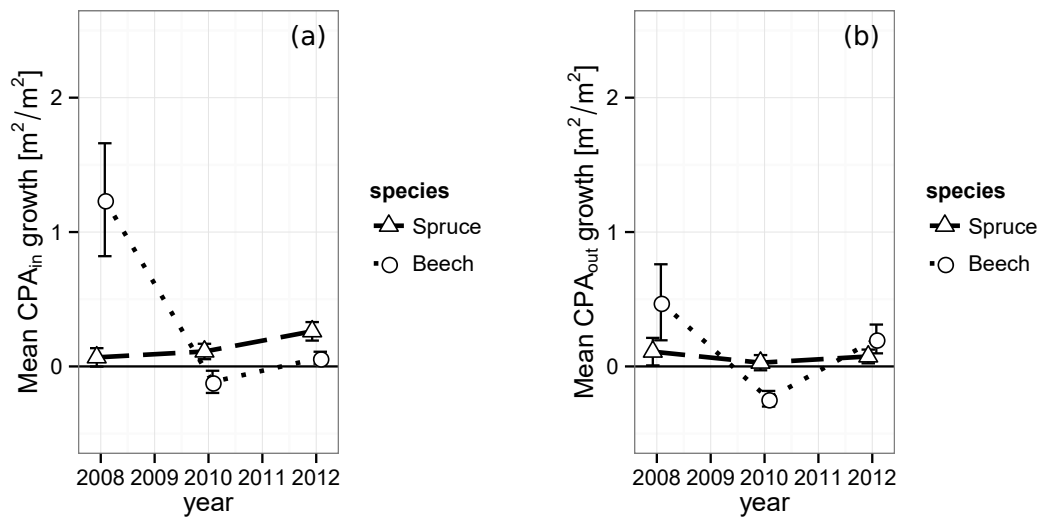

Figure 18.: CPA growth **(a)** towards the gap center and **(b)** towards the remaining stand (Bayer and Pretzsch 2017).
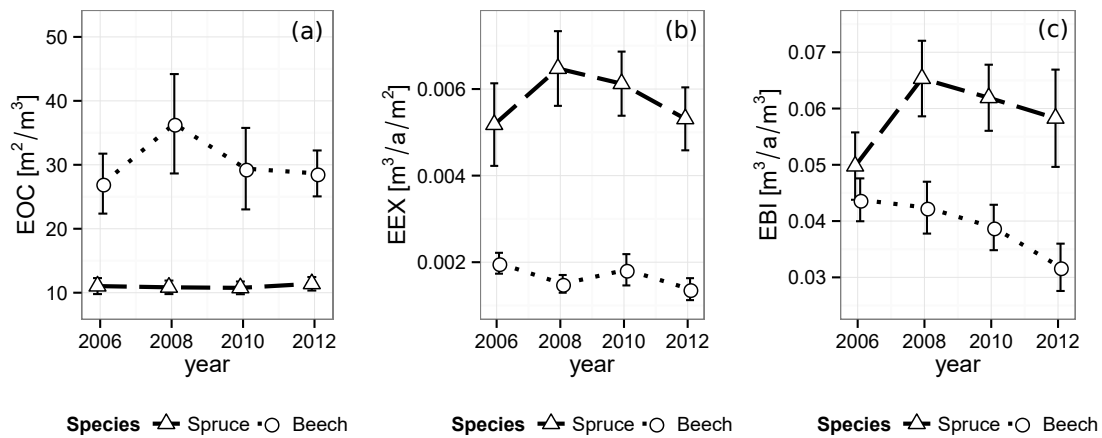
Figure 19.: (a) *EOC*: Efficiency of space occupation **(b)** *EEX*: Efficiency of space exploitation and **(c)** *EBI*: Efficiency of biomass investment for Norway spruce and European beech by year (Bayer and Pretzsch 2017).

Norway spruce. European beech, while alredy on lower levels than spruce, displays a declining trend in all later observations (Figure 19c, Table 5).

Overall, the development of the gaps displayed closure of the vacant canopy space. The spruce gap increased its single-layer gap projection area (*GPA*) of 70.2% of the gap polygon in 2006 to 84.0% in 2012. European beech increased its gap polygon cover from 59% in the beginning up to 90% at the last observation. The mixed gap cover started at 73.3% and increased to 90.9%. Concurrently, the multi-layering area *ML* of all three gaps increased, whereby the absolute multi-layering as well as its increase was least prominent in the pure spruce gap. Both, the pure beech and the mixed-species gap reached relative multi-layering *RML* values of 27.0% at the end of the study. Yet, the European beech gap featured a higher level during the observations in 2008 and 2010.

4.4. Structural parameters of small-leaved lime and black locust and their response to varying urban environments

Within the municipal area of Munich, small-leaved lime displayed significantly larger crown volumes than black locust at comparable *dbh* and *h* levels (Figure 20). Crown volumes depended significantly on measured branch angles and lengths. However,
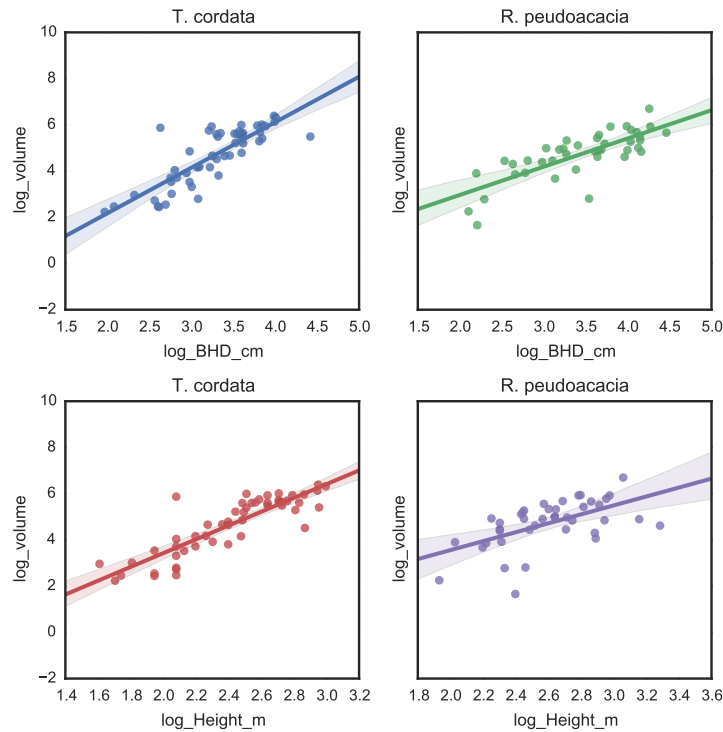
Figure 20.: Volume-*dbh* (top row) and Volume-*h* (bottom row) relation of small-leaved lime (*Tilia cordata*, left column) and black locust (*Robinia pseudoacacia*, right column) (Bayer et al. 2017).

species and growing location had no significant influence on branch parameters (Figure 21, Table 6). It is conceivable, since only main branches, i.e. of the first order, have been measured that the structural diversification of branching patterns was primarily caused by branches of second and higher order and therefore not recorded in this study. Tree species and growing location displayed a significant influence in the *h-bdh* relationship. Crown length l_c, besides *dbh* and *h*, was significantly dependent on species and growing location. With comparable crown volume, black locust covered more ground in terms of *CPA* than small-leaved lime.

In case of black locust, all three growing locations displayed significantly different indicators for crown surface complexity, with street featuring the least and park trees the most complexity (Figure 22). Small-leaved lime displayed no statistical difference
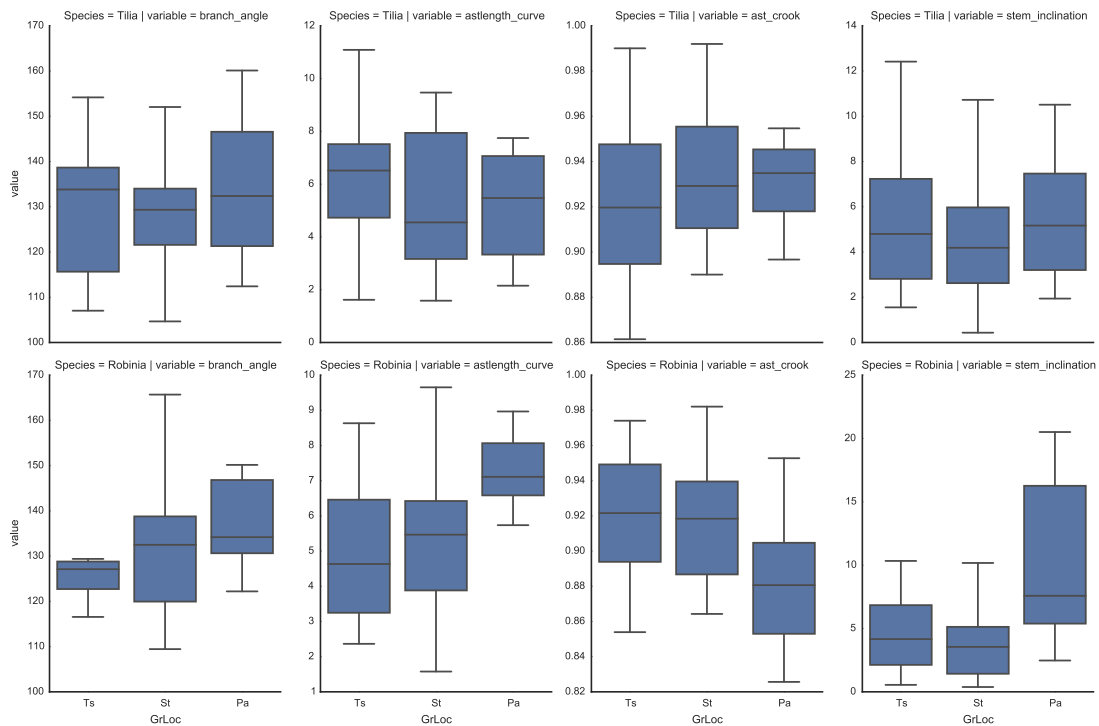
Figure 21.: Skeleton parameters branch angle φ_b, branch length l_b, branch bending *crook* and stem inclination φ_s by species (top row: small-leaved lime, bottom row: black locust) and growing location (Bayer et al. 2017).

between park and town square but street trees significantly stood out with considerably less crown surface complexity.

The growing location has no significant influence on small-leaved lime's horizontal crown center displacement CD_h. Black locust growing in parks significantly stand out from both, street and town square locusts and all small-leaved limes (Table 6). Obviously, stem inclination and tree height are major determining factors for the horizontal crown displacement. Yet, black locust shows an additional significant difference of the growing location park, suggesting that competition with surrounding trees has a meaningful effect on CD_h. Branch angle, branch length, species and growing location are significant factors determining the vertical crown center displacement CD_v. As in the case of the horizontal crown center displacement, a significant difference of CD_v among the growing locations of small-leaved lime could not be verified. A larger sample size however, might have yielded a clear difference between town squares and the park.

41

Table 6.: Tree skeleton parameters. φ_s stem inclination, CD_h horizontal crown displacement, CD_v vertical crown displacement, φ_b branch angle from branch base to branch end, l_b branch length, *crook* relation between actual branch length and straight line from branch base to branch end (Bayer et al. 2017).

	φ_s [°]	se	CD_h	se	CD_v	se	φ_b [°]	se	l_b [m]	se	crook	se
T. cordata												
Park	5.5	1.1	0.66	0.12	0.49	0.013	134.1	5.7	5.17	0.79	0.93	0.007
Place	7.7	2.6	0.81	0.24	0.43	0.015	132.1	5.0	5.96	0.71	0.93	0.011
Street	4.4	0.5	0.87	0.13	0.47	0.012	128.6	2.9	5.21	0.47	0.93	0.006
R. pseudoacacia												
Park	10.6	2.7	2.82	0.47	0.64	0.045	137.3	4.0	7.62	0.70	0.88	0.018
Place	4.7	1.0	0.95	0.22	0.54	0.026	128.9	4.5	4.89	0.62	0.92	0.012
Street	4.9	1.1	0.72	0.12	0.54	0.014	131.9	3.1	5.43	0.50	0.91	0.010

Black locust growing in park environments significantly differs from both street and town square trees in regards to the vertical crown center position.
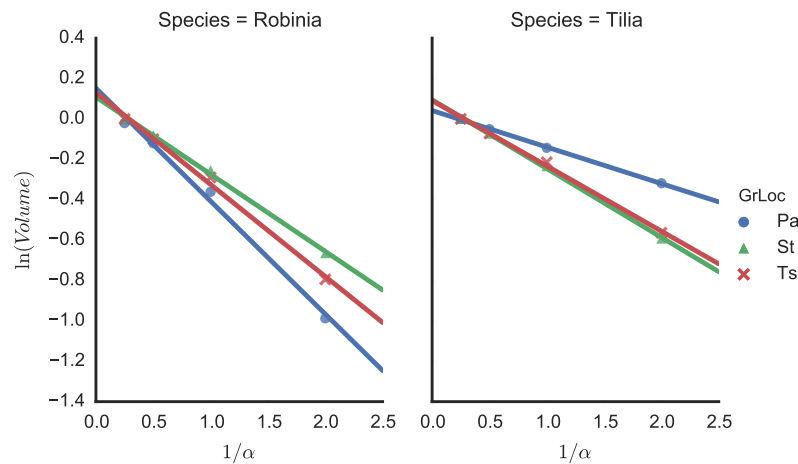
Figure 22.: Linearized α-shape volume series for **(l)** *Robinia pseudoacacia* and **(r)** *Tilia cordata* by growing location. For better visual presentation and illustration of the slopes (β_1), absolute values have been shiftet so that $\alpha_{0.25} = 0.0$. Due to the $1/\alpha$-transformation, more negative slopes mean higher fractal-like surface complexity (Bayer et al. 2017).

Black locust displays significant difference between trees located in parks and streets. Among the growing locations of small-leaved lime, and between both species in general, no further significant differences could be identified. The branch bending is significantly related to species, *CPA* and φ_b. Branch angles φ_b as well as branch length l_b significantly affect crown volume. No distinct differences between species or growing locations could
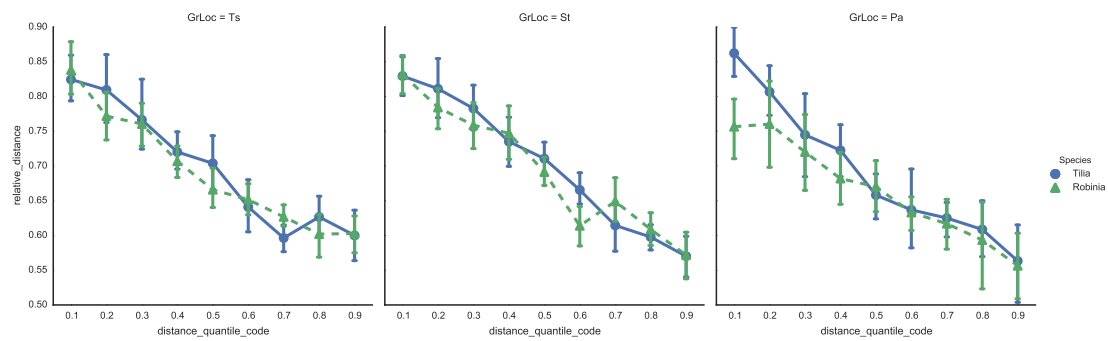
Figure 23.: Mean radial distance of the point density quantiles from the crown center in relation to the spherical crown radius for *Tilia cordata* and *Robinia pseudoacacia*. (**l**) Town square (**m**) street canyon (**r**) park (Bayer et al. 2017)

be found. However, between black locust growing at town squares and the other two locations a remarkable difference in variance is present.

Tree species had no significant effect on the mean distance of voxels belonging to an individual tree crown's point density quantiles in relation to the spherical crown radius (Figure 23). Within the species of small-leaved lime, the growing location as well had no significant effect on the relation between density quantile and its mean relative distance from the crown center. Black locust however, displayed a significant role of the respective growing location in the density quantile-distance relation.

5. Discussion

This thesis highlights the many facets of tree morphology and the conditions affecting them. The included studies span across a variety of aspects in regards to structure. Detailed measurements of crown parameters from simple convex hulls down to surface properties, density distribution within the crown, to structural attributes at branch level as well as repeated observations of dynamic processes and the according structural responses have been investigated. In order to achieve this, extensive methodological developments in the field of the analysis of terrestrial laser scanner data of forest and urban trees have been carried out.

5.1. Intra- and interspecific competition and crown structure

Spruce and beech embody rather different species in terms of functional and structural attributes. Spruce is a quick, vertically oriented but comparatively unplastic species, while beech is a slow, rather laterally oriented and very plastic species. A combination of such complementary species leads to a meaningful modification of the canopy structure compared to pure stands, which might produce the particular broad intraspecific plasticity not known from pure stands. Other common species combinations such as oak/beech, pine/beech, eucalypt/acacia, populus/white spruce for example, represent similarly diverse structural and functional stands and might display comparable crown plasticity in inter- versus intraspecific environments (Bauhus et al. 2004).

Differing crown structures of European beech and Norway spruce have already been subject of detailed analysis (Assmann 1961; Droste zu Hülshoff 1969; Pretzsch and Schütze 2005). Research article I of this thesis (Bayer et al. 2013) however, focuses on variation and additional information on parameters such as branch angles not only between species but the disparities between pure and mixed stands as well (Figure 24). Intra- and interspecific crown plasticity in regards to mixture has hardly been elucidated so far (Purves et al. 2007; Richards et al. 2010). The revealed crown development of
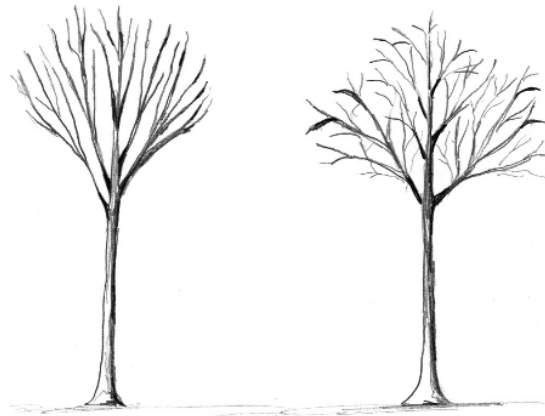
44

Figure 24.: Schematic drawing of the qualitative differences between individual European beech trees growing in **(l)** pure and **(r)** mixed-species stands found by Bayer et al. (2013)

mixed stands is beyond the known range of pure stands. It therefore indicates structural crown attributes emerging from interspecific environments.

The competition of beech versus spruce through shallower branch angles, wider crown extension and denser space filling in interspecific versus intraspecific neighborhoods might be favored in two different ways. Namely by accessing contested resources and blocking the approaches of neighbors by effective shading and space occupation. Increased structural crown plasticity and more structural complexity within the canopy results in a higher variability of environmental conditions. This in return triggers the plasticity at organ, crown or tree level in order to optimally capture resources or acclimate to competing neighbors and the resulting altered environment. As a result of the interaction between growth, structure and local environment, the structural variability affects interspecific competition, production as well as structural diversity and biodiversity.

The results of research paper I suggest, that European beech features significantly higher variability in terms of branch angles and lateral branch extension in mixture. This strengthens beech's ability to increase growing space and may contribute to explaining, why under interspecific competition with spruce, beech is able to penetrate and occupy crown space very efficiently while commiting only to relativeley low biomass investments (Pretzsch and Schütze 2005). Organs such as branches, twigs and leaves are responsible for a considerable share of a tree's productivity. Therefore, structural

variation may not only have an effect on the filling of canopy space but the efficiency of tree crowns in terms of biomass production per unit of crown projection area and year. The competitive strength regarding resource exploitation may be affected as well (Matyssek et al. 2005).

Its plasticity regarding lateral crown expansion prevents Norway spruce from being out-competed by beech, drives it into higher canopy layers where less shading is prevalent and light may be captured easily and efficiently. This reaction may contribute to the understanding of over-yielding of spruce when grown in mixture with beech (Pretzsch 2009; Pretzsch et al. 2010). Combinations of Norway spruce and European beech may achieve an average over-yielding of about 20 % in relation to the respective pure stands (Pretzsch et al. 2010). Because improvements of soil properties caused by mixture are not as beneficial to European beech as they are to spruce, the over-yielding of beech is supposedly related to differing crown structure attributes such as those found by research paper I.

Besides productivity, the structural richness found in tree crowns plays an important role in habitat formation and its effect on biodiversity. The habitat heterogenity hypothesis suggests that increased complexity induces increased species diversity by providing more niches and opportunities to exploit environmental resources (e.g. MacArthur and MacArthur 1961; Bazzaz 1975). Animal species, regarding their distribution and interaction, are often affected by the plant community of its habitat which usually provides a majority of the physical structure of the environment (Lawton 1983; McCoy and Bell 1991). The majority of studies about habitat heterogeneity found positive correlations between plant species diversity and structural complexity of the habitat defined by attributes such as branching patterns of tree crowns (Tews et al. 2004). Mixed species stands might therefore not only be beneficial to animal species diversity because of plant species diversity but as well by the potentially increased structural complexity of the habitat forming trees themselves.

5.2. TLS validation of structural-functional tree models

Research paper II (Beyer et al. 2017a) is a special case regarding the fact that it was mainly written in order to validate the functional-structural tree model presented by Beyer et al. (2017c). It is however, a valuable contribution because it demonstrated how TLS data

can be incorporated and used for the thorough investigation of functional-structural growth models.

Especially considering the potential TLS imagery offers in terms of detailed tree morphology and structure, growth modelers might benefit from working closely together with LiDAR practitioners. Eventually, novel spatially explicit empirical data might become a solid basis for growth model parameter estimations. Further technical advancements in LiDAR technology are still required to make it more accessible, practicable and efficient. Simultaneously, more development and progress in TLS data processing and interpretation algorithms such as those developed and applied in the scope of this thesis continue to be necessary.

5.3. Forest gap structure and dynamics

Size-asymmetric competition caused by larger individuals claiming disproportionate shares of the contested resources and thus supressing less competitive neighbors is a common occurrence in plant communities (Schwinning and Weiner 1998; Weiner and Damgaard 2006). In temperate forest stands, where the primary limit to tree growth often is light availability, the existence of taller trees with their according high potential for light interception often cause such a size-asymmetric competition (Wichmann 2002). Seeing that the actual availability and distribution of resources, for example light, within the canopy space are hard to measure, space functions as an important abstraction for above-ground resources. Following this, some authors argue that space may be thought-about as a resource itself (Grams and Lüttge 2011).

Shape, size and abundance of openings in the canopy thus are essential regarding the mechanisms of stand dynamics. Assuming a 3% annual rate of tree loss caused by thinning or mortality results in the formation of an open gap area of 300 $m^2/ha/year$. Let's further assume a rotation period of 100 years. Over this amount of time, the temporal gap areas caused by this drop-out process amount to about 30,000 m^2 or 300% of the actual stand area (Pretzsch 2014). Repeatedly, the growing space is released, contested, occupied and released again due to the dynamics of mortality and thinning as well as the recapturing of the most competitive induviduals (Bauhus 2009). Beginning with several thousand planted - or even millions if naturally regenerated - individual trees taking part in the process of competing for space and the involved capturing and recapturing, only about 50 to 100 trees per ha finally form a mature stand. Species

characterized by high crown plasticity are able to occupy these ever-emerging gaps faster and more thoroughly than less plastic competitors. Especially predominantly mono-layered stands undergo a constant opening and following closure by crown extension in the canopy. Crown and thus gap size as well, increases with tree age. Because the filling of larger gaps by adjacent trees is more time consuming, the reoccupation of space becomes more sluggish with increasing stand age. Even in an un-thinned mono-layered stand with pure species composition, 5 - 15% of the total stand area remains open (Wiedemann 1951). Individual tree growth in temperate forests is often light-limited. Gaps are closed faster above-ground than below-ground, the corresponding vacancies in the root space can finally be covered by root extension (Bauhus 2009). Individuals displaying the highest crown plasticity are able to gain more additional space by faster and wider ranging gap occupation and consequently better resource capture and higher competitive strength. Sudden and abrupt gap emergence caused by thinning for example, favor species capable of quick and far-reaching occupation. Vacancies in the canopy produced by mortality in contrast, emerge rather continuously and are under slow and steady occupation by neighbors already in advance of the tree's death.

The findings of research paper III (Bayer and Pretzsch 2017) suggest, that the mixture of the gap (mixed or pure) has no significant impact on the observed reactions of Norway spruce and European beech. Obviously, the mechanisms of intra- and inter-specific competition are important drivers of stand development, structure as well as functions and processes of forest stands (Hari 1985; Pretzsch 2009). In the case of gaps located in stands where light availability constitutes the main limitation to growth however, the abrupt abundance of free above-ground resources may likely overshadow any potential mixing effects between the two species at least during the initial years of reoccupation. Both species displayed rather opposing reactions to the emergence of the gaps. For Norway spruce the results indicate no shifts in resource allocation. However, space exploitation and biomass investment efficiencies are increased during the first two years after gap emergence. In conclusion, Norway spruce's development is mainly characterized by increased *dbh* growth and hardly any substantial morphological adaptions. Asymmetry of lateral growth is existent, however it develops slowly, so that statistical significant differences between observations was only given after for the first

and last observation. Due to conifers' low directional growth towards light, this was not unexpected (Muth and Bazzaz 2002; Seidel et al. 2016).

European beech in contrast, displayed fast lateral crown expansion followed by a sharp decrease in crown size during the first two years after the gap creation. From the available data, the decrease could not be attributed to a specific cause with certainty. It seems likely, that the crown retreat was caused by one or several weather events, resulting in mechanical damage. However it is conceivable that, as a result of the rapid initial crown expansion and the following increase in competition, mechanical abrasion between crowns contributed to the loss of crown mass. According to some authors, abrasion might even be one of the substantial drivers of above ground competition (Franco 1986; Hajek et al. 2015). Overall, the high plasticity of European beech resulted in meaningful morphological reactions to the emergence of gaps. The investigated allocation ratios showed a strong bias towards lateral crown expansion immediately after the gap creation. In conclusion, the individual tree dynamics of European beech with its rapid closing approach suggests resource allocation heavily in favor of space occupation and its associated competitive effects, even to the cost of reduced DBH and biomass growth initially.

European beech obtains much of its exceptional competitive strength in most of Central Europe's natural forest systems from its morphological adaption capabilities (Dieler and Pretzsch 2013; Bayer et al. 2013) as well as the fast and efficient ability to occupy free canopy space it demonstrated in the study of research paper III (Bayer and Pretzsch 2017). In this context, beech is not only able to secure above-ground resources for itself, but also to exclude competitors from accessing the same resources and to hold back potential future competitors from the undersoty (Pretzsch and Schütze 2009). Quick and thorough exploitation of growing space by fast crown expansion is favorable in regards to future growth and yield potential. However, negative economic effects of large crowns, especially on tree value have to be considered. Lower crown base, knottiness, stem-bending, tree-ring width irregularities for instance, are often economically detrimental side-effects of structurally complex stands (Macdonald et al. 2010; Pretzsch and Rais 2016). Similarly to individual tree structures, the size and structure of crowns and gaps and their development over time also determine habitat formation. Opposed to trees developing in the stand interior under relatively regular spacing, individual trees growing at the borders of stands or gaps develop different

49

crown shapes. Plastic species especially, develop asymmetric crown shapes, longer and often more irregularly shaped branches and lower crown base heights. The larger set of varying habitat structures may enable particular animal species to inhabit a stand which would otherwise not be suitable (North et al. 1999; Hinsley et al. 2009; Müller et al. 2012).

5.4. Urban tree structure and ecosystem functions and services

Spiritual, moral and aesthetic values are often influenced by the urban environment (Chiesura 2004; Tyrväinen et al. 2005). Thus, green spaces are an important aspect of social and cultural values within cities (Chan et al. 2012). Beneficial effects on physical and mental health, social cohesion, as well as multitude of recreational opportunities may enhance the overall quality of life in urban areas (Gómez-Baggethun and Barton 2013; Livesley et al. 2016). Most, if not all contributions of urban trees to these benefits can directly or indirectly be related to structure.

Regarding temperature regulation and shading for example, the results of research paper IV (Bayer et al. 2017) show that small-leaved lime featured larger crown volumes than black locust at comparable tree sizes. Black locust displayed larger crown projection areas per m^3 of crown volume. Small-leaved lime however, is known to feature denser crowns as well and therefore promotes an overall stronger shading effect. Additionally, with its higher leaf area, small-leaved lime is able to produce a stronger average cooling effect through evapotranspiration than black locust (Moser et al. 2015; Rahman et al. 2017). Both species did not show significant differences in terms of structure in relation to growing location.

Windspeed is one of the most important factors for pedestrian comfort in urban landscapes. Next to buildings, trees are among the largest objects in those environments. Hence, trees are stationary subgrid-scale obstacles within the turbulent wind-flowfield of street canyons (Mochida et al. 2008; Mochida and Lun 2008). Crown size and inner structure define an individual tree's effect as an obstacle to wind (Roodbaraky et al. 1994; Stathopoulos 2006). For the mitigation of strong winds, small-leaved lime might be more effective than black locust. Its larger crowns as well as its in comparison lower, and therefore closer to pedestrian levels, crown center make it a sensible choice for wind exposed locations such as town squares.

Small-leaved lime with its larger and denser crowns in comparison to black locust (Moser et al. 2015) has the higher potential for rain interception. However, under space

restrictions, black locust with its ability to cover more ground area per m^3 of crown volume while maintaining comparably smaller crowns, might be a better choice for rain sheltering.

Structurally, black locust has a higher potential for air purification than small-leaved lime. Its more complex crown surfaces in combination with a more complex leaf morphology provide good prerequisites for efficient filtering of air pollutants. Furthermore, the lower LAI values of black locust compared to small-leaved lime are likely beneficial for its air purification potential as well. The inner crown's wind speed is not reduced as much and therefore the turbulent decomposition of atmospheric particles through impaction is not inhibited as much (Hofman et al. 2014) in the case of black locust. The differences found in crown surface complexity in relation to growing location suggest, that black locust features the highest purification potential in parks, followed by town squares with the least potential in street canyons.

Black locust displayed more complex crown surfaces than small-leaved lime. The highest complexity was found in parks where animal sighting often contributes to the desired recreational value. High crown complexity means a larger abundance of concavities and gaps in the crown periphery and thus a larger abundance of potential habitats (Müller et al. 2012; Blakey et al. 2017).

Next to the numerous benefits urban trees are able to provide, some ecosystem disservices have to be considered as well (Lyytimäki and Sipilä 2009). These negative aspects are often neglected in the assessment of urban tree effects on the environment. Among the disservices related to tree structure are mechanical damage to pavements by rooting activities, the blocking of views (Lyytimäki et al. 2008), the corrosion of buildings caused by bird excrements or animal digging related to the habitat-forming aspects of tree structure (De Stefano and Deblinger 2005; Lyytimäki and Sipilä 2009), for example. The provision of certain habitats may also result in an abundance of species like rats, wasps, pigeons or mosquitoes, which are perceived as pests by a many people and may take part in the transmission of diseases. Furthermore, several health issues may be caused or enhanced by allergenic pollen (Dales et al. 2008; Cariñanos and Casares-Porcel 2011). The allergenicity values of wind-pollinated species might be affected by structural attributes determining their wind interaction and crown permeablility (Cariñanos et al. 2016).

6. Conclusion

By the combination of voxel based, α-shape based, and skeletonization based evaluations of TLS data, novel insights into structural tree attributes could be acquired within the scope of the research articels this dissertation is based on. The specifically developed methods have been applied to the intra- and interspecific variations of crown structure in forest stands, to forest gaps as well as their dynamics over several years and to the individual tree structure of urban trees. The results were discussed in regards to their implications for the respective study's subject in order to contribute to a better understanding of the feedback loop between structure and function and its implications. To what extent the findings of the research papers this dissertation is based on, can be transferred to other species, stands or cities is subject to further research.

Terrestrial laser scanning has been shown to be highly suitable for non-destructive, high precision measurements of tree and stand structure. Many of the measured parameters are novel and hardly - in some cases not at all - obtainable with classical dendrometrical measurement methods. Today's, and even more so future LiDAR devices have tremendous potential. Full-waveform or drone-based devices for example, continue to improve as do methodologies for data evaluation and the extraction of novel information for a more comprehensive understanding of tree and stand structure.

Literature

Akbari, H. (2005). Energy Saving Potentials and Air Quality Benefits of Urban Heat Island Mitigation. *Sol Energy*, 1–19.

Akbari, H., Pomerantz, M. and Taha, H. (2001). Cool surfaces and shade trees to reduce energy use and improve air quality in urban areas. *Sol Energy* 70.(3), 295–310.

Assmann, E. (1961). Waldertragskunde. Organische Produktion, Struktur, Zuwachs und Ertrag von Waldbeständen. BLV Verlagsgesellschaft, München.

Assmann, E. (1970). The principles of forest yield study. Pergamon Press, Oxford, New York, 506p.

Aylor, D. (1972). Noise reduction by vegetation and ground. *J Acoust Soc Am* 51, 197–205.

Badoux, E. (1946). Krone und Zuwachs. *Mitt Schweiz Anst Forstl Versuchswesen* 24.(2), 405–513.

Bauhus, J., Winden, A. P. van and Nocotra, A. B. (2004). Above-ground interactions and productivity in mixed-species plantations of Acacia mearnsii and Eucalyptus globulus. *Can J For Res* (34), 686–694.

Bauhus, J. (2009). Rooting Patterns of Old-Growth Forests: is Aboveground Structural and Functional Diversity Mirrored Belowground? In: *Old-Growth Forests: Function, Fate and Value*. Ed. by C. Wirth, G. Gleixner and M. Heimann. Berlin, Heidelberg: Springer Berlin Heidelberg, 211–229.

Bayer, D. and Pretzsch, H. (2017). Reactions to gap emergence: Norway spruce (*Picea abies* [L.] Karst.) increases growth while European beech (*Fagus sylvatica* L.) features horizontal space occupation – evidence by repeated 3D TLS measurements. *Silva Fennica* 51.(5), article id 7748.

Bayer, D., Seifert, S. and Pretzsch, H. (2013). Structural crown properties of Norway spruce (Picea abies [L.] Karst.) and European beech (Fagus sylvatica [L.]) in mixed versus pure stands revealed by terrestrial laser scanning. *Trees* 27 (4), 1035–1047.

Bayer, D., Pretzsch, H., Moser, A. and Rötzer, T. (2017). Structural response of black locust (Robinia pseudoacacia L.) and small-leaved lime (Tilia cordata Mill.) to varying ur-

ban environments analyzed by terrestrial laser scanning. Implications for ecological functions and services. *Urban Forestry & Urban greening* under review.

Bazzaz, F. (1975). Plant species diversity in old-field successional ecosystems in southern Illinois. *Ecology* 56, 485–488.

Beyer, R., Bayer, D., Letort, V., Pretzsch, H. and Cournède, P.-H. (2017a). Validation of a functional-structural tree model using terrestrial Lidar data. *Ecol Modell* 357, 55–57.

Beyer, R., Bayer, D., Pretzsch, H. and Cournède, P.-H. (2017b). Reconstructing minimal length tree branch systems from leaf positions. *Ecological Informatics* 42.(Supplement C), 61–66.

Beyer, R., Letort, V., Bayer, D., Pretzsch, H. and Cournède, P.-H. (2017c). Leaf density-based modelling of phototropic crown dynamics and long-term predictive application to European beech. *Ecol Modell* 347, 63–71.

Binkley, D., Stape, J. L. and Ryan, M. G. (2004). Thinking about efficiency of resource use in forests. *For Ecol Manage* 193, 5–16.

Blakey, R. V., Law, B. S., Kingsford, R. T. and Stoklosa, J. (2017). Terrestrial laser scanning reveals below-canopy bat trait relationships with forest structure. *Remote Sensing of Environment* 198, 40–51.

Bolund, P. and Hunhammar, S. (1999). Ecosystem services in urban areas. *Ecol Econ* 29.(2), 293–301.

Bremer, M., Jochem, A. and Rutzinger, M. (2012). Comparison of branch extraction for deciduous single trees in leaf-on and leaf-off conditions – an eigenvector based approach for terrestrial laser scanning point clouds. In: vol. 11, 33-43. (1/2012). EARSeL eProceedings, 33–43.

Bucksch, A., Lindenbergh, R. and Menenti, M. (2010). SkelTre - Robust skeleton extraction from imperfect point clouds. *The Visual Computer* 26.(10), 1283–1300.

Bucksch, A. K. (2011). Revealing the skeleton from imperfect point clouds. Dissertation. PhD Thesis at Delft University of Technology.

Buddle, C. M., Langor, D. W., Pohl, G. R. and Spence, J. R. (2006). Arthropod responses to harvesting and wildfire: implications for emulation of natural disturbance in forest management. *Biol Conserv* 128.(3), 346–357.

Burger, H. (1939). Holz, Blattmenge und Zuwachs. *Mitt Schweiz Anst Forstl Versuchswesen 1939-1953* vol 15-29.

Burschel, P. and Huss, J. (1997). Grundriss des Waldbaus. Parey, Berlin.

Cariñanos, P., Adinolfi, C., Guardia, C. D. de la, Linares, C. D. and Casares-Porcel, M. (2016). Characterization of Allergen Emission Sources in Urban Areas. *J. Environ. Qual.* 45, 244–252.

Cariñanos, P. and Casares-Porcel, M. (2011). Urban green zones and related pollen allergy: A review. Some guidelines for designing spaces with low allergy impact. *Landscape and Urban Planning* 101.(3), 205–214.

Chan, K., Satterfield, T. and Goldstein, J. (2012). Rethinking ecosystem services to better address and navigate cultural values. *Ecol Econ* 74, 8–18.

Chiesura, A. (2004). The role of urban parks for the sustainable city. *Landscape Urban Plann* 68, 129–138.

Côté, J.-F., Fournier, R. A. and Egli, R. (2011). An architectural model of trees to estimate forest structural attributes using terrestrial LiDAR. *Environ Modell Softw* 26.(6), 761–777.

Dales R, E., S, C., S, J. and F, C. (2008). Tree Pollen and Hospitalization for Asthma in Urban Canada. *Int Arch Allergy Immunol* 146, 241–247.

De Stefano, S. and Deblinger, R. (2005). Wildlife as valuable natural resources vs intolerable pests: a suburban wildlife management mode. *Urban Ecosystems* 8, 131–137.

Dieler, J. and Pretzsch, H. (2013). Morphological plasticity of European beech (Fagus sylvatica L.) in pure and mixed-species stands. *For Ecol Manage* 295, 97–108.

Drössler, L., Feldmann, E., Glatthorn, J., Annighöfer, P., Kucbel, S. and Tabaku, V. (2016). What Happens after the Gap ?— Size Distributions of Patches with Homogeneously Sized Trees in Natural and Managed Beech Forests in Europe. *Open Journal of Forestry* 6.(June), 177–190.

Droste zu Hülshoff, B. von (1969). Struktur und Biomasse eines Fichtenbestandes auf Grund einer Dimensionsanalyse an oberirdischen Baumorganen. PhD thesis. LMU München.

DWD (2015). *Deutscher Wetterdienst*.

Edelsbrunner, H., Kirkpatrick, D. G. and Seidel, R. (1983). On the shape of a set of points in the plane. *IEEE T Inform Theory* 29, 551–559.

Edelsbrunner, H. and Mücke, E. P. (1994). Three-Dimensional Alpha Shapes. *ACM Trans. Graphics* 13.(1), 43–72.

55

Enquist, B. J., Brown, J. H. and West, G. B. (1998). Allometric scaling of plant energetics and population density. *Nature* 395.(6698), 163–165.

Escobedo, F. and Nowak, D. (2009). Spatial heterogeneity and air pollution removal by an urban forest. *Landscape Urban Plann* 90, 102–110.

Fang, C.-F. and Ling, D.-L. (2003). Investigation of the noise reduction provided by tree belts. *Landscape Urban Plann* 63, 187–195.

Franco, M. (1986). The Influences of Neighbours on the Growth of Modular Organisms with an Example from Trees. *Philosophical Transactions of the Royal Society of London B: Biological Sciences* 313.(1159), 209–225.

Goetz, S. J., Steinberg, D., Betts, M. G., Holmes, R. T., Doran, P. J., Dubayah, R. and Hofton, M. (2010). Lidar remote sensing variables predict breeding habitat of a Neotropical migrant bird. *Ecology* 91.(6), 1569–1576.

Gómez-Baggethun, E. and Barton, D. N. (2013). Classifying and valuing ecosystem services for urban planning. *Ecol Econ* 86, 235–245.

Grams, T. E. E. and Lüttge, U. (2011). Space as a Resource. In: *Progress in Botany 72*. Ed. by E. U. Lüttge, W. Beyschlag, B. Büdel and D. Francis. Berlin, Heidelberg: Springer Berlin Heidelberg, 349–370.

Hackenberg, J., Spiecker, H., Calders, K., Disney, M. and Raumonen, P. (2015). SimpleTree —An Efficient Open Source Tool to Build Tree Models from TLS Clouds. *Forests* 6.(11), 4245–4294.

Hajek, P., Seidel, D. and Leuschner, C. (2015). Mechanical abrasion, and not competition for light, is the dominant canopy interaction in a temperate mixed forest. *For Ecol Manage* 348, 108–116.

Hardin, P. J. and Jensen, R. R. (2007). The effect of urban leaf area on summertime urban surface kinetic temperatures: A Terre Haute case study. *Urban Forestry & Urban Greening* 6.(2), 63–72.

Hari, P. (1985). "Theoretical aspects of eco-physiological research". In: *Crop physiology of forest trees*. Ed. by P. M. A. Tigerstedt, P. Puttonen and V. Koski. Helsinki Univ Press, Helsinki, pp. 21–30.

Higgens, S., Turpie, J., Costanza, R., Cowling, R., Le Maitre, D., Marais, C. and Midgley, G. (1997). An ecological simulation model of mountain fynbos ecosystems: dynamics, valuation and management. *Ecol Econ* 22, 155–169.

Hilker, T., Leeuwen, M. van, Coops, N., Wulder, M., Newnham, G., Jupp, D. and Culvenor, D. (2010). Comparing canopy metrics derived from terrestrial and airborne laser scanning in a Douglas-fir dominated forest stand. *Trees* 24.(5), 819–832.

Hinsley, S. A., Hill, R. a. R. A., Fuller, R., Bellamy, P. E. and Rothery, P. (2009). Bird species distributions across woodland canopy structure gradients. *Community Ecology* 10.(1), 99–110.

Hofman, J., Bartholomeus, H., Calders, K., Wittenberghe, S. V., Wuyts, K. and Samson, R. (2014). On the relation between tree crown morphology and particulate matter deposition on urban tree leaves: A ground-based LiDAR approach. *Atmospheric Environment* 99, 130–139.

Huang, P. and Pretzsch, H. (2010). Using terrestrial laser scanner for estimating leaf areas of individual trees in a conifer forest. *Trees* 24.(4), 609–619.

Kragh, J. (1981). Road traffic noise attenuation by belts of trees. *J Sound Vib* 74, 235–241.

Kuuluvainen, T. and Grenfell, R. (2012). Natural disturbance emulation in boreal forest ecosystem management—theories, strategies, and a comparison with conventional even-aged management. *Can J For Res* 42.(7), 1185–1203.

Lawton, J. H. (1983). Plant Architecture and the Diversity of Phytophagous Insects. *Annu. Rev. Entomol.* 28, 23–39.

Leeuwen, M. van, Hilker, T., Coops, N. C., Frazer, G., Wulder, M. a., Newnham, G. J. and Culvenor, D. S. (2011). Assessment of standing wood and fiber quality using ground and airborne laser scanning: A review. *For Ecol Manage* 261.(9), 1467–1478.

Leeuwen, M. van and Nieuwenhuis, M. (2010). Retrieval of forest structural parameters using LiDAR remote sensing. *Eur J Forest Res* 129, 749–770.

Lertzmann, K. P., Sutherland, G. D., Inselberg, A. and Saunders, S. (2015). Canopy gaps and the landscape mosaic in a coastal temperate rain forest. *Statewide Agricultural Land Use Baseline 2015* 1.(4), 1254–1270. arXiv: `arXiv:1011.1669v3`.

Livesley, S. J., McPherson, E. G. and Calfapietra, C. (2016). The Urban Forest and Ecosystem Services: Impacts on Urban Water, Heat, and Pollution Cycles at the Tree, Street, and City Scale. *J Environ Qual* 45, 119–124.

Lyytimäki, J., Kjerulf Petersen, L., Normander, B. and Bezák, P. (2008). Nature as nuisance? Ecosystem services and disservices to urban lifestyle. *Environnemental Sciences* 5, 161–172.

Lyytimäki, J. and Sipilä, M. (2009). Hopping on one leg—the challenge of ecosystem disservices for urban green management. *Urban Forestry & Urban Greening* 8, 309–315.

MacArthur, R. and MacArthur, J. (1961). On bird species diversity. *Ecology* 42, 594–598.

Macdonald, E., Gardiner, B. and Mason, W. (2010). The effects of transformation of even-aged stands to continuous cover forestry on conifer log quality and wood properties in the UK. *Forestry* 83.(1), 1–16.

Mandelbrot, B. (1967). How Long Is the Coast of Britain? Statistical Self-Similarity and Fractional Dimension. *Science* 156, 636–638.

Mandelbrot, B. (1983). The Fractal Geometry of Nature. W.H. Freeman and Co.

Maneewongvatana, S. and Mount, D. M. (1999). It's okay to be skinny, if your friends are fat. In: *Proceedings of the 4th Annual CGC Workshop on Computational Geometry*.

Matyssek, R., Agerer, R., Ernst, D., Munch, J.-C., Oßwald, W., Pretzsch, H., Priesack, E., Schnyder, H. and Treutter, D. (2005). The Plant's Capacity in Regulating Resource Demand. *Plant Biology* 7.(6), 560–580.

McCoy, E. D. and Bell, S. S. (1991). "Habitat structure: The evolution and diversification of a complex topic". In: *Habitat Structure: The physical arrangement of objects in space*. Ed. by S. S. Bell, E. D. McCoy and H. R. Mushinsky. Dordrecht: Springer Netherlands, pp. 3–27.

Metz, J., Seidel, D., Schall, P., Scheffer, D., Schulze, E. D. and Ammer, C. (2013). Crown modeling by terrestrial laser scanning as an approach to assess the effect of above-ground intra- and interspecific competition on tree growth. *For Ecol Manage* 310, 275–288.

Mochida, A. and Lun, I. Y. (2008). Prediction of wind environment and thermal comfort at pedestrian level in urban area. *J Wind Eng Ind Aerodyn* 96.(10-11), 1498–1527.

Mochida, A., Tabata, Y., Iwata, T. and Yoshino, H. (2008). Examining tree canopy models for CFD prediction of wind environment at pedestrian level. *J Wind Eng Ind Aerodyn* 96.(10-11), 1667–1677.

Moser, A., Rötzer, T., Pauleit, S. and Pretzsch, H. (2015). Structure and ecosystem services of small-leaved lime (Tilia cordata Mill.) and black locust (Robinia pseudoacacia L.) in urban environments. *Urban Forestry and Urban Greening* 14.(4), 1110–1121.

Mueller-Dombois (1991). "The mosaic theory and the spatial dynamics of natural dieback and regeneration in Pacific forests". In: *The mosaic-cycle concept of ecosystems*. Springer Berlin / Heidelberg, pp. 46–60.

Müller, J., Mehr, M., Bässler, C., Fenton, M. B., Hothorn, T., Pretzsch, H., Klemmt, H.-J. and Brandl, R. (2012). Aggregative response in bats: Prey abundance versus habitat. *Oecologia* 169.(3), 673–684.

Muth, C. C. and Bazzaz, F. a. (2002). Tree canopy displacement at forest gap edges. *Can J For Res* 32.(2), 247–254.

Niklas, K. J. (1994). Plant Allometry. Univ Chicago Press, Chicago, IL.

North, M. P., Franklin, J. F., Carey, A. B., Forsman, E. D. and Hamer, T. (1999). Forest stand structure of the northern spotted owl's foraging habitat. *Forest Science* 45.(4), 520–527.

Nowak, D. J. (1996). Estimating leaf area and leaf biomass of open-grown deciduous urban trees. *Forest Science* 42.(Walton), 504–507.

Nowak, D. (1994). Air pollution removal by Chicago's urban forest. In McPherson, E.G., Nowak, D.J., Rowntree, R.A.(eds): Chicago's urban forest ecosystem: results of the Chicago Urban Forest Climate Project. Gen. Tech. Rep. NE-186. U.S. Department of Agriculture, Forest Service, Northeastern Forest Experiment Station, Radnor PA. Chap. Air pollution removal by Chicago's urban forest, pp. 63–81.

Oldeman, R. A. (1990). Forests: Elements of Silvology. Springer Verlag, Berlin.

Pataki, D., Carreiro, M., Cherrier, J., Grulke, N., Jennings, V., Pincetl, S., Pouyat, R., Whitlow, T. and Zipperer, W. (2011). Coupling biogeochemical cycles in urban environments: ecosystem services, green solutions, and misconceptions. *Front Ecol Environ* 9, 27–36.

Pateiro-López, B. and Rodríguez-Casal, A. (2010). Generalizing the convex hull of a sample: The R package alphahull. *Journal of Statistical Software* 5, 1–28.

Pauleit, S., Jones, N., Garcia-Martin, G., Garcia-Valdecantos, J. L., Rivière, L. M., Vidal-Beaudet, L., Bodson, M. and Randrup, T. B. (2002). Tree establishment practice in towns and cities – results from a european survey. *Urban Forestry and Urban Greening* 1, 83–96.

Potapov, I., Järvenpää, M., Åkerblom, M., Raumonen, P. and Kaasalainen, M. (2016). Data-based stochastic modeling of tree growth and structure formation. *Silva Fennica* 50.(1), article id 1413.

Pretzsch, H. (1992). Modellierung der Kronenkonkurrenz von Fichte und Buche in Rein- und Mischbeständen. *AFJZ* 163.(11/12), 203–213.

Pretzsch, H. (2006). Species-specific allometric scaling under self-thinning: Evidence from long-term plots in forest stands. *Oecologia* 146.(4), 572–583.

Pretzsch, H. (2009). Forest dynamics, growth and yield, From measurement to model. Springer, Berlin, Heidelberg.

Pretzsch, H., Block, J., Dieler, J., Dong, P., Kohnle, U., Nagel, J., Spellmann, H. and Zingg, A. (2010). Comparison between the productivity of pure and mixed stands of Norway spruce and European beech along an ecological gradient. *Ann For Sci* 67.(7), 712.

Pretzsch, H. and Schütze, G. (2005). Crown Allometry and Growing Space Efficiency of Norway Spruce (Picea abies [L.] Karst.) and European Beech (Fagus sylvatica L.) in Pure and Mixed Stands. *Plant Biology* 7.(6), 628–639.

Pretzsch, H. and Schütze, G. (2009). Transgressive overyielding in mixed compared with pure stands of Norway spruce and European beech in Central Europe: evidence on stand level and explanation on individual tree level. *Eur J Forest Res* 128.(2), 183–204.

Pretzsch, H. (2003). Diversität und Produktivität von Wäldern. *AFJZ* 174, 88–98.

Pretzsch, H. (2014). Canopy space filling and tree crown morphology in mixed-species stands compared with monocultures. *For Ecol Manage* 327, 251–264.

Pretzsch, H., Biber, P., Uhl, E. and Dauber, E. (2015). Long-term stand dynamics of managed spruce-fir-beech mountain forests in Central Europe: Structure, productivity and regeneration success. *Forestry* 88.(4), 407–428.

Pretzsch, H. and Rais, A. (2016). Wood quality in complex forests versus even-aged monocultures: review and perspectives. *Wood Sci Technol* 50.(4), 1–36.

Pretzsch, H., Seifert, S. and Huang, P. (2011). Beitrag des terrestrischen Laserscannings zur Erfassung der Struktur von Baumkronen. *Schweiz. Z. Forstwes.* 162, 186–194.

Price, C. A., Gilooly, J. F., Allen, A. P., Weitz, J. S. and Niklas, K. J. (2010). The metabolic theory of ecology: prospects and challenges for plant biology. *New Phytol.* 188.(3), 696–710.

Puettmann, K. J., Coates, K. D. and Messier, C. C. (2012). A critique of silviculture: managing for complexity. *Island Press, Washington, Coveolo, London.*

Purves, D. W., Lichstein, J. W. and Pacala, S. W. (2007). Crown Plasticity and Competition for Canopy Space: A New Spatially Implicit Model Parameterized for 250 North American Tree Species. *PLoS One* 2.(9), e870.

Quine, C. P. and Gardiner, B. A. (2007). Understanding how the interaction of wind and trees results in wind- throw, stem breakage, and canopy gap formation. Elsevier, Amsterdam, pp. 103–156.

Rahman, M. A., Moser, A., Rötzer, T. and Pauleit, S. (2017). Microclimatic differences and their influence on transpirational cooling of Tilia cordata in two contrasting street canyons in Munich, Germany. *Agric For Meteorol* 232, 443–456.

Ramachandran, P. and Varoquaux, G. (2008). Mayavi: Making 3D Data Visualization Reusable. In: *Proceedings of the 7th Python in Science Conference*. Ed. by G. Varoquaux, T. Vaught and J. Millman. Pasadena, CA USA, 51–56.

Remmert, H. (1991). The mosaic-cycle concept of ecosystems — an overview. Springer, Berlin, Heidelberg, pp. 1–21.

Richards, A. E., Forrester, D. I., Bauhus, J. and Scherer-Lorenzen, M. (2010). The influence of mixed tree plantations on the nutrition of individual species: a review. *Tree Physiol.* 30.(9), 1192–1208.

Röhle, H. and Huber, W. (1985). Untersuchungen zur Methode der Ablotung von Kronenradien und der Berechnung von Kronengrundflächen. *Forstarchiv* 56.(6), 238–243.

Roloff, A. (2001). Baumkronen: Verständnis und praktische Bedeutung eines komplexen Naturphänomens. Ulmer, Stuttgart.

Roodbaraky, H., Baker, C., Dawson, A. and Wright, C. (1994). Experimental observations of the aerodynamic characteristics of urban trees. *J Wind Eng Ind Aerodyn* 52, 171–184.

Schwinning, S. and Weiner, J. (1998). Mechanisms determining the degree of size asymmetry in competition among plants. *Oecologia* 113.(4), 447–455.

Seidel, D., Hoffmann, N., Ehbrecht, M., Juchheim, J. and Ammer, C. (2015). How neighborhood affects tree diameter increment - New insights from terrestrial laser scanning and some methodical considerations. *For Ecol Manage* 336, 119–128.

Seidel, D., Leuschner, C., Müller, A. and Krause, B. (2011). Crown plasticity in mixed forests—Quantifying asymmetry as a measure of competition using terrestrial laser scanning. *For Ecol Manage* 261.(11), 2123–2132.

Seidel, D., Ruzicka, K. J. and Puettmann, K. (2016). Canopy gaps affect the shape of Douglas-fir crowns in the western Cascades, Oregon. *For Ecol Manage* 363, 31–38.

Seifert, T. (2003). Integration von Holzqualität und Holzsortierung in behandlungssensitive Waldwachstumsmodelle. PhD thesis. Technische Universität München.

Stathopoulos, T. (2006). Pedestrian level winds and outdoor human comfort. *J. Wind Eng. Ind. Aerodyn.* 94.(11), 769–780.

Tews, J., Brose, U., Grimm, V., Tielbörger, K., Wichmann, M. C., Schwager, M. and Jeltsch, F. (2004). Animal species diversity driven by habitat heterogeneity/diversity: the importance of keystone structures. *J Biogeogr* 31.(1), 79–92.

Tyrväinen, L., Pauleit, S., Seeland, K. and Vries, S. de (2005). Benefits and uses of urban forests and trees. In Konijnendijk, C., Nilsson, K., Randrup, T. and Schipperijn, J. (eds). *Urban Forests and Trees, Springer*.

Van der Meer, P. J. and Bongers, F. (1996). Formation and closure of canopy gaps in the rain forest at Nouragues, French Guiana. *Vegetatio* 126.(2), 167–179.

Villarreal, E. L. and Bengtsson, L. (2005). Response of a Sedum green-roof to individual rain events. *Ecol Eng* 25.(1), 1–7.

Vosselmann, G. and Maas, H.-G. (2010). Airborne and terrestrial laser scanning. Whittles Publishing, ISBN 978–1904445–87–6, 320 p.

Walter, H. (1931). Die Hydratur der Pflanzen und ihre physiologisch-ökologische Bedeutung. Gustav Fischer Verlag, Jena.

Weiner, J. and Damgaard, C. (2006). Size-asymmetric competition and size-asymmetric growth in a spatially explicit zone-of-influence model of plant competition. *Ecol Res* 21.(5), 707–712.

West, G. B., Enquist, B. J. and Brown, J. H. (2009). A general quantitative theory of forest structure and dynamics. *PNAS* 106.(17), 7040–7045.

Wichmann, L. (2002). Modelling the effects of competition between individual trees in forest stands. PhD Thesis. Royal Veterinary University Copenhagen.

Wiedemann, E. (1951). Ertragskundliche und waldbauliche Grundlagen der Forstwirtschaft. JD Sauerländer's Verlag, Frankfurt am Main.

Wilhelmsson, L., Arlinger, J., Spångberg, K., Lundqvist, S.-O., Grahn, T., Hedenberg, Ö. and Olsson, L. (2002). Models for Predicting Wood Properties in Stems of Picea abies and Pinus sylvestris in Sweden. *Scand. J. For. Res.* 17.(4), 330–350.

Zobel, B. J. and Van Buijtenen, J. P. (1989). Wood Variation - Its Causes and Control. Springer, Berlin.

List of Figures

List of Tables

Abbreviations

dbh	Diameter at breast height (1.3 m)
h	Tree height
LAI	Leaf Area Index
V	Crown volume derived by α-shape computations
S	Crown surface area derived by α-shape computations
CPA	Crown Projection Area derived from 2D α-shape computations
GPA	Whole Gap Projection Area derived from 2D α-shape computations
l_c	Crown length
l_b	Branch length
φ_b	Branch angle
φ_s	Stem inclination
CD_h	Crown center displacement horizontally
CD_v	Relative vertical crown center position
ML	Multi-Layering
RML	Relative Multi-Layering
A_{dbh}	Allocation ratio between crown diameter and *dbh*
A_h	Allocation ratio between crown diameter and *h*
A_B	Allocation ratio between crown diameter and biomass
EOC	Efficiency of space occupation
EEX	Efficiency of space exploitation
EBI	Efficiency of biomass investment

TLS Terrestrial laser scanning

LiDAR Light Detection and Ranging

TLiDAR Terrestrial Light Detection and Ranging

SOP Matrix Scanner Position and Orientation - Matrix

MST Metabolic Scaling Theory

St Growing location: Street canyon

Pa Growing location: Public Park

Ts Growing location: Public Town Square

GUI Graphical User Interface

VTK Visualization Toolkit

List of Species

Picea abies **[L.] Karst:** Norway spruce

Fagus sylvatica **L.:** European beech

Tilia cordata **Mill.:** Small leaved lime

Robinia pseudoacacia **L.:** Black locust

DOMINIK BAYER

Curriculum Vitae

Von-Fürer-Str.45
90491 Nürnberg

☎ *(+49) 911 278 78 72*
📱 *(+49) 179 130 53 04*
✉ *domink.bayer@lrz.tu-muenchen.de*
✉ *bayer.dom@gmail.com*

Persönliche Daten

Geboren am 01.01.1983 in München

Berufliche Tätigkeiten

12/2012 - 01/2017	**Doktorand, Wissenschaftlicher Mitarbeiter**, *Technische Universität München (TUM)*, Freising.
seit 07/2017	**Data Scientist**, *DATEV eG*, Nürnberg.

Dissertation (Dr. rer. nat.)

05/2011 - 06/2017	**Doktorand**, *Technische Universität München (TUM)*, Freising.
Arbeitstitel	*Three-dimensional tree structure on various levels and its impact on functions and services - New evidence by innovative TLS-Methodologies.*
Beschreibung	Entwicklung innovativer und komplexer Methoden zur Auswertung und Interpretation terrestrischer LiDAR-Daten im Kontext komplexer Ökosysteme.

Bildung

10/2004 - 06/2010	**Studium**, *Technische Universität München*, Freising, Diplomstudiengang *Forstwissenschaft*, Abschluss Dipl.-Ing., Abschlussnote - 1,8. Schwerpunkte: Methoden der Holzforschung, Produktionssysteme und Management, Holzwirtschaft
09/1993 - 06/2003	**Gymnasium**, *Luitpold-Gymnasium*, München. Abschluss: Allgemeine Hochschulreife (Abitur)
09/1989 - 07/1993	**Grundschule**, *Grund- und Teilhauptschule Unterföhring*, Unterföhring.
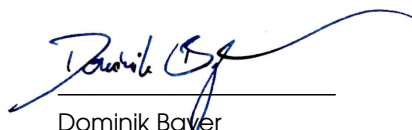
Sprachen

Deutsch	Muttersprache
Englisch	Verhandlungssicher in Wort und Schrift (wiss. Publikationen und Fachvorträge)

Nürnberg, 5. November 2017

Dominik Bayer

Part III.

Appendix: Published Articles and Submitted Manuscripts

Bayer et al. 2013

ORIGINAL PAPER

Structural crown properties of Norway spruce (*Picea abies* [L.] Karst.) and European beech (*Fagus sylvatica* [L.]) in mixed versus pure stands revealed by terrestrial laser scanning

Dominik Bayer · Stefan Seifert · Hans Pretzsch

Abstract How tree morphology develops in mixed-species stands is essential for understanding and modelling mixed-stand dynamics. However, research so far focused on the morphological variation between tree species and neglected the variation within a species depending on intra- and interspecific competition. Our study, in contrast, addresses crown properties of nine mature Norway spruces (*Picea abies* [L.] Karst.) of a pure stand and compares them with ten spruces growing in mixture with European beech (*Fagus sylvatica* [L.]). The same was done with 11 pure stand beeches and 12 beeches growing in mixture with spruce. Through application of a terrestrial laser scanner and a new skeletonization approach, we deal with both species'-specific morphological traits such as branch angle, branch length, branch bending, crown volume and space occupation of branches within the crown, some of which were hardly accessible so far. Special attention is paid to distinct differences between trees growing in mixed and pure stands: for spruce, our study reveals significantly longer branches and greater crown volumes in the mixed stand when compared to the pure stand. In case of European beech, individuals growing in mixture show flatter branch angles, more distinct ramification, greater crown volumes and a lower share of a single branch's space occupation in the total crown volume. The results show that the presented methods yield detailed information on the morphological traits analyzed in this study and that interspecific competition on its own may have a significant impact on crown structures. Implications for production ecology and stand dynamics of mixed-species forests are discussed.

Keywords Crown allometry · Crown plasticity · Allometric variability · TLS · Skeletonization

Introduction

According to the principle of function convergence the structure, physiology and phenology of plants indicate the prevailing environmental conditions under which they grow (see e.g., Assmann 1970; Walter 1931). This explains why Oldemann (1990) or Roloff (2001) use tree morphology and foliation for assessing tree vitality. For tree crowns that mean that their size and form result from the local environmental factors and resource supply which in forest stands are mainly determined by the tree's inter- or intraspecific neighbourhood within the stand.

The structure of a tree's crown is crucial in the feedback loop between tree functioning, structure and environment in pure stands (Hari 1985), but even more important in mixed stands where different species demonstrate their abilities to acclimate their structures to capture contested resources more efficiently or deny competitors access to the same resources (Pretzsch 2009).

The importance of crown structure and crown plasticity for the dynamic of mixed species stands is recognized and addressed (Pretzsch 2003; Price et al. 2010; Richards et al.

Communicated by R. Matyssek.

D. Bayer (✉) · S. Seifert · H. Pretzsch
Department of Ecology and Ecosystem Management,
Chair for Forest Growth and Yield Science,
Technische Universität München, Hans-Carl-von-
Carlowitz-Platz 2, 85354 Freising, Germany
e-mail: dominik.bayer@lrz.tu-muenchen.de

S. Seifert
Department of Forest and Wood Science, Stellenbosch
University, Private Bag X1, Matieland 7602, South Africa

2010) but hardly elucidated so far, especially in mature stands where crown structure is difficult to measure.

Measurement of tree crowns by e.g., Badoux (1946) and Burger (1939) constitutes the paradigm shift from stand to individual tree level thinking and modelling in forest science. Terrestrial methods for measuring (Röhle and Huber 1985), quantifying (Assmann 1970) and modelling (Pretzsch 1992, 2009) tree crowns were continuously refined. The main objective was to understand, predict and maximize tree growth based on empirical relationships between growing space of the tree, crown size and stem volume growth (Assmann 1970; Pretzsch 2006). A further aspect was the effect of silviculture on crown structure and wood quality (Zobel and van Buijtenen 1989 Wilhelmsson et al. 2002; Seifert 2003). New motivation for crown analysis came from allometry (Niklas 1994) and especially from the metabolic scaling theory (MST) which provides promising synthesis, scaling approaches and models for the functioning and structure of plants from organ to ecosystem level (Enquist et al. 1998; West et al. 2009).

Understanding and modelling of tree growth in mixture require tracing of the causes of over- or underyielding from stand to the tree or even organ level. Space-filling principles within the crown such as branch angle, branch length, branch number and ramification in mixture may differ from pure stands and indicate changed resource supply, resource capture, or resource use efficiency (Binkley et al. 2004). However, these space filling principles and the according morphological patterns triggered by interspecific competition can hardly be revealed by classical crown measurement by recording the crown length and cross section area in order to estimate the extension of the convex hull (Röhle and Huber 1985).

Terrestrial laser scanning (TLS) is widely utilized for high precision measurements in architecture, engineering and archaeology (Vosselman and Maas 2010) and in the last decade also used to measure forest parameters for inventory and even individual tree parameters (Huang and Pretzsch 2010; Pretzsch et al. 2011). The extraction of a structure description from TLS point clouds such as a collection of connected lines is called skeletonization and allows detailed analysis of morphological traits. Automated skeletonization approaches already exist and show great potential (e.g., van Leeuwen et al. 2011; Bucksch et al. 2010; Bremer et al. 2012). These methods however, are often highly species specific, require several scan positions per tree as well as generally free-standing test trees and suffer from difficulties dealing with inhomogeneous point densities, data gaps and noise within the dataset (Bucksch 2011; Côté et al. 2011). Thus, there is still a lot of need for further research until those methods can be used to reliably measure crown parameters at the branch level, especially within forest stands where occlusion is considerably stronger.

In order to contribute to the understanding of inter- and intraspecific competition and its impact on structural parameters, we developed and applied a new, software based manual skeletonization method for TLS point clouds to Norway spruce (*Picea abies* [L.] Karst.) and European beech (*Fagus sylvatica* [L.]) dealing with the following questions:

1. Is the presented method suitable to reveal structural crown properties, what problems arise and how may they be overcome?
2. What are the characteristic branch angles of both species and does growing within a mixed stand cause variations of these angles?
3. What are the characteristic branch length and branch bending of both species and does growing within mixture influence them?
4. What are the specific length-sum of the branches, number of branches and their distribution regarding branch order of both species and does interspecific competition affect these parameters?
5. How large is the crown volume and the space that individual branches occupy within the crown on a fine scale and do these parameters in mixed stands differ from those in pure stands?

Material and methods

Study area

For scrutiny of structural traits of spruce and beech and their differences in pure versus mixed stands, we selected the age series SON 814 (west–east spread: 10°28′45″E– 0°31′39″E, north–south spread: 47°31′05″N–47°32′31″N) which includes both, pure and mixed stands of Norway spruce and European beech and is located 785–800 m above sea level in the ecological region 14.4 "Schwäbisch-Bayerische Jungmoräne und Molassevorberge. Westliche kalkalpine Jungmoräne" in southern Bavaria, about 60 km southwest of Munich, Germany. The mean annual temperature is 6.8 °C with a precipitation of 1,114 mm. During the vegetation period of 140 days (days ≥10 °C) the temperature averages 13.9 °C accompanied by 648 mm of precipitation. The natural vegetation would be a *Luzulo-Fagetum* association.

We took our sample trees from plot SON814/3 which is composed of parts where both species occur in pure as well as in mixed stands with otherwise equal underlying conditions. An overview of the stand characteristics for SON814/3 is given in Table 1. We considered a tree that had no other tree's crown in between its own crown and the crown of the sample tree a neighbour. The selection of our

Table 1 Stand characteristics for the experimental plot SON814/3

	Age	dg (cm)	Basal area (m² ha⁻¹)	Volume (m³ ha⁻¹)
Norway spruce	128	56.1	36.8	640.6
European beech	143	42.3	19.4	360.0
Total	–	–	56.2	1,000.6

Volume indicates merchantable wood above 7 cm in diameter at the thinner end

dg diameter of median basal area tree

Table 2 Tree characteristics for the analyzed Norway spruces and European beeches in pure and mixed stands on the experimental plot SON814/3

	Norway spruce				European beech			
	Pure		Mixed		Pure		Mixed	
	Mean	SE	Mean	SE	Mean	SE	Mean	SE
N	9	–	10	–	11	–	12	–
Age	128	–	128	–	143	–	143	–
DBH (cm)	45.7	3.05	59.1	3.79	43.7	1.82	42.2	2.30
H (m)	38.9	0.51	39.2	1.07	36.8	0.62	35.9	0.37
Rel. H	0.93	0.01	0.94	0.02	0.94	0.02	0.91	0.02
Local basal area (m²/ha)	64.82	3.24	63.28	2.32	52.83	2.36	53.39	3.25

N number of sample trees, *DBH* diameter at 1.3 m, *Rel H* height relative to highest stand member within a 10 m radius, *Local basal area* sum of basal areas of all trees within a radius of 10 m from sample tree up scaled to ha

sample trees was done in such a way as to ensure that trees classified as growing in pure stand were surrounded exclusively by neighbours belonging to the same species. Accordingly, a sample tree was only classified as growing in mixture if all of its neighbours are members of the opposite species. Furthermore, we closely paid attention to tree size and competitive situation to ensure that trees of both pure and mixed stands grow under comparable conditions and differences in structural crown properties are caused by mixture itself and not by differences in local stand density or tree size. The sample spruces in pure and mixed stand are 128-year old and of comparable average height (pure 38.9 m, mixed 39.2 m) and relative height (pure 0.93, mixed 0.94), i.e. their height in relation to the highest neighbour within a radius of 10 m around the sample tree. The local basal area (pure 64.82 m²/ha, mixed 63.28 m²/ha), i.e. the sum of basal areas of all trees also in a 10 m radius around the sample tree, up-scaled to ha is approximately the same. Spruce's average dbh differs significantly between pure (45.7 cm) and mixed stand

(59.1 cm). The selected beeches are at the age of 148 years in both pure and mixed stand. Mean height (pure 36.8 m, mixed 35.9 m), relative height (pure 0.94, mixed 0.91), local basal area (pure 52.83 m²/ha, mixed 53.39 m²/ha) and dbh (pure 43.7 cm, mixed 42.2 cm) are comparable. A summary of the characteristics of our sample trees is given in Table 2.

Data acquisition

We used the Riegl LMS-Z420i TLS system. This laser scanner system works on the so-called time-of-flight principle. A short laser impulse is fired in a specified direction to a target. A part of the light is reflected back to the scanner. The scanner measures the time between the firing and the return of the signal. Multiplying this time with the speed of light in air gives the double distance to the object. The accuracy for these distance measurements is about 1 cm. The angles azimuth and inclination to the target are recorded with a precision of 0.002°. For each laser impulse the angles are slightly varied (0.06°) resulting in a scanning action. The consecutive distance measurements result in a range image of the desired region. With one setup of the Riegl LMS-Z420i the maximum region is 360° (horizontally) by 80° (vertically) wide. Tilting the scanner by 90° and doing a second scan results in a nearly complete scan of the whole sphere. The originally spherical coordinates (azimuth, inclination and distance) are translated to Cartesian coordinates (x, y, z) for further processing.

Obviously, the measurement density drops with increasing distance to the scanner as the angles are widening with distance. Moreover, the infrared the laser beam is normally not able to penetrate the tree compartments and so it is not possible to make measurements behind an obstacle. These two effects result in rather sparse measurement densities in higher crown regions, especially if the crown parts near to the scanner are dense, like the conifer crowns are (Hilker et al. 2010). Keeping this in mind we set up the scanner between the trees of interest, in a way that the tree crown was covered as much as possible by the laser scan. In addition, we used a distance measurement mode which is called last-pulse or last-target. In this mode the last echo of the laser impulse is used for distance recording, allowing the laser beam to penetrate the tree crown further than using the normal, first-pulse mode.

Skeletonization

In order to determine crown structures as entirely as necessary to gain insights on crown structures, we developed a software-based approach for the manual skeletonization of

measured TLS point clouds where the skeletonization of a tree's point cloud is done semi-manually, using software specifically developed for this purpose. The code is written in the programming language Python to facilitate fast and relatively unproblematic adjustments and good interoperability with other programming languages such as C/C++ for time-critical calculations or R for statistical analysis.

First, trees of sufficient scan quality were manually extracted from the point cloud of the whole scan position retrieved by the terrestrial laser scanner. These single tree point clouds were then skeletonized by visualizing the tree, utilizing the Mayavi program library for Python (Ramachandran and Varoquaux 2008) and letting the user measure the course of a branch by successively defining as many branch segments as possible through a dedicated user interface to get a sufficient image of the tree structure (Fig. 1). The definition of the branch segments is done by picking appropriate members of the point cloud, i.e. points that actually belong to the specific branch with the help of interactive call-back functions and internal plausibility checks. Additional queried information for every branch through user input includes branch type (main axis, secondary axis or branch), the branch order, the branch's parent-branch and whether the branch is dead or alive. The entirety of the measured branches finally defines the tree's skeletal structure.

After the skeletonization process, the skeletal structure serves as a basis for various calculations such as branch angles, branch length and branch bending. Furthermore, the point cloud of a tree or the combination of point cloud and skeletal structure facilitates the calculation of crown volume and the space requirement of a branch, i.e. the volume of a branch including smaller branches, twigs and foliage.

Branch angles

We defined a branch's angle φ as the angle between the vectors $\overrightarrow{bs}$ and $\overrightarrow{z}$ where $\overrightarrow{bs}$ is the vector from the branch's base to a point s lying on the branch in an arbitrary distance r. $\overrightarrow{z}$ is a vector of arbitrary length along the z-axis of the coordinate system which is aligned to the centre of gravity in negative direction. Since the skeletal approach allows for angle investigation in different distances r and therefore angle distributions along the course of a branch, the coordinates of s are dependent on r. The point s

$$\overrightarrow{s} = \overrightarrow{p_1} + \frac{-t_2 + \sqrt{t_2^2 - 4t_1t_3}}{2t_1}\left(\overrightarrow{p_2} - \overrightarrow{p_1}\right) \tag{1}$$

with

$$t_1 = (x_{p2} - x_{p1})^2 + (y_{p2} - y_{p1})^2 + (z_{p2} - z_{p1})^2 \tag{2}$$

$$t_2 = 2((x_{p2} - x_{p1})(x_{p1} - b_x) + (y_{p2} - y_{p1})(y_{p1} - b_y) \\ + (z_{p2} - z_{p1})(z_{p1} - b_z)) \tag{3}$$

$$t_3 = b_x^2 + b_y^2 + b_z^2 + x_{p1}^2 + y_{p1}^2 + z_{p1}^2 \\ - 2(b_x x_{p1} + b_y y_{p1} + b_z z_{p1}) - r^2 \tag{4}$$

can be determined by calculating the intersection point of the surface of a sphere with radius r and centre b and the line segment with $|\overrightarrow{bp_1}| < r < |\overrightarrow{bp_2}|$ where p_1 is the first point defining the branch segment and p_2 is the second respectively (Fig. 2). Finally, the branch angle φ is determined by the scalar product of $\overrightarrow{bs}$ and $\overrightarrow{z}$ (Eq. 5).

$$\cos\varphi = \frac{\overrightarrow{bs} * \overrightarrow{z}}{|\overrightarrow{bs}| * |\overrightarrow{z}|} \tag{5}$$

For each branch of each skeletonized tree, we calculated branch angles in absolute distances ranging from 0.5 to 10 m in steps of 0.5 m. In addition, we determined angles ranging from 0.5 to 5.0 m measurement distance in reverse direction, meaning from the branch's top to its base in 0.5-m steps as well and lastly, we calculated angles in distances relative to the branch in steps of 10 % of the branch's length.

Branch length

We defined two different lengths of a branch. One described simply by the straight distance l_s between the branch base b and its end e (Eq. 6).

$$l_s = \left|\overrightarrow{e} - \overrightarrow{b}\right| \tag{6}$$

The second length l_c we defined achieves higher accuracy by following the curvature of the branch and summing up the lengths of all n segments belonging to the branch's skeletal structure as shown in Eq. (7).

$$l_c = \sum_{i=1}^{n} \sqrt{(p_{2x} - p_{1x})_i^2 + (p_{2y} - p_{1y})_i^2 + (p_{2z} - p_{1z})_i^2} \tag{7}$$

Volume calculations

In order to estimate the spatial occupation of branches within the crown, additional points in a distance of 10 cm or less from each other were created within every branch segment to achieve higher density and homogeneity of the skeleton's defining points. Then, every member of the TLS point cloud was assigned to its nearest neighbour of the enriched skeleton point crowd by application of the kd-tree-based nearest neighbour algorithm described by Maneewongvatana and Mount (1999). In computational

Fig. 1 From point cloud to a tree's skeletal structure: (*l*) isolated individual tree from scan position image (*m*) skeletal structure surrounded by original point cloud data (*r*) isolated tree skeleton
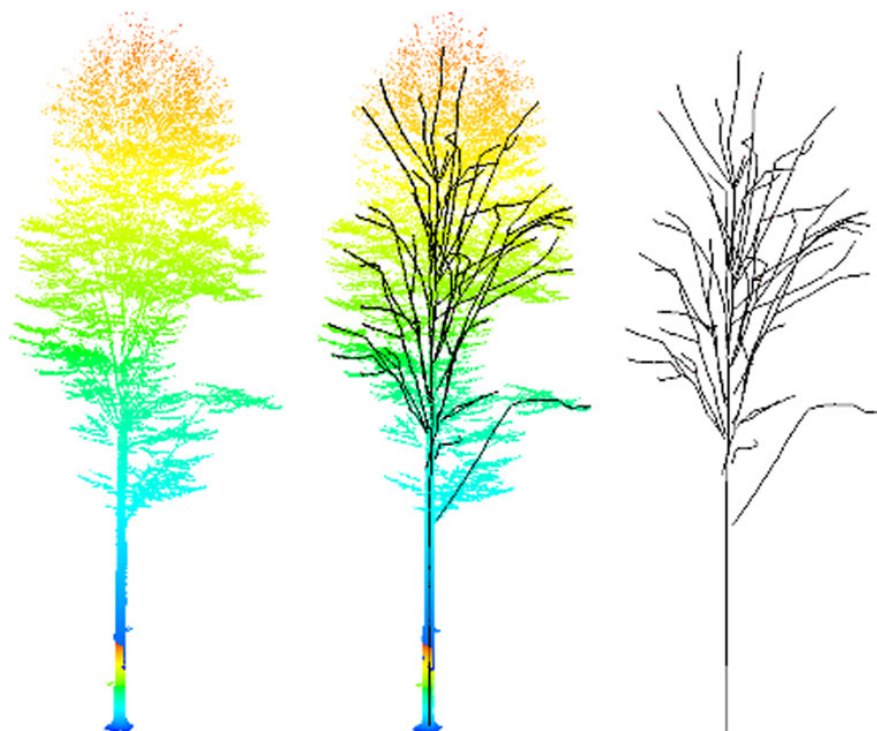
geometry, an α-shape is a generalization of the convex hull of a point set based on Delaunay triangulation. The so-called α-value is a parameter that controls the level of detail in which the calculated shape represents the point cloud. It can range from $\alpha \rightarrow 0$ which yields the point cloud itself to $\alpha \rightarrow \infty$ yielding the convex hull of the point cloud. For detailed explanation see Edelsbrunner and Mücke (1994).

The specific point cloud for every single branch resulting from the nearest neighbour assignment was used for three-dimensional α-shape calculations. The volume V_α of the α-shape of a branch was calculated by summing up the volumes of all *n* tetrahedrons being part of the α-shape as shown in Fig. 3 and Eq. (8).

$$V_\alpha = \sum_{i=1}^{n} \sqrt{\frac{1}{288} * \det \begin{pmatrix} 0 & u_i^2 & v_i^2 & w_i^2 & 1 \\ u_i^2 & 0 & W_i^2 & V_i^2 & 1 \\ v_i^2 & W_i^2 & 0 & U_i^2 & 1 \\ w_i^2 & V_i^2 & U_i^2 & 0 & 1 \\ 1 & 1 & 1 & 1 & 0 \end{pmatrix}} \tag{8}$$

Since we calculated the α-shape for several alpha values, ranging from coarse (convex hull: $\alpha = \infty$) to fine ($\alpha = 0.25$ m), it is possible to estimate the three-dimensional hull and spatial requirement of a tree's

branches including smaller branches, twigs and foliage originating from it in different resolutions (Fig. 4).

To estimate the crown volume of a given tree's point cloud, a three-dimensional α-shape of all members of the cloud with a *z*-value higher than that of the point where the crown commences was calculated. Its volume was determined analogue to the calculation of a single branch volume. It represents the growing space occupied by the tree, respectively its branches.

Results

The results summarized in Table 3 refer to all branches that were alive and exceeded 5 % of their tree's height in length at the time the scans were made. For spruce, our study reveals significantly longer branches and significantly higher crown volumes in the mixed stand when compared to the pure stand. In case of European beech, individuals growing in mixture show flatter branch angles, more distinct ramification, higher crown volumes and a lower proportion of single branch volumes within the crown. In order to take the grouping of the branches on tree level into account, we applied a linear mixed effects model (lme) whenever it was appropriate.
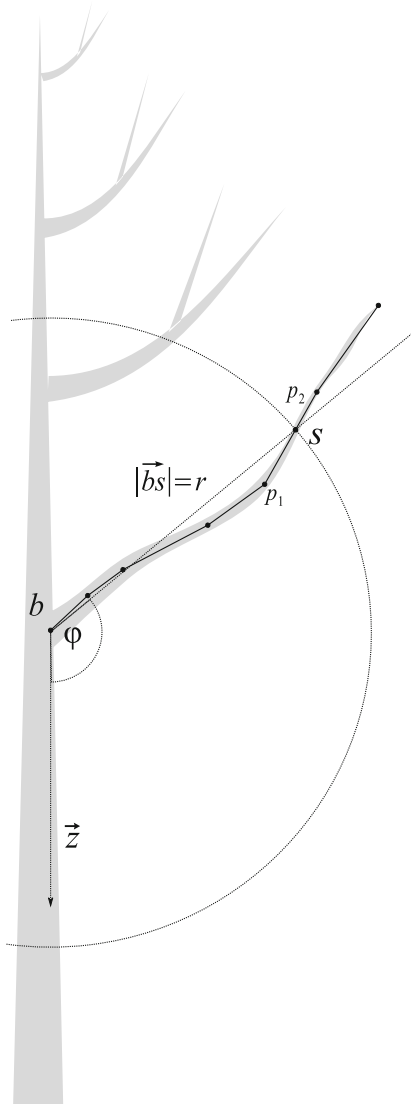
Fig. 2 Angle between branch base b and point on the branch in distance r

Fig. 3 Tetrahedron edges as in Eq. (8)
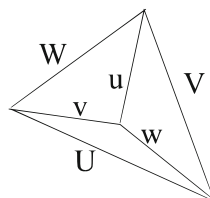
Branch angles

The branch angles, measured from branch base to branch end, over the entirety of all branches show significant
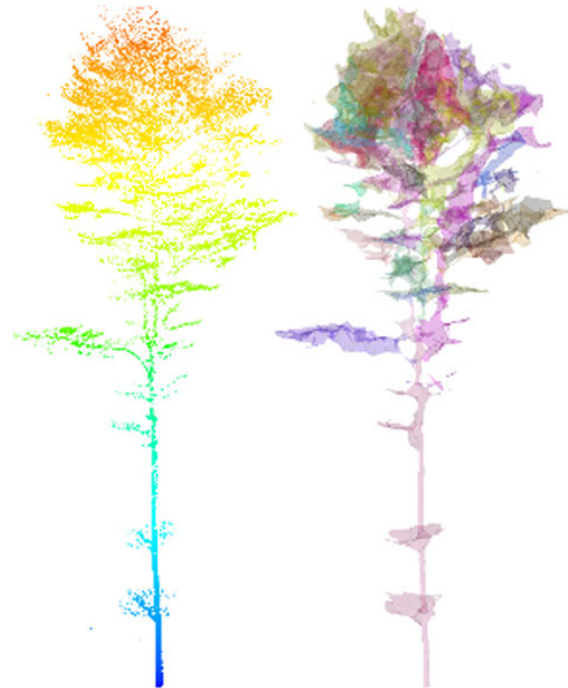
Fig. 4 Original point cloud (*l*) and three-dimensional model of the same tree assembled by its single branch α-shapes (*r*)

differences between pure and mixed stands for European beech (Fig. 5). The mean angles of Norway spruce both in the pure stand and the mixed stand are about 89° on average (Table 3). European beech's branch angles average at 138.6° in pure stands and 128.5° in mixed stands ($p < 0.001$). Moreover, the results for European beech present significant differences between pure and mixed stands for branch angles over the whole course of a branch in all measurement distances relative to the total branch length. While the angles derived from a lme stay on a relatively constant level at about 140° in pure stands, in mixed stand they decline from about 133.8° to 128.5° with increasing measuring distance (Fig. 6). Both pure and mixed stand branch angles flatten towards the branch end. To illustrate this, the branch angles of beech's crown periphery measured in reversed direction, i.e. from branch top in direction to the branch base in absolute measurement distance intervals of 0.5 m, are presented in Fig. 7.

Branch length and branch bending

Norway spruce features significantly distinct branch lengths l_s. In pure stands the mean measured branch length is 2.16 m compared to 2.78 m in mixed stands ($p = 0.047$; see Table 3). For European beech, the results show no

Table 3 Descriptive statistics for the analyzed sample trees

| | Norway spruce | | | | | | European beech | | | | |
| | Pure stand | | Mixed stand | | | | Pure stand | | Mixed stand | | |
	Model	Mean	SE	Mean	SE	p	Mean	SE	Mean	SE	p
N	lm	20.1	4.493	26.0	3.092	0.261	18.6	2.663	35.8	3.687	<0.001
φ (°)	lme	89.55	3.175	88.12	4.365	0.747	138.56	2.220	128.52	2.870	0.0022
l_s (m)	lme	2.16	0.210	2.78	0.289	0.0476	4.81	0.209	4.31	0.261	0.0702
BB	lme	95.72e-2	5.631e-3	96.27e-2	7.525e-3	0.475	96.21e-2	4.188e-3	94.39e-2	5.281e-3	0.0024
SBL (m)	lm	45.82	12.536	68.98	8.628	0.0821	89.26	15.560	153.84	10.760	<0.001
RLBV (m^3)	lme	–	–	–	–	–	−3.777	0.121	−4.286	0.160	0.0045
CV (m^3)	lm	21.07	7.120	46.23	9.814	0.0202	25.25	5.763	58.97	7.978	<0.001

Volume calculations are based on α-shapes with α = 0.25 m

N number of branches per tree, *φ* branch angle measured from branch base to branch end, *l_s* branch length in straight line from branch base to branch end, *BB* branch curvature, *SBL* sum of branch lengths per tree, *RLBV* relative logarithmic branch volume, *CV* crown volume, *lm* standard linear model, *lme* linear mixed effects model
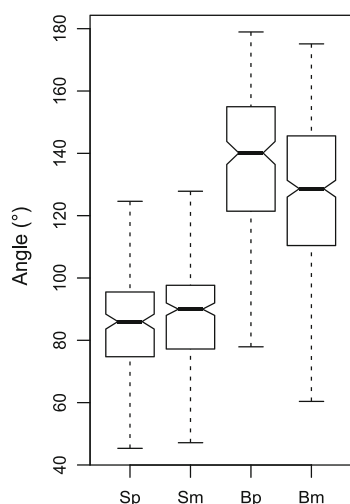
Fig. 5 All branch angles measured from branch base to branch top for Norway spruce and European beech in pure and mixed stands. Differences between pure and mixed stands are highly significant for European beech (linear model, $p < 0.001$). *Sp* Norway spruce in pure stand, *Sm* Norway spruce in mixed stand, *Bp* European beech in pure stand, *Bm* European beech in mixed stand

Fig. 6 Mean relative angles and single standard error bars for European beech in pure and mixed stands derived from a linear mixed effects model. Trees growing in pure stands show significantly higher values than trees growing in mixture over the whole course of a branch. While the angles stay on a relatively constant level in pure stands, they decline with increasing measurement distance. *p* values range from 0.047 (worst) to 0.002 (best)

significant differences over the entirety of all branches ($p = 0.070$) as well as within the various branch orders.

Regarding the branch bending (BB), here defined as the quotient l_s/l_c of branch length measured from branch base to top and the branch length revealed by the sum of all measured branch segments belonging to a branch, Norway spruce features mean values of about 96×10^{-2} in pure stands and in mixed stands without significant differences ($p = 0.556$). European beech however shows significantly distinct values of 96.21×10^{-2} in pure stand and 94.39×10^{-2} in mixed stand, meaning that branches in mixed stands are less straight ($p = 0.002$).

Length sum, branch count and branch orders

For Norway spruce the number of measured branches fulfilling the above-mentioned criteria averages 20.1 branches in pure and 26.0 branches in mixed stands resulting in no significant difference ($p = 0.261$). European beech, however, with 18.6 branches in the pure stand compared to 35.8 branches in the mixed stand, showed significantly more measureable branches over all in mixed stands ($p < 0.001$; Table 3). Especially branches of the second, third and fourth orders are significantly more numerous in mixed stands as shown in Fig. 8. While there is a tendency but no significant difference in the average branch length of European beech in pure and mixed stand ($p = 0.070$; see Table 3), due to the higher quantity of branches the sum branch lengths (SBL) differs significantly between pure (89.3 m) and mixed (153.8 m) stands ($p < 0.001$).

🖄 Springer
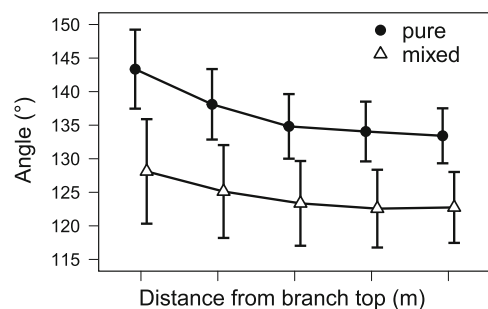
Fig. 7 Absolute branch angle means and double *standard error bars* of European beech measured from branch end towards branch base. Means and errors are derived from a linear mixed effects model. *p* values range from 0.002 (worst) to <0.001 (best)
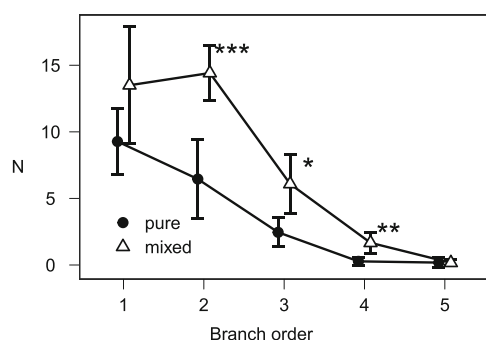
Fig. 8 Mean number of branches and double standard error for European beech in pure and mixed stands by branch order. In mixture, European beech shows significantly more branches of the second, third and fourth order ($p_2 < 0.001$, $p_3 = 0.011$, $p_4 = 0.004$)

Volume of the α-shape of individual branches and the crown as a whole

Crown volumes (CV), based on volume calculations of α-shapes (α = 0.25 m) of the individual tree point clouds, were significantly higher in mixed stands for both Norway spruce and European beech as presented in Table 3. In the case of Norway spruce, the differences in crown volumes between pure and mixed stands are mainly caused by the greater average branch lengths in mixed stands compared to pure stands ($R^2 = 0.34$, $p = 0.005$) (see Fig. 9). Branch angles of spruce appear to have no significant influence on crown volume. The differences in crown volumes of European beech on the other hand are related to the differences of the branch angles ($R^2 = 0.36$, $p = 0.002$) (see Fig. 10), while branch length shows no significant influence.

The relative branch volume (RBV), i.e. the branch volume in relation to the tree's crown volume, shows no significant differences between pure and mixed stands
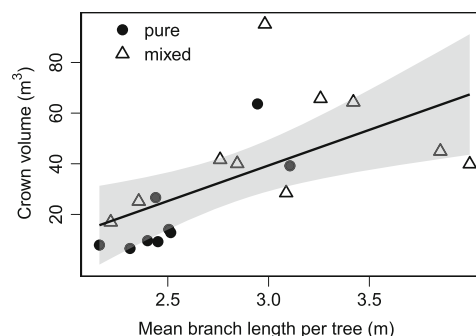
Fig. 9 Relation between average branch length and crown volume derived from α-shapes with α = 0.25 m for Norway spruce. $\overline{V_\alpha} = -45.0 + 28.1 * l_s$, $R^2 = 0.34$, $p = 0.005$, shaded area marks the 95 % confidence region of the regression line

when a linear mixed effects model is applied. However, the logarithmic relative branch volume (RLBV) is significantly higher in pure stands for European beech for both standard linear models as well as linear mixed effects models ($p_{lme} = 0.005$; Table 3). Since due to occlusion caused by foliage, the skeletonization of Norway spruce proved to be difficult in the higher crown regions, branch volume calculations did not yield reliable results.

Discussion

How different tree crowns may develop under intra- and interspecific competition is illustrated in Fig. 11 by the example of the results we found for European beech. Tree crown development plays an essential role during stand development of pure and even more of mixed-species forests. In order to explain the relevance of crown development and intraspecific plasticity in the interaction between two tree species during stand development, Fig. 12 illustrates the feedback between their functioning, structure, and local environment within the stand. The distinction between functioning (e.g., growth), structure formation (e.g., crown extension, crown space filling) and environment (e.g., light supply in the canopy, water supply below ground) is made in accordance to the ecosystem approach by Hari (1985, p 28) and Pretzsch (2009, p 226). The trees can modify their local environment within the stand via their structure and their functioning.

The functioning (e.g., growth, partitioning) can change the tree structure (e.g., crown width, branch angles) and the resulting tree and stand structure affects the local environmental conditions for tree and stand growth (slow feedback loop functioning → structure → environment → functioning, represented by bold arrows). The extinction of light in the stand canopy results from the tree and stand structure which are analyzed in this study. The tree
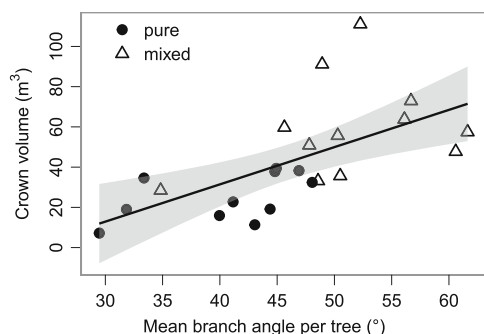
Fig. 10 Relation between mean branch angle measured from branch base to branch end per tree and crown volume derived from α-shape with $\alpha = 0.25$ m for Europen beech. For better readability, angles were subtracted from 180°. Here, increasing angles mean flatter branches resulting in a larger crown volume. $\overline{V_\alpha} = -42.7 + 1.9 * (180 - \varphi)$, $R^2 = 0.36$, $p = 0.002$, shaded area marks the 95 % confidence region of the regression line
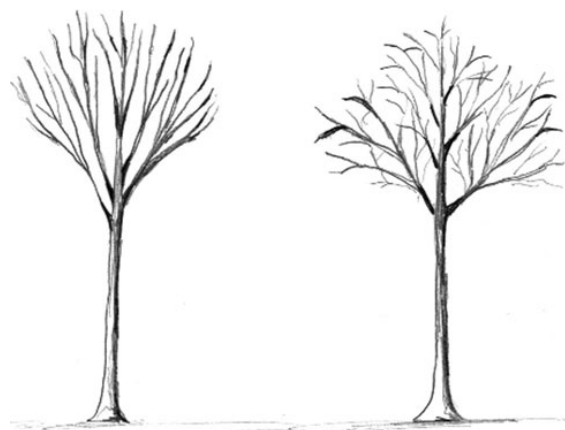
Fig. 11 Schematic drawing of crown structures of European beech in pure (*left*) and mixed (*right*) stands to illustrate the different branching structures. While individuals growing in pure stands develop steeper branches, those growing in mixture with Norway spruce show flatter branches with a higher number of smaller branches originating from them

functioning can also directly affect the environment (rapid feedback loop functioning → environment → functioning, represented by bold arrow and opposite thin arrow). Supply or efficiency of soil water and nutrient exploitation may be reduced or enhanced e.g., if shallow rooting species and deeper rooting neighbours complement each other (Grams et al. 2002; Bolte and Villanueva 2006).

Our results on the variability of crown structure concern the slow feedback loop functioning → structure → environment → functioning. The crown development revealed for mixed stands is beyond the range known from pure stands and indicates crown properties emerging in interspecific environment.
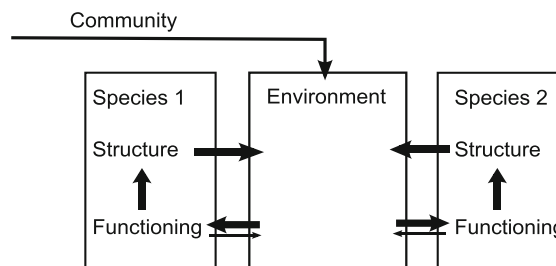
Fig. 12 Feedback between stand structure, environmental conditions and tree functioning in a two-specific mixed forest stand. Further explanation is given in the text

The principle differences in the crown properties between spruces and beeches in mono-specific stands were already subject of detailed analysis (Assmann 1961; von Droste zu Hülshoff 1969; Pretzsch and Schütze 2005) and we just discuss additional details like species-specific branch angles, numbers and volumes. In contrast, the intra-specific crown plasticity of both species in mixed versus pure stands which we focused on was hardly analyzed so far (Purves et al. 2007; Richards et al. 2010).

The shallower branch angle, further crown extension, and denser crown space filling of beech in interspecific versus intraspecific neighbourhood may favour the competition of beech versus spruce in two different ways, via access to contested resources and hindering of a neighbour's approach by effective shading and space occupation.

A higher structural crown plasticity and more complex canopy structure creates a higher variability of environmental conditions and in return triggers the plasticity at organ, crown or tree structure level for an optimal capture of resource or acclimation to the environment altered by competing neighbours. As a result of the feedback between growth, structure and local environmental conditions, structural variability can have an effect on interspecific competition, production ecology, structural diversity and biodiversity as shown in the following.

Methodological considerations on TLidar application

Our semi-manual skeletonization approach facilitates the retrieval of crown structures from imperfect TLS point cloud data and does so regardless of tree species. Even, due to occlusion and little scan positions, imperfect data as retrieved within actual forest stands yield usable tree architectures. However, occlusion, inhomogeneous point densities and noise within the dataset can still be an issue. Especially crown regions of Norway spruce which are higher than about 70 % of the tree's height were hard to capture due to high occlusion caused by its foliage. Because of that, our method did not deliver reliable branch

α-shapes and their volumes for Norway spruce sample trees. In fact the number of measurable branches in the higher crown regions is much lower than the actual number of branches of the tree, which in combination with the nearest neighbour assignment of the TLS point cloud members leads to a large overestimation of the actual point cloud of a branch. The establishment of more scan positions and the utilization of a more advanced TLS-device such as a full waveform scanner may help to overcome this problem. European beech on the other hand, if scanned outside the vegetation period under foliage free condition, proves to be a lot less problematic in that regard and yields viable tree architectures even in the higher crown regions.

Another issue that needs further investigation is the optimal α-value for the hull and volume calculations. The higher the chosen value the coarser the hull, which means that noisy point cloud members lying outside the actual crown or branch gain larger influence on the resulting volume calculation. On the other hand, α-values that are too small can lead to an underestimation of the actual crown or branch volume since holes in the point cloud data that are caused by occlusion are omitted in the hull calculation (Edelsbrunner and Mücke 1994). Therefore, depending on the quality of the dataset and the applied scan resolution, the range of reasonable α-values can vary. In our case, an α-value of 0.25 m provided a practicable trade-off between over- and underestimation of the actual growing space while ensuring that the potential point density in an assumed maximum measurement distance of 50 m is still sufficient for every α-shape facet.

Intraspecific variation of morphological traits in mixed-species versus pure stands

The longevity of forests enables a particular continuous formation of complex crown and stand structure. Due to uniform crown structure the canopy as a whole is rather homogeneous in pure stands but can become much more heterogeneous in mixed stands, e.g., when species such as spruce and beech with different compensation points of photosynthesis establish in multiple layers.

In order to avoid a mixing of merely size- and density-dependent changes in tree allometry and architecture with reactions triggered by an interspecific environment (Poorter et al. 2012), we selected trees with rather similar tree size in terms of stem diameter at breast height and local competition (Table 2). The structural traits our method reveals were presented in isolation in the "Results" section but are discussed in connexion with each other because of their close mechanical and physiological relationship.

The characteristic branch angles we report do not significantly differ between the pure and the mixed stand for Norway spruce. European beech, however, turned out to be much more variable in branch angles and lateral branch extension in mixed versus pure stands. This contributes to an increase in growing space (see Fig. 10) and may explain why under interspecific competition with spruce, beech is able to penetrate and occupy crown space very efficiently with low biomass investments (Pretzsch and Schütze 2005).

Regarding branch length and branch bending we found that compared to the pure stand, Norway spruce in mixture with European beech developed longer branches, thus resulting in more voluminous crowns. European beech shows no difference in branch lengths. However, it demonstrates its plasticity by growing branches that are less straight in mixture.

The number of branches, their distribution among branch orders and the length sum of branches within a crown for Norway spruce in a pure stand does not differ significantly from spruces in a mixed stand. European beech again shows its high crown plasticity by developing more branches, especially in the second, third and fourth branch order resulting in considerably more ramified crowns. While the branch length does not change, beech's increased number of branches in mixed stand leads to significantly higher sums of branch lengths within the crown, contributing to a considerably denser filling of the growing space and increased fractal scaling of crown surface structure.

Tree crowns as described by Oldemann (1990), Purves et al. (2007) and Roloff (2001) lie somewhere in the continuum between the borderline cases of an umbrella-like crown with the whole leave surface area allocated close to the convex hull (surface dimension $n = 2$) and a broom-like crown with leave surface area distributed all over the crown space (surface dimension $n = 3$) (Zeide 1998). Species mixing can obviously modify the fractal dimension of the crown surface area and leaf area from a lower space filling (Euclidian scaling) towards higher space filling of the crown volume (fractal scaling) (Pretzsch and Dieler 2012). Concerning crown volume and the space that individual branches occupy within the crown, Norway spruce features larger crowns in mixture. The crown volumes of European beech too are significantly larger in the mixed stand. The average share of a single branch on beech's crown volume however is smaller in the mixed stand. This may be explained through the finding that the larger overall crown volume in mixture is outweighed by the higher number of smaller branches when compared to the pure stand.

The considered higher crown plasticity in mixed versus pure stands is a emergent property which is crucial for better analyzing, understanding and modelling of stand dynamics (Purves et al. 2007; Richards et al. 2010). The

latter applies in particular to mixed species forests where the structural as well as functional heterogeneity are much higher compared to pure stands and trigger manifold space occupation strategies, plant forms and shapes. Spruce and beech represent rather different species in terms of functional and structural traits: spruce is a quick, vertically oriented but rather unplastic species, while beech is a slow, rather laterally and very plastic one. Combination of such complementary species means a significant change of the canopy structure compared with pure stands and might trigger the particular broad intraspecific plasticity not known from pure stands. However, other common species combinations, e.g., oak/beech, pine/beech, eucalypt/acacia, populus/white spruce, represent similar structural and functional differences and might trigger comparable crown plasticity in inter- versus intraspecific environments (e.g., Bauhus et al. 2004).

Relevance of the structural crown variability for the growth performance of mixed versus pure stands

Crown structures at the individual tree level constitute a key aspect in the mechanisms of inter- and intraspecific interaction and its impact on a successful exploitation of potentially available environmental resources. Above ground, differences in growth and yield between pure and mixed stands can be caused by the occupation of more canopy space, by variations in the utilization efficiency of the given space or a combination of both. Since organs such as branches, twigs and leaves constitute a considerable share of the productivity; structural differences may presumably not only influence the filling of canopy space but crown efficiency (biomass production per unit of crown projection area and year) and competitiveness in resource exploitation as well (Matyssek et al. 2005).

The plasticity in lateral crown expansion prevents spruce from being outcompeted by beech, drives it into higher canopy layers where light can be captured more efficiently due to less shading. Latter reaction may explain the overyielding of spruce in mixture with beech (Pretzsch et al. 2010). Combination of both species can finally result in an average overyielding of about 20 % compared with pure stands (Pretzsch and Schütze 2009).

While our results for Norway spruce, apart from longer branches and higher crown volume in the mixed stand, show no statistically significant differences in structural crown parameters between pure and mixed stands, an increase in crown efficiency is likely at least partially caused by structural differences within the crown on branch or smaller level. European beech on the other hand is known to feature no considerable increase of crown efficiency when grown in mixture on our experimental plot. In fact, the crown efficiency slightly decreases (Pretzsch and Schütze 2009). As European beech does not profit from mixture-induced improvements of soil properties as much, the overyielding is presumably directly related to the differing structural crown properties we found. Since the actual distribution and availability of resources within the canopy space is hard to measure, space serves as an abstraction for above-ground resources. According to Grams and Lüttge (2011) space may even be considered a resource itself. In pure stands under intraspecific competition, potential niches and gaps in canopy space are heavily contested. Larger crowns, higher branch ramification, higher branch bending as well as flatter branch angles and more branches overall lead to a denser filling of the available canopy space, thus enhancing space occupation efficiency, adaption and multi-layering which enhances light interception and diameter growth (Binkley et al. 2011) and contributes to the frequently reported overyielding of beech in mixed versus pure stands (Pretzsch 2009; Pretzsch et al. 2010). The space occupation and suppression of neighbouring species reflect the competitive strength of beech and explain its domination in most Central European mixed stands (Fischer 1995).

Structural heterogeneity as component of biodiversity

Apart from productivity, structural crown properties also play an important role in habitat formation and its impact on biodiversity. The habitat heterogeneity hypothesis assumes that more complex habitats likely induce increased species diversity as they provide more niches and means to utilize potential environmental resources (e.g. MacArthur and MacArthur 1961; Bazzar 1975). The distribution and interaction of animal species are often notably influenced by the plant community of a habitat which defines the majority of the physical environmental structure (Lawton 1983; McCoy and Bell 1991). In our case, more complex habitats is equivalent to mixed stands due to their higher complexity achieved by two instead of one main tree species and by more complex crown structures of European beech when grown in mixture with Norway spruce. According to Tews et al. (2004), the majority of studies about habitat heterogeneity and its relation to animal species diversity found a positive correlation with plant species diversity or structural complexity defined by parameters such as branch angles and ramification. Therefore, not only the mixture of Norway spruce and European beech in itself but also its impact on crown structures on branch or even lower level may significantly enhance animal species diversity.

Conclusions

A new method using terrestrial LiDAR in combination with point cloud skeletonization and other methods such as alpha shape calculations to determine structural crown properties of trees independent of tree species was developed. This method was applied to sample trees of an experimental plot providing comparable trees of both Norway spruce and European beech in pure stand as well as in mixture with each other. The results of this study have shown that our method may constitute a valuable non-destructive tool to facilitate a deeper understanding of the intra- and interspecific interaction of trees and its impact on productivity and ecological traits, e.g., biodiversity in pure and mixed-species forest stands.

Whether, and to what extent, our results may be applied to other stands is subject to further research. The experimental plot SON 814 is considered highly productive for both species. It can be assumed that nutrition and soil properties are provided in sufficient magnitude for each of the sample trees, largely independent of competition. It is imaginable that inter- and intraspecific competition for the most part manifest in above-ground structural differences induced by the competition for light. Hence, it is conceivable that structural differences in terms of structural reactions on differing neighbour species are less distinct on stands which offer less optimal growth conditions where below-ground competition mechanisms or the general resource supply and soil properties become more of an issue.

The potential applications of our method are manifold. For instance, not only may structural crown properties be analyzed, but also the interaction between crowns and the occupation of canopy space of stand neighbours on individual tree level. The method is currently applied on plots along an ecological gradient to analyze how the intraspecific crown plasticity is modified by site conditions.

References

Assmann E (1961) Waldertragskunde. Organische Produktion, Struktur, Zuwachs und Ertrag von Waldbeständen. BLV Verlagsgesellschaft, München

Assmann E (1970) The principles of forest yield study. Pergamon Press, Oxford

Badoux E (1946) Krone und Zuwachs. Mitt Schweiz Anst Forstl Versuchswesen 24:405–513

Bauhus J, van Winden AP, Nicotra AB (2004) Above-ground interactions and productivity in mixed-species plantations of Acacia mearnsii and Eucalyptus globulus. Can J For Res 34:686–694

Bazzaz FA (1975) Plant species diversity in old-field successional ecosystems in southern Illinois. Ecology 56:485–488

Binkley D, Stape JL, Ryan MG (2004) Thinking about efficiency of resource use in forests. For Ecol Manag 193:5–16

Binkley D, Campoe OC, Gspaltl M, Forrester DI (2011) Light absorption and use efficiency in forests: Why patterns differ for trees and stands. For Ecol Manage. doi:10.1016/j.foreco.2011.11.002

Bolte A, Villanueva I (2006) Interspecific competition impacts on the morphology and distribution of fine roots in European beech (Fagus sylvatica L.) and Norway spruce (Picea abies (L.) Karst.). Eur J For Res 125:15–26

Bremer M, Jochem A, Rutzinger M (2012) Comparison of branch extraction for deciduous single trees in leaf-on and leaf-off conditions—an eigenvector based approach for terrestrial laser scanning point clouds. EARSeL eProc 11(1):33–43

Bucksch AK (2011) Revealing the skeleton from imperfect point clouds. Dissertation, Delft University of Technology

Bucksch AK, Lindenbergh R, Menenti M (2010) SkelTre—Robust skeleton extraction from imperfect point clouds. Vis Comput 26:1283–1300

Burger H (1939) Holz, Blattmenge und Zuwachs. Mitt Schweiz Anst Forstl Versuchswesen 1939–1953, vol 15–29

Côté JF, Fournier RA, Egli R (2011) An architectural model of trees to estimate forest structural attributes using terrestrial LiDAR. Environ Model Softw 26:761–777

Edelsbrunner H, Mücke EP (1994) Three-Dimensional Alpha Shapes. ACM Transact Graph 13:43–72

Enquist BJ, Brown JH, West GB (1998) Allometric scaling of plant energetics and population density. Nature 395:163–165

Fischer A (1995) Forstliche Vegetationskunde. Pareys Studientexte 82. Blackwell Wissenschaft, Berlin, Wien

Grams TEE, Lüttge U (2011) Space as a resource. Prog Bot 72:349–370

Grams TEE, Kozovits AR, Winkler JB, Sommerkorn M, Blaschke H, Häberle K-H, Matyssek R (2002) Quantifying competitiveness in woody plants. Plant Biol 4:153–158

Hari P (1985) Theoretical aspects of eco-physioligical research. In: Tigerstedt PMA, Puttonen P, Koski V (eds) Crop physiology of forest trees. Helsinki Univ Press, Helsinki, pp 21–30 336p

Hilker T, van Leeuwen M, Coops NC, Wulder MA, Newnham GJ, Jupp DLB, Culvenor DS (2010) Comparing canopy metrics derived from terrestrial and airborne laser scanning in a Douglas-fir dominated forest stand. Trees 24:819–832

Huang P, Pretzsch H (2010) Using terrestrial laser scanner for estimating leaf areas of individual trees in a conifer forest. Trees 24:609–619

Lawton JH (1983) Plant architecture and the diversity of phytophagous insects. Ann Rev Entomol 28:23–39

MacArthur RH, MacArthur JW (1961) On bird species diversity. Ecology 42:594–598

Maneewongvatana S, Mount D (1999) It's okay to be skinny, if your friends are fat. In: Proceedings of the 4th Annual CGC Workshop on Computational Geometry

Matyssek R, Agerer R, Ernst D, Munch JC, Oßwald W, Pretzsch H, Priesack E, Schnyder H, Treutter D (2005) The Plant's Capacity in Regulating Resource Demand. Plant Physiol 7:560–580

McCoy ED, Bell SS (1991) Habitat structure: the evolution and diversification of a complex topic. In: Bell SS, McCoy ED, Mushinsky HR (eds) Habitat structure: the physical arrangement of objects in space. London, Chapman & Hall, pp 3–27

Niklas KJ (1994) Plant Allometry. Univ Chicago Press, Chicago

Oldemann RAA (1990) Forests: elements of Silvology. Springer, Berlin

Poorter H, Niklas KJ, Reich PB, Oleksyn J, Poot P, Mommer L (2012) Biomass allocation to leaves, stems and roots: meta-analysis of interspecific variation and environmental control. New Phytol 193:30–50

Pretzsch H (1992) Modellierung der Kronenkonkurrenz von Fichte und Buche in Rein- und Mischbeständen. AFJZ 163(11/12):203–213

Pretzsch H (2003) Diversität und Produktivität von Wäldern. AFJZ 174:88–98

Pretzsch H (2006) Species-specific allometric scaling under self-thinning. Evidence from long-term plots in forest stands. Oecologia 146:572–583

Pretzsch H (2009) Forest dynamics, growth and yield: From measurement to model. Springer, Berlin

Pretzsch H, Dieler J (2012) Evidence of variant intra- and interspecific scaling of tree crown structure and relevance for allometric theory. Oecologia. doi:10.1007/s00442-011-2240-5

Pretzsch H, Schütze G (2005) Crown allometry and growing space efficiency of Norway spruce (Picea abies (L.) Karst.) and European beech (Fagus sylvatica L.) in pure and mixed stands. Plant Biol 7:628–639

Pretzsch H, Schütze G (2009) Transgressive overyielding in mixed compared with pure stands of Norway spruce and European beech in Central Europe: evidence on stand level and explanation on individual tree level. Eur J For Res 128:183–204

Pretzsch H, Seifert S, Huang P (2011) Beitrag des terrestrischen Laserscannings zur Erfassung der Struktur von Baumkronen. Schweiz Z Forstwes 162:186–194

Pretzsch H, Block J, Dieler J, Dong PH, Kohnle U, Nagel J, Spellmann H, Zingg A (2010) Comparison between the productivity of pure and mixed stands of Norway spruce and European beech along an ecological gradient. Ann For Sci 67. doi:10.1051/forest/2010037

Price CA, Gilooly JF, Allen AP, Weitz JS, Niklas KJ (2010) The metabolic theory of ecology: prospects and challenges for plant biology. New Phytol 188:696–710

Purves DW, Lichstein JW, Pacala SW (2007) Crown plasticity and competition for canopy space: a new spatially implicit model parameterized for 250 North American tree species. PLoS ONE 2:e870. doi:10.1371/journal.pone.0000870

Ramachandran P, Varoquaux G (2008) Mayavi: making 3D data visualization reusable. In: Varoquaux G, Vaught T, Millman J (eds) Proceedings of the 7th Python in Science Conference. Pasadena, CA USA, pp 51–56

Richards AE, Forrester DI, Bauhus J, Scherer-Lorenzen M (2010) The influence of mixed tree plantations on the nutrition of individual species: a review. Tree Physiol 30:1192–1208

Röhle H, Huber W (1985) Untersuchungen zur Methode der Ablotung von Kronenradien und der Berechnung von Kronengrundflächen. Forstarchiv 56:238–243

Roloff A (2001) Baumkronen. Verständnis und praktische Bedeutung eines komplexen Natur-phänomens, Ulmer

Seifert T (2003) Integration von Holzqualität und Holzsortierung in behandlungssensitive Waldwachstumsmodelle. Dissertation, Technical University of Munich

Tews J, Brose U, Grimm V, Tielbörger K, Wichmann MC, Schwager M, Jeltsch F (2004) Animal species diversity driven by habitat heterogeneity/diversity: the importance of keystone structures. J Biogeogr 31:79–92

van Leeuwen M, Hilker T, Coops NC, Frazer G, Wulder MA, Newnham GJ, Culvenor DS (2011) Assessment of standing wood and fiber quality using ground and airborne laser scanning: a review. For Ecol Manag 261:1467–1478

von Droste zu Hülshoff B (1969) Struktur und Biomasse eines Fichtenbestandes auf Grund einer Dimensionsanalyse an oberirdischen Baumorganen. Ph.D thesis, LMU München, 209 p

Vosselman G, Maas HG (2010) Airborne and terrestrial laser scanning. Whittles Publishing, Dunbeath

Walter H (1931) Die Hydratur der Pflanzen und ihre physiologisch-ökologische Bedeutung. Gustav Fischer Verlag, Jena

West GB, Enquist BJ, Brown JH (2009) A general quantitative theory of forest structure and dynamics. PNAS 106:7040–7045

Wilhelmsson L, Arlinger J, Spångberg K, Lundqvist SO, Grahn T, Hedenberg Ö, Olsson L (2002) Models for predicting wood properties in Stems of picea abies and pinus sylvestris in Sweden. Scand J For Res 17:330–350

Zeide B (1998) Fractal analysis of foliage distribution in loblolly pine crowns. Can J For Res 28:106–114

Zobel B, van Buijtenen J (1989) Wood Variation—its causes and control. Springer, Berlin

Beyer et al. 2017
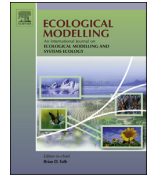
Validation of a functional-structural tree model using terrestrial Lidar data

Robert Beyer [a],[*],[1], Dominik Bayer [c],[1], Véronique Letort [b], Hans Pretzsch [c], Paul-Henry Cournède [b]

[a] McDonald Institute for Archaeological Research, University of Cambridge, Cambridge CB2 3ER, United Kingdom
[b] Laboratoire de Mathématiques et Informatique pour la Complexité et les Systèmes, CentraleSupélec, Université Paris-Saclay, Grande Voie des Vignes, 92295 Châtenay-Malabry, France
[c] Technische Universität München, Chair for Forest Growth and Yield Science, Hans-Carl-von-Carlowitz-Platz 2, 85354 Freising, Germany

ARTICLE INFO

ABSTRACT

We compared the spatial output of the functional-structural tree growth model recently presented by Beyer et al. (2017) to empirical tree crowns of European beech (*Fagus sylvatica* L.) obtained via terrestrial laser scanning. Simulations are found to be morphologically similar to the observed 3D data in terms of size and shape, as well as, quantitatively, contained withing its standard range. We argue that Lidar data provides an unprecedented degree of information on tree geometry compared to traditional forest inventory measurements, and can thus greatly contribute to the parameterisation and validation of tree growth models.

© 2017 Elsevier B.V. All rights reserved.

1. Introduction

In recent years, the acquisition and analysis of 3D spatially resolved tree and forest data has been considerably shaped by terrestrial Lidar imagery (Van Leeuwen and Nieuwenhuis, 2010; Pretzsch et al., 2011; Bayer et al., 2013; Moskal, 2014; Durrieu and Véga, 2015). These applications drive the simultaneous development of algorithms allowing the efficient and robust reconstruction of tree crown shape and branch geometries from Lidar point clouds (Pfeifer et al., 2004; Zhu et al., 2008; Yan et al., 2009; Livny et al., 2010; Preuksakarn et al., 2010; Raumonen et al., 2013; Gibbs et al., 2017).

(Functional-)Structural tree growth models (Prusinkiewicz and Lindenmayer, 1990; Kurth, 1994; Sievänen et al., 2000; Godin and Sinoquet, 2005; Sievanen et al., 2014) can greatly benefit from this novel type of data, which offer a degree of spatial information that traditional forest inventory data such as tree height, trunk diameter or crown radius cannot provide. However, with the recent exception of Potapov et al. (2016), 3D Lidar data has not yet found its way into the parametrisation or validation of spatially explicit tree growth models. Challenges that may be associated with the use of

Lidar data for modelling may include high financial and personal costs linked to data collection, the need for technical expertise to apply the appropriate point cloud processing methods, if necessary, as well as the task of developing suitable metrics in order to compare model simulation outputs to empirical 3D data.

In a recent article (Beyer et al., 2017), we presented a functional-structural tree growth model based on the notion of 3D spatial leaf area density. Based on Beer-Lambert's law, we determined local light conditions within the crown, which are used to compute local biomass production. The local transport of biomass, prior to its allocation in accordance with the pipe model theory, is directed along the local light gradient, which induces an upward and horizontal expansion of the simulated crown over time that adapts to the presence of competitors. Our calibrated model accurately predicted long-term tree height and trunk diameter dynamics of 16 stands of European beech (*Fagus sylvatica* L.), crown radius as well as the allometric 3/4-rule (Beyer et al., 2017, Figs. 2–5).

Beyond the qualitative comparison to the typical shape of a mature beech crown in the original article (Beyer et al., 2017, Fig. 3), here, we quantitatively compare the simulated tree crown, characterised in terms of its 3D spatial leaf density, to empirical crowns obtained from terrestrial Lidar scans. While our approach is by no means without technical caveats, we intend for it to be a contribution towards a more pronounced role of Lidar data in the parametrisation and validation of functional-structural tree growth models.

---

* Corresponding author.
E-mail address: rb792@cam.ac.uk (R. Beyer).
[1] Both authors joint as first authorship.
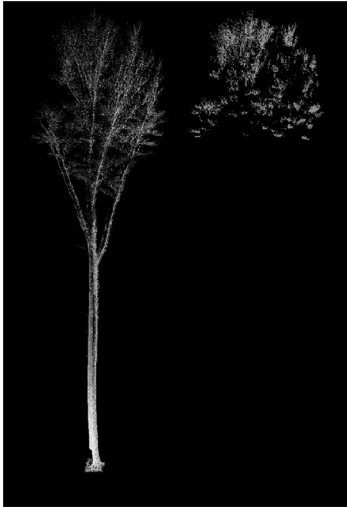
Fig. 1. Tree laser scan point cloud and isolated twig structures.

2. Materials and methods

We acquired Lidar scans for sub-plot 3 of the European beech experimental site "Fabrikschleichach" (cf. Section 3.1 of Beyer et al., 2017, for details) in March 2012 (when the stand aged 180 years) using the Riegl LMS-Z420i laser scanning system. Its infrared laser beams do typically not penetrate tree compartments, hence a dense canopy can significantly distort a scan image. This motivated to scan trees in leafless conditions and to compare the model's simulated leaf area density to a spatial twig density, as described below. For the same reason, we used the last-pulse distance measurement mode in which the last echo of the laser impulse is used for distance recording, allowing the laser beam to penetrate the tree crown further than using the regular, first-pulse mode. In order to cover the trees thoroughly and minimise additional distortion, we took a total of ten upright and tilted scans from five regularly distributed positions within the stand, and merged those into one image. Bayer et al. (2013) elaborated further on general technical and procedural details, and addressed the impracticality of applying automatic skeletonisation algorithms to scans at the forest stand scale. Individual trees and subsequently their respective twigs were manually isolated from the final scan image (Fig. 1). Altogether we obtained a total of 10 samples.

We presume that the empirical 3D twig density and leaf area density essentially differ only by a multiplicative constant. Equivalently, relative twig density and relative leaf area density, both normed such that their integrals equal 1, are assumed to roughly coincide. For a given 3D grid, the former is obtained from a given laser scan point cloud by first assigning to each voxel the number of laser points contained in it. Dividing this absolute frequency by the total number of points and the voxel volume yields a (step-function) density with integral 1 for each sample. Denote these by $\tilde{v}_i(x), x \in \mathbb{R}^3, i = 1, \ldots, m$, with $m = 10$. Let

$$x \mapsto \bar{v}(x) = \frac{1}{m} \cdot \sum_{i=1}^{m} \tilde{v}_i(x) \text{ and } \sigma_{\tilde{v}} = \sqrt{\frac{1}{m} \cdot \sum_{i=1}^{m} \|\bar{v} - \tilde{v}_i\|^2}$$

denote their mean and standard deviation, respectively, where $\|\cdot\|$ denotes the L^2-norm ($\|f\| = \sqrt{\int_{\mathbb{R}^3} |f(x)|^2 \, dx}$).

We can quantitatively compare the empirical densities $\tilde{v}_1 \ldots, \tilde{v}_m$ to the relative leaf density $x \mapsto \widetilde{u}(x) = \frac{u(x, 180 \, \text{years})}{\int_{\mathbb{R}^3} u(\xi, 180 \, \text{years}) \, d\xi}$ (in the notation of Beyer et al., 2017) provided by the growth model. The model performs well if the simulated density $\tilde{u}$ is not more distant from the average empirical density $\bar{v}$ than the standard deviation $\sigma_{\tilde{v}}$, i.e. if

$$\|\tilde{u} - \bar{v}\| \leq \sigma_{\tilde{v}}.$$

3. Results

Fig. 2 gives a visual comparison of $\bar{v}$ and the relative leaf density $\tilde{u}$ provided by the model simulations at 180 years. We note similar dimensions in terms of height and radius (cf. Beyer et al., 2017, Figs. 2i and 3a]) as well as a distinct concavity for both crowns. While the simulated crown corresponds well to the typical structure of beech crowns in the given growth conditions that is pictured by Horn (1971), Roloff (2001) and Pretzsch (2014, Fig. 9a), where the bulk of foliage is concentrated in a thin layer along the upper crown hull, we also note a positive density in lower regions of the empirical data. This may in parts be attributed to the relatively small size of ten samples: Whereas single unusually low branches resulting from randomness have presumably little relevance in the case of a large sample set, they may act distortively otherwise. Nevertheless, this also points to limitations of the idealised monolayer stereotype. Overall, however, we observe a concentration of the empirical
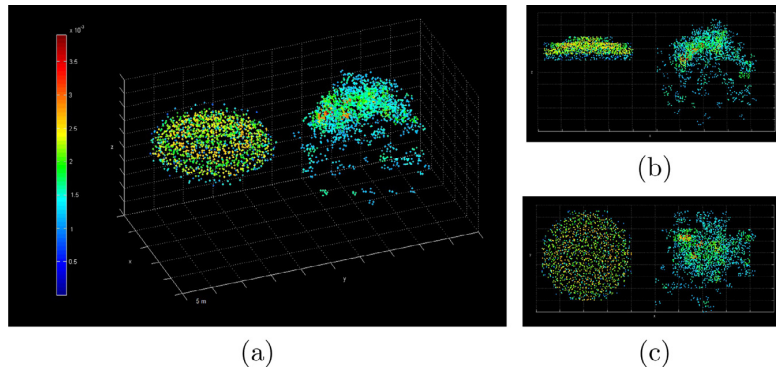
Fig. 2. (a) Oblique, (b) side and (c) top view of mean empirical (right) and simulated (left) relative twig- and leaf area density, $\bar{v}$ and $\tilde{u}$, respectively (cf. Beyer et al., 2017, Fig. 3 for a vertical cross-section of u).

density in the upper regions, in accordance with the simulation output.

On a quantitatively level, we find that $\tilde{u}$ is contained in the $\sigma_{\tilde{v}}$-ball about $\bar{v}$ with $\|\tilde{u} - \bar{v}\| = 0.0135 < 0.0182 = \sigma_{\tilde{v}}$. The simulated crown is thus within the standard range of crown shapes for the given age and growth conditions, as desired.

4. Discussion

In addition to long-term forest inventory and allometric data, here, we used 3D terrestrial Lidar data to evaluate the tree growth model previously presented by Beyer et al. (2017). The extracted empirical relative twig densities and the simulated relative leaf density proved morphologically similar in terms of size and shape, and were found to be reasonably close under an appropriate metric. We thereby illustrated how Lidar data can be linked to and used for the analysis of spatial simulation output of a functional-structural growth model.

Resorting to twig density, and consequently considering relative densities, was inevitable in view of the technical and logistic impossibility of obtaining realistic leaf densities throughout the crown from leafed trees, especially in the forest stand, as opposed to for solitary trees (Bayer et al., 2013), and for a reasonably large number of individuals. For monolayer species, additional airborne Lidar images, e.g. using drones (Tang and Shao, 2015; Zhang et al., 2016), may be able to complement terrestrial data, and thus allow an improved, direct comparison of absolute empirical and simulated 3D leaf densities.

In view of the potential in the field of structural tree modelling that 3D Laser scan data offers in terms of detailed tree geometry, tree growth modellers could greatly benefit from working closely with Lidar technicians, data collectors and empiricists. Thus, the appropriate type, scale, detail and amount of 3D data can be specifically identified, and eventually used to contribute to the estimation of growth model parameters or to model validation, based on empirical data. In parallel, hard- and software advances to make Lidar more accessible, logistically practicable and efficient, as well as the development of readily applicable data processing algorithms continue to be needed.

References

Bayer, D., Seifert, S., Pretzsch, H., 2013. Structural crown properties of Norway spruce (*Picea abies* [L.] Karst.) and European beech (*Fagus sylvatica* [L.]) in mixed versus pure stands revealed by terrestrial laser scanning. Trees 27, 1035–1047.

Beyer, R., Letort, V., Bayer, D., Pretzsch, H., Cournède, P.-H., 2017. Leaf density-based modelling of phototropic crown dynamics and long-term predictive application to European beech. Ecol. Model. 347, 63–71.

Durrieu, S., Véga, C. (Eds.), 2015. Proceedings of SilviLaser 2015. 14th Conference on Lidar Applications for Assessing and Managing Forest Ecosystems.

Gibbs, J.A., Pound, M., French, A.P., Wells, D.M., Murchie, E., Pridmore, T., 2017. Approaches to three-dimensional reconstruction of plant shoot topology and geometry. Funct. Plant Biol. 44 (1), 62–75.

Godin, C., Sinoquet, H., 2005. Functional-strucutral plant modelling. New Phytologist 166, 705–708.

Horn, H.S., 1971. The Adaptive Geometry of Trees, vol. 3. Princeton University Press.

Kurth, W., 1994. Morphological models of plant growth: possibilities and ecological relevance. Ecol. Model. 75, 299–308.

Livny, Y., Yan, F., Olson, M., Chen, B., Zhang, H., El-Sana, J., 2010. Automatic reconstruction of tree skeletal structures from point clouds. In: ACM Transactions on Graphics (TOG), vol. 29. ACM, pp. 151.

Moskal, L.M. (Ed.), 2014. Special Issue: Lidar and Other Remote Sensing Applications in Mapping and Monitoring of Forests Structure and Biomass. Forests.

Pfeifer, N., Gorte, B., Winterhalder, D., et al., 2004. Automatic reconstruction of single trees from terrestrial laser scanner data. In: Proceedings of 20th ISPRS Congress, ISPRS, Istanbul, pp. 114–119.

Potapov, I., Järvenpää, M., Åkerblom, M., Raumonen, P., Kaasalainen, M., 2016. Data-based stochastic modeling of tree growth and structure formation. Silva Fennica 50 (1).

Pretzsch, H., 2014. Canopy space filling and tree crown morphology in mixed-species stands compared with monocultures. Forest Ecol. Manage. 327, 251–264.

Pretzsch, H., Seifert, S., Huang, P., 2011. Beitrag des terrestrischen laserscannings zur erfassung der struktur von baumkronen| application of terrestrial laser scanning for measuring tree crown structures. Schweiz. Z. Forstwes. 162 (6), 186–194.

Preuksakarn, C., Boudon, F., Ferraro, P., Durand, J.-B., Nikinmaa, E., Godin, C., 2010. Reconstructing plant architecture from 3d laser scanner data. 6th International Workshop on Functional-Structural Plant Models, 12–17.

Prusinkiewicz, P., Lindenmayer, A., 1990. The Algorithmic Beauty of Plants. Springer.

Raumonen, P., Kaasalainen, M., Åkerblom, M., Kaasalainen, S., Kaartinen, H., Vastaranta, M., Holopainen, M., Disney, M., Lewis, P., 2013. Fast automatic precision tree models from terrestrial laser scanner data. Remote Sens. 5 (2), 491–520.

Roloff, A., 2001. Baumkronen: Verständnis und praktische Bedeutung eines komplexen Naturphänomens. Ulmer.

Sievänen, R., Nikinmaa, E., Nygren, P., Ozier-Lafontaine, H., Perttunen, J., Hakula, H., 2000. Components of a functional-structural tree model. Ann. Forest Sci. 57, 399–412.

Sievanen, R., Godin, C., DeJong, T.M., Nikinmaa, E., 2014. Functional-structural plant models: a growing paradigm for plant studies. Ann. Bot. 114, 599–603.

Tang, L., Shao, G., 2015. Drone remote sensing for forestry research and practices. J. For. Res. 26 (4), 791–797.

Van Leeuwen, M., Nieuwenhuis, M., 2010. Retrieval of forest structural parameters using Lidar remote sensing. Eur. J. Forest Res. 129 (4), 749–770.

Yan, D.-M., Wintz, J., Mourrain, B., Wang, W., Boudon, F., Godin, C., 2009. Efficient and robust reconstruction of botanical branching structure from laser scanned points. In: 11th IEEE International Conference on Computer-Aided Design and Computer Graphics, CAD/Graphics'09, IEEE, pp. 572–575.

Zhang, J., Hu, J., Lian, J., Fan, Z., Ouyang, X., Ye, W., 2016. Seeing the forest from drones: testing the potential of lightweight drones as a tool for long-term forest monitoring. Biol. Conserv. 198, 60–69.

Zhu, C., Zhang, X., Hu, B., Jaeger, M., 2008. Reconstruction of tree crown shape from scanned data. International Conference on Technologies for E-Learning and Digital Entertainment, 745–756.

Bayer and Pretzsch 2017

SILVA FENNICA

Dominik Bayer and Hans Pretzsch

Reactions to gap emergence: Norway spruce increases growth while European beech features horizontal space occupation – evidence by repeated 3D TLS measurements

Highlights

- Analysis of the closure dynamics of a Norway spruce, a European beech and a mixed forest gap by repeated TLS measurements.
- Norway spruce allocated additional resources predominantly into DBH growth and displayed stronger resilience against mechanical crown damage.
- European beech allocated resources towards space occupation and displayed higher crown plasticity.
- Species mixture had no significant effect.

Abstract

The reach of different tree species' crowns and the velocity of gap closure during the occupation of canopy gaps resulting from mortality and thinning during stand development determine species-specific competition and productivity within forest stands. However, classical dendrometric methods are rather inaccurate or even incapable of time- and cost-effectively measuring 3D tree structure, crown dynamics and space occupation non-destructively. Therefore, we applied terrestrial laser scanning (TLS) in order to measure the structural dynamics at tree and stand level from gap cutting in 2006 until 2012 in pure and mixed stands of Norway spruce (*Picea abies* [L.] Karst.) and European beech (*Fagus sylvatica* L.). In conclusion, our results suggest that Norway spruce invests newly available above-ground resources primarily into DBH as well as biomass growth and indicate a stronger resilience against loss of crown mass induced by mechanical damage. European beech showed a vastly different reaction, investing gains from additional above-ground resources primarily into faster occupation of canopy space. Whether our sample trees were located in pure or mixed groups around the gaps had no significant impact on their behavior during the years after gap cutting.

1

Abbreviations

The following abbreviations are used in this manuscript:

A_{DBH}: Temporal allometric coefficient for the allocation ratio between crown diameter and DBH
A_H: Temporal allometric coefficient for the allocation ratio between crown diameter and H
A_B: Temporal allometric coefficient for the allocation ratio between crown diameter and B
DBH: Diameter at Breast Height (1.3 m)
CPA: Crown Projection Area
CPAG: Crown Projection Area Growth
D: Diameter of a hypothetical circle encompassing the same area as the respective sample tree's CPA
GPA: Gap Projection Area
EOC: Efficiency of Space Occupation
EEX: Efficiency of Space Exploitation
EBI: Efficiency of Biomass Investment
H: Tree height
TLiDAR: Terrestrial Light Detection and Ranging (see also: TLS)
TLS: Terrestrial Laser Scanning
ML: Multi-Layering
RML: Relative Multi-Layering

1 Introduction

During the long lifetime of forest stands, various kinds of disturbances (e.g., tree mortality due to competition, storm damage, bark beetle attacks or thinning) repeatedly cause openings in the canopy and vacancies in the root space. In the past, these forest gaps were mainly of interest regarding the mosaic-cycle concept of natural unmanaged ecosystems (Mueller-Dombois 1991; Remmert 1991; Lertzman et al. 1996). However, in the ongoing transition from rather homogeneous monocultures to more heterogeneous mixed-species stands, silviculturally generated gaps play an essential role (Burschel and Huss 1997; Puettmann et al. 2012; Drössler et al. 2016).

Gaps are, for instance, cut into stands of middle or advanced age to initiate natural regeneration, to promote light demanding underplanting or to prepare the establishment of light demanding species as well as to enhance and promote structural and habitat diversity (Pretzsch et al. 2015). Silvicultural concepts such as selection cutting, femel coupe, or gap cutting, which result in opened canopies, gain currency. In addition, gaps often result from disturbances such as bark beetle attacks, wind throw, and snow-breakage. So, apart from the juvenile stand phase fully stocked, stands without gaps were standard in the past but have become rather an exception at present. This tendency towards gap rich stand structures has been strongly promoted by the concept of emulation of natural disturbance in forest management (Buddle et al. 2006; Kuuluvainen and Grenfell 2012). In most European forest ecosystems the natural dynamics would follow the mosaic-cycle dynamics with a gap phase caused by randomly distributed natural death of trees or tree groups. By anticipating their natural death and cutting them when still of merchantable value, forest management nowadays partly emulates the natural stand development regime (Kuuluvainen and Grenfell 2012).

Methods for measurement and quantification (Assmann 1970; Röhle and Huber 1985) as well as modelling (Pretzsch 1992; Pretzsch 2006) have been improved and refined in the past. However, although it is evident that the competition for canopy space and its associated resources is a major

2

driver of forest dynamics (Purves et al. 2007), and forests are more and more dominated by gaps and border trees, knowledge of tree and stand dynamics at the border to gaps is still scarce. The main reason for this deficit is that the establishment, structure and dynamics of gaps and trees at gap borders are difficult to measure (van der Meer and Bongers 1996) by classical methods due to constraints of measuring the three-dimensional structure of tree crowns. Leaning and straightness of border trees, their branches and crown eccentricity for example, are hardly measurable by optical plummet or hypsometer but determine wood quality (Pretzsch and Rais 2016). Crown extension, layering, and transparency are difficult to access by hemispherical photography but important for understanding and modelling light conditions within the gap, velocity of gap closure, and growth resilience after gap cutting (Dieler and Pretzsch 2013; Seidel et al. 2015). Furthermore, the roughness of the canopy surface and the borderline of gaps is important to know as it can increase the susceptibility to wind-throw (Quine and Gardiner 2007), the habitat quality and species diversity (Goetz et al. 2010; Müller et al. 2012).

The progress of three-dimensional high-precision techniques for measurements within forest stands, such as terrestrial laser scanning (TLS) during the last decade however, makes these highly valuable, yet hard to determine parameters more and more accessible. Studies utilizing TLS have, especially during recent years, started to outgrow the stage of pure methodological (Bucksch et al. 2010; Côté et al. 2011; Hackenberg et al. 2015) development towards important contributions to the understanding of ecological questions. Bayer et al. 2013 for example was one of the first studies investigating relationships between the inner crown morphology as well as crown shape and the surrounding stand. Former studies used TLS-derived individual tree parameters to relate a tree's shape (Seidel et al. 2011) or growth (Metz et al. 2013) to its surrounding stand. Other studies have for example dealt with TLS measurements in forest gaps and the impact of gaps on tree diameter increment and crown shape (Seidel et al. 2015; Seidel et al. 2016).

Our study analyzes forest gap border trees using repeated measurements to scrutinize their actual development over time. Based on repeated TLS measurements of the crown structure from 2006–2012 and additional longer term terrestrial measurement of annual growth rates of pure and mixed stands of Norway spruce (*Picea abies* [L.] Karst.) and European beech (*Fagus sylvatica* L.), we scrutinize (i) the species- and gap type specific effect of gap-emergence on the crown structure and allometric relations on tree level, (ii) the utilization of the newly available above-ground resources and (iii) the development of the crown cover in the gap area concerning space occupation and multi-layering.

2 Materials and methods

2.1 Study area

The analyzed gaps lie within the experimental plot FRE 813/1, located at the "Kranzberger Forst" near Freising in Southern Bavaria, Germany (48°42´N, 11°66´E). The study site is located 490 m above sea-level in the ecological region "Tertiäres Hügelland. Oberbayerisches Tertiärhüggelland" on a Luvisol, derived from loess over tertiary sediments. The long-term averages of annual air temperature range between 7 °C and 8 °C, accompanied by an annual precipitation of 750–850 mm (BayFORKLIM 1996). Norway spruce and European beech are the main tree species. There are occasional single members of other species present, however they do not contribute significantly to the overall stand structure and are not located in proximity to our sample trees. The sample trees themselves are members of a pure spruce and a beech group as well as a group composed of both species in mixture. During 2007, the average stand age was determined as 56 (spruce) and 66

3

years (beech). In order to create gaps, two trees have been harvested in the middle of the respective group before the first laser scan acquisition has been made in autumn 2006.

We defined and quantified the gap area of each gap as a polygon using the middle of the stem bases of the surrounding trees as vertices. This way, the areas are fixed over the different scan acquisition dates and take the specific shape of each gap into account. The resulting gap polygon areas cover 32.18 m^2 (spruce), 54.77 m^2 (beech) and 84.03 m^2 (mixed).

2.2 Scan acquisition

The TLS scans were acquired during the leafless state of the sample trees in the years 2006, 2008, 2010 and 2012. Fixed, permanently installed reflectors facilitated the precise alignment of the repeated measurements' point clouds. The Riegl LMS-Z360 laser scanning system was used in 2006 and 2008, while the newer, more advanced Riegl LMS-Z420i, was used for the later data acquisitions of 2010 and 2012. In order to cover the gaps, three scan positions arranged roughly in a triangle formation around the trees representing the respective gap have been set up for each measurement. Additionally, we set up a fourth scan position in the middle of each gap, in order to gain undisturbed and sharp data of the boundaries of the available free space. During each position-ing of the scanner, we closely paid attention to ensure a field of view with as little occultation of the crowns as possible. The vertical and horizontal angular resolution was set to 0.06° in order to achieve a sensible trade-off between scan-time, risk of disturbances due to tree movement caused by wind and resolution.

Both systems work according to the time-of-flight principle. A short laser impulse is fired in a specified direction towards a target. Part of the light is reflected back to the scanner which measures the time between firing and the return of the laser impulse. The speed of light in air c_{air}, adjusted by air temperature, pressure and moisture, in combination with the time of flight of the laser impulse results in the measurement distance $d_l = 0.5t \times c_{air}$. Distance and direction yield the spherical coordinates of the target which are translated to Cartesian coordinates for further processing. The many consecutive measurements finally result in a three-dimensional image of the scanned region.

Due to the widening of the scan angles with increasing distance to the scanner, the measure-ment density drops with distance. Furthermore, the laser beam is normally not able to penetrate tree compartments in order to perform measurements behind obstacles. These two effects result in rather sparse measurement densities in the upper crown regions, especially if the crown parts near to the scanner are dense, like those of conifers (Hilker et al. 2010). In the case of this study however, these effects are less relevant because (i) for every gap measurement, one of the scanner positions lied in the middle of the respective gap and was therefore located closest to the crown regions of the most interest, namely the regions directed towards the gap middle and (ii) we used a distance measurement mode which is called last-pulse or last-target, gaining a higher proportion of returns from inner crown regions than by using the devices' first-pulse modes.

2.3 Structure analysis

After the acquisition of our scans, the data of all scan positions and dates were referenced to each other. Then, the individual tree scans were manually extracted and exported using the scanner manufacturer's software RiSCAN PRO. Further processing was done within the programming environments of Python and R.

In order to derive projected areas and volumes from our point clouds, we utilized two- and three-dimensional α-shapes. These α-shapes are generalizations of the convex hull of a point

4

set based on Delaunay triangulation (Edelsbrunner et al. 1983; Edelsbrunner and Mücke 1994). Thereby, the so-called α-value is a parameter controlling the level of detail in which the calculated shape represents the point cloud. It can range from α→0, which yields the point cloud itself, to α→∞, yielding the convex hull of the point cloud.

The biggest issue in using α-shapes for the reconstruction of shapes from point sets is the choice of an appropriate α-value. Applying too large α-values leads to coarse hulls, which is not desirable since much of the detailed information in the original TLS point cloud is lost. However, too small values result in incomplete reconstructions of the original TLS data if the distance between measured points cannot be covered by the application radius of the α-shape. In our study, we determined α-values which yield solid, yet detailed α-shapes by calculating various α-shapes using a series of α-values ranging from very small (0.05 m) to relatively large (10 m). Real perimeters and surfaces show fractal-like properties, meaning that their measured values rise with smaller measurement units (Mandelbrot 1967). Therefore, in an ideal world with unlimited data resolution, the perimeter (2D) or the surface (3D) of an α-shape of the same point cloud must increase with decreasing α-value as long as the calculation yields robust results. For our data, this behavior held true until α=0.25 m for 2D and α=0.30 m for 3D calculations which are the values we used.

The crown projection areas CPA_{tot} were calculated by projecting the respective point cloud onto the xy-plane. After the projection, the sum of all surfaces of the triangles generated by the involved Delauny triangulation determine the respective 2D α-shape's surface area. Furthermore, we calculated the surface areas of subsets of each crown's point cloud which represent the share of the crown projection lying in- (CPA_{in}) and outside (CPA_{out}) the defined gap polygon (Fig. 1, blue and green shaded areas). Analogously, the volumes of 3D α-shapes were computed by summation of their contained tetrahedrons' volumes.

In order to determine the crown volumes, we cut the point clouds at the point where the crown commences and calculated the 3D α-shape volumes of the remaining points. To specify the vertical shape of a sample tree's crown, its point cloud was horizontally sliced into compartments of 1m height. Each compartment was projected flat to the xy-plane. Then, its surface was derived from its 2D α-shape as described above. The height of the slice with the largest surface within the crown in relation to the overall crown height describes the vertical crown shape H_{CPA}. Each of the described calculations were done for every sample tree and measurement in order to scrutinize the respective development over time.

To describe the gap's impact on resource allocation, we also computed temporal allometric coefficients which describe the allocation ratio between crown diameter and DBH (A_{DBH}, Eq. 1), crown diameter and height H (A_H, Eq. 2) as well as crown diameter and biomass B (A_B, Eq. 3)

$$A_{DBH} = \frac{\Delta D / D}{\Delta DBH / DBH}, \tag{1}$$

$$A_H = \frac{\Delta D / D}{\Delta H / H}, \tag{2}$$

$$A_B = \frac{\Delta D / D}{\Delta B / B} \tag{3}$$

whereby D is the diameter of a hypothetical circle encompassing the same area as the respective sample tree's CPA to normalize crown diameter despite a crown's natural irregularities. Biomasses used here and later have been estimated using the set of biomass functions provided by (Pretzsch et al. 2014).

5
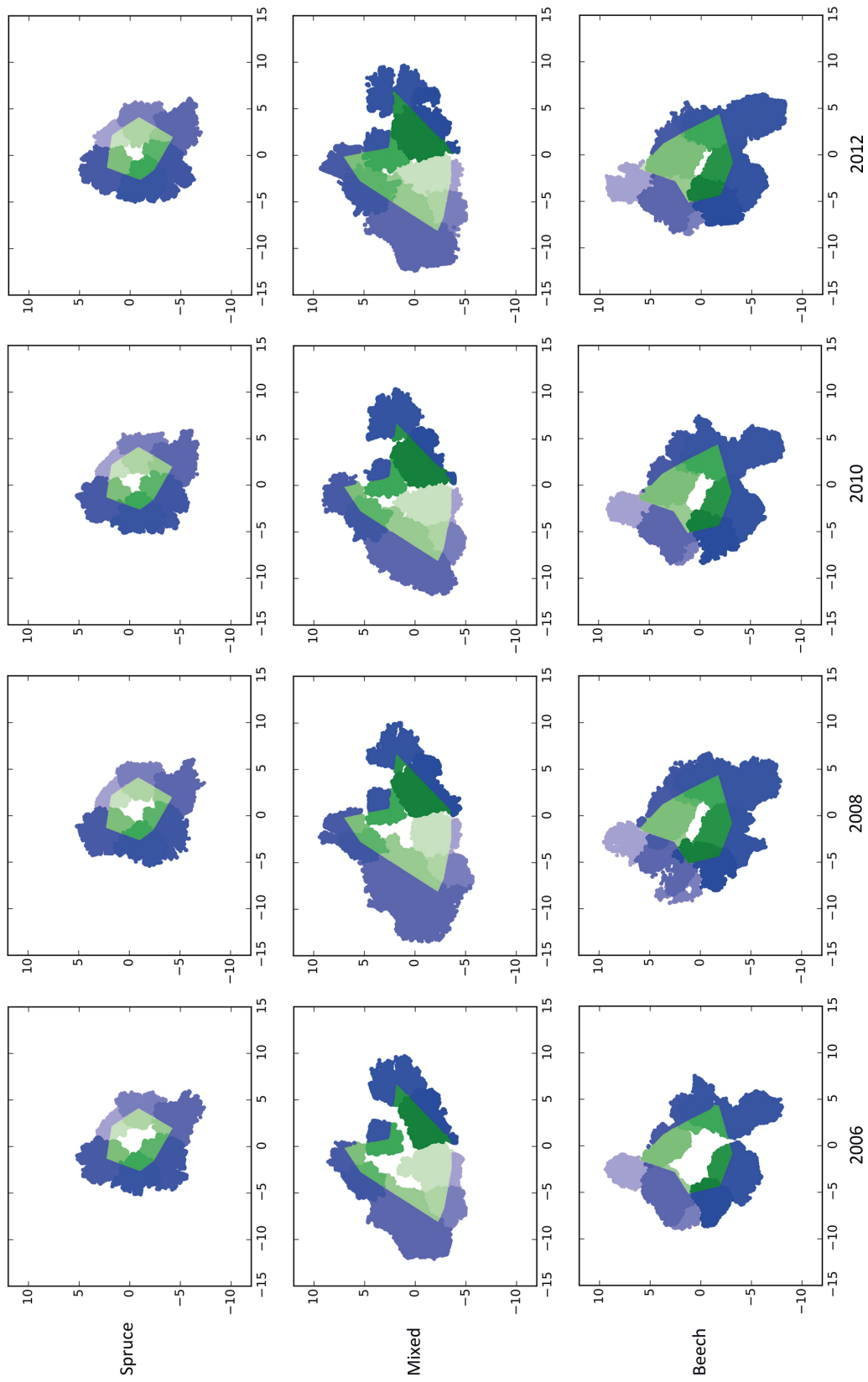
Fig. 1. Bird's eye view of the TLS scans showing the crown closure from 2006–2012 in pure stands of Norway spruce (top row), a mixed stand of Norway spruce and European beech (middle row) and European beech (bottom row) after generating gaps (white centres) by thinning on the experimental plot FRE 813/1 in 2006. The green areas mark the portion of the crowns lying inside the gap polygon. Blue areas mark the crown regions outside the polygon borders. Different shades of green and blue are given to make the gap's individual trees visible.

The increase in total crown projection area (CPA_{tot}) was scrutinized not only by computing the change of the CPA_{tot} itself over time, but also by distinguishing between the crown parts in- and outside the defined gap polygon, so the relative CPA growth towards ($CPAG_{in}$) and away from the gap area ($CPAG_{out}$) could be determined (Eq. 4, Eq. 5).

$$CPAG_{in} = \frac{CPA_{in_i} - CPA_{in_{i-1}}}{CPA_{in_{i-1}}}, \tag{4}$$

$$CPAG_{out} = \frac{CPA_{out_i} - CPA_{out_{i-1}}}{CPA_{out_{i-1}}}, \tag{5}$$

In line with Matyssek et al. 2002 and the idea that growth can be conceived as a resource investment in order to occupy space, we quantified a sequence of cost/benefit relations. Thereby a measure of biomass efficiency in terms of space occupation is given by the efficiency of space occupation EOC (Eq. 6) which sets the CPA in relation to the existing biomass. Another descriptive parameter we used in this study is the efficiency of space exploitation EEX, quantifying the relation between biomass increase and projected crown area (Eq. 7) as well as the efficiency of biomass investment EBI which quantifies the relation between existing biomass and biomass growth G_B (Eq. 8).

$$EOC = \frac{CPA}{B}, \tag{6}$$

$$EEX = \frac{\Delta B}{CPA}, \tag{7}$$

$$EBI = \frac{\Delta B}{B}, \tag{8}$$

On gap level, we derived the total projection area for every gap GPA within its polygon borders, viewing the gap as a whole. By comparing the GPA with the sum of the individual tree crowns the gap is comprised of, we can derive the multi-layered area i.e. the area which is overshadowed by more than one crown (Eq. 9). Furthermore, for comparability we calculated gap closure values and multi-layering values relative to the respective gap sizes.

$$ML = -GPA + \sum_{i=1}^{n} CPA_i, \tag{9}$$

3 Results

Fig. 1 gives a bird's eye view of the spruce, beech and mixed gap trees' TLS point cloud representations of all four measurement dates. As expected, within all three groups, crown expansion, especially towards the newly emerged free space, is clearly visible.

7

Table 1. Individual tree parameters by species from 2006 to 2012.

Species	Year	N	DBH [cm]	SE	H [m]	SE	CPA_{tot} [m²]	SE	H_{CPA} [%]	SE
Norway spruce	2006	10	33.9	2.04	28.3	0.52	14.3	1.49	54.2	0.03
	2008	10	35.0	2.03	28.6	0.50	15.1	1.24	52.1	0.02
	2010	10	36.1	2.06	28.8	0.48	15.9	1.05	53.4	0.03
	2012	10	37.1	2.04	29.0	0.46	17.8	1.12	54.0	0.03
European beech	2006	12	25.6	1.77	26.6	0.30	19.4	2.75	57.1	0.04
	2008	12	26.1	1.80	27.0	0.30	26.3	4.12	59.0	0.05
	2010	12	26.4	1.82	27.3	0.31	22.0	3.22	60.1	0.04
	2012	12	26.7	1.83	27.6	0.31	24.4	3.62	58.3	0.04

N = number of trees, DBH = diameter at breast height, H = height, CPA_{tot} = mean crown projection area derived from two-dimensional α-shapes (α = 0.25 m), H_{CPA} = relative height within crown with maximum projection area, SE = standard error.

3.1 Individual tree paramneters

During the observation period from 2006 to 2012, Norway spruce's mean height increased from 28.3 m to 29.0 m and from 26.6 m to 27.6 m in case of European beech. The mean DBH of our sample spruces increased from 33.9 cm in 2006 to 37.1 cm in 2012, the mean DBH of beech grew from 25.6 cm to 26.7 cm over the same period (Table 1).

While Norway spruce increased its α-shape derived mean crown projection area (CPA_{tot}) from 14.3 m² (2006) to 17.8 m² (2012) in a steady fashion, European beech presents a jump during the observation period from 2006 (19.4 m²) to 2008 (26.3 m²) directly following the cutting and a retreat back to 22.0 m², suggesting events leading to mechanical damage during the period from 2008 to 2010 (Fig. 2).

The relative height of the maximum crown projection area (H_{CPA}), describing the vertical crown shape averages to 53.4 % (spruce) and 58.6 % (beech) over all observation periods. However, no clear development trend can be observed.
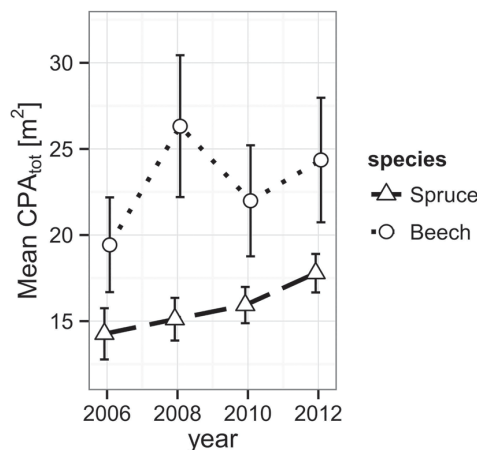
Fig. 2. Development of the mean crown projection area (CPA) derived from α-shapes (α = 0.25 m) of the individual trees' TLS point clouds for both species from 2006 to 2012. The error bars mark the one-fold standard error.

8

Table 2. Allometric parameters.

Species	Year	A_{DBH}	SE	A_H	SE	A_B	SE
Norway spruce	2008	1.39	1.01	4.40	5.52	0.67	0.51
	2010	0.95	0.66	4.74	2.84	0.47	0.32
	2012	1.56	0.44	6.97	2.64	0.77	0.22
European beech	2008	11.02	3.75	12.60	1.95	3.74	0.99
	2010	−7.48	2.51	−10.19	3.75	−2.74	0.93
	2012	4.18	1.10	2.14	2.96	−1.54	3.06

A_{DBH} = allocation ratio between crown diameter and DBH, A_H = between crown diameter and height, A_B = crown diameter and biomass, SE = standard error.

Spruce's growth in DBH during the period directly after the cut (2006–2008: 1.07 cm period^{-1}) is significantly higher than in the period before (2004–2006: 0.74 cm period^{-1}, $p = 0.006$) and stays at an increased level until 2012. Beech does not significantly react immediately in terms of DBH growth (0.44 cm period^{-1} before and 0.43 cm period^{-1} after cut), nor at a later point in our study.

The temporal allometric crown diameter parameters (Table 2), indicating the allocation bias of exploited resources, do not show distinct reactions in case of Norway spruce (Fig. 3). The ratio between crown diameter growth in relation to existing crown diameter and DBH growth in relation to existing DBH, A_{DBH} (Eq. 1), changes from 1.39 in 2008 to 1.56 in 2012 with a minimum of 0.95 in 2010, exposing a slight bias towards CPA growth. A_H being at an overall higher level and therefore suggesting an allocation bias towards CPA over height, rises from 4.40 in 2008 to 6.97 in 2012. The A_B however, being below 1.0 (0.67 in 2008, 0.47 in 2010, 0.77 in 2012) shows a substantial bias towards biomass production compared to lateral crown expansion. In contrast to Norway spruce with its rather steady parameters, European beech reacts significantly stronger to the emergence of the gaps. All three allometric parameters reach their maximum value in the observation period directly after gap emergence, displaying an immediate strong allocation bias towards lateral crown expansion over stem diameter, height and biomass growth in 2008 (A_{DBH}: 11.02, A_H: 12.60, A_B: 3.74). On the other hand, European beech's crowns prove to be less resilient against
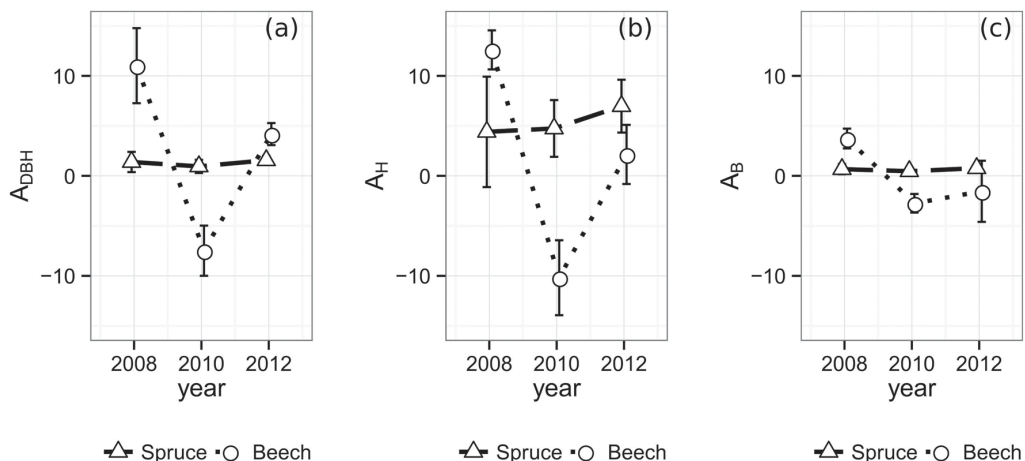
Fig. 3. Allometric relations and one-fold standard error bars over time between (a) crown diameter and DBH, (b) crown diameter and tree height (c) and crown diameter and biomass. In order to take different crown shapes into account, the crown diameter was substituted by the diameter of a hypothetical circle encompassing the same area as its respective tree's two-dimensional α-shape (α = 0.25 m).

9

mechanical influences resulting in loss of crown size. Due to the substantial loss of crown projection area during the period from 2008 to 2010, the according values of A_{DBH} (–7.48), A_H (–10.19), and A_B (–2.74) are negative. Finally, in 2012 the allocation reaches more stable levels at an A_{DBH} of 4.18, A_H of 2.14 and an A_B of –1.54.

3.2 Space utilization

The projected area growth $CPAG_{in}$ of spruce's crown sections from 2006 to 2008 within the defined gap borders was 0.07 m² m⁻², successively rising to 0.11 m² m⁻² (2010) and 0.26 m² m⁻² in 2012 (Fig. 4). While a trend could be assumed from the data, it is not significant (2008 and 2012, $p = 0.064$). European beech shows a totally different behavior. The period immediately after the gap cutting features quite a strong boost of 1.24 m² m⁻² in $CPAG_{in}$. In the following period, the space occupation is even negative (–0.12 m² m⁻²) and reaches 0.06 m² m⁻² in the final observation period. The initial value was significantly higher than both other observations ($p_{2010} = 0.005$, $p_{2012} = 0.011$).

The projected area growth $CPAG_{out}$ of the crown sections lying outside the defined gap borders does not react as strong to the newly created gaps. Spruce starts with 0.11 m² m⁻² in the first period, shows 0.03 m² m⁻² in the second and finally reaches 0.07 m² m⁻² in the last period, which is significantly less than its corresponding $CPAG_{in}$ (0.26 m² m⁻², $p = 0.045$). The development of European beech's $CPAG_{out}$ behaves quite similar to its $CPAG_{in}$. However, the initial growth boost of the first period is less pronounced outside the inner gap borders resulting in a $CPAG_{out}$ of only 0.48 m² m⁻². Furthermore, the $CPAG_{out}$ of the second period is even more negative (–0.24 m² m⁻²) than its corresponding $CPAG_{in}$, indicating either a better resistance against mechanical crown damage, a lower actual projected area growth compensating for the damage or a combination of both.

The efficiency of space occupation of spruce ($EOC_{2006} = 11.0$ m² m⁻³, $EOC_{2008} = 10.8$ m² m⁻³, $EOC_{2010} = 10.8$ m² m⁻³, $EOC_{2012} = 11.4$ m² m⁻³) is significantly lower than beech's corresponding value over all periods. ($EOC_{2006} = 27.1$ m² m⁻³, $EOC_{2008} = 36.4$ m² m⁻³, $EOC_{2010} = 29.4$ m² m⁻³, $EOC_{2012} = 28.7$ m² m⁻³, $p_{2006} = 0.010$, $p_{2008} = 0.011$, $p_{2010} = 0.022$, $p_{2012} < 0.001$). While the EOC
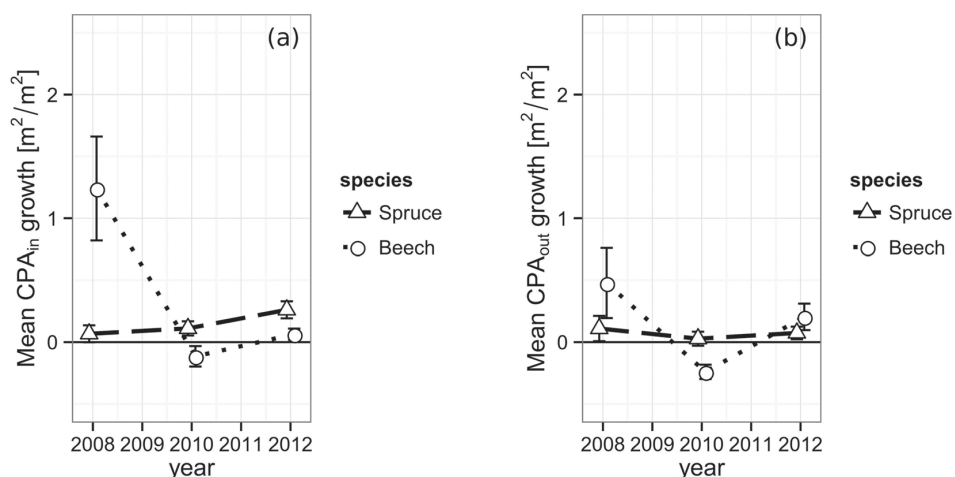
Fig. 4. (a) Increase of the crown projection area by species within the gap polygon, i.e. towards the gap center and (b) increase of the crown projection by species area outside of the gap polygon, towards competing neighbors from 2006 to 2012. The vertical bars indicate the one-fold standard error.

10
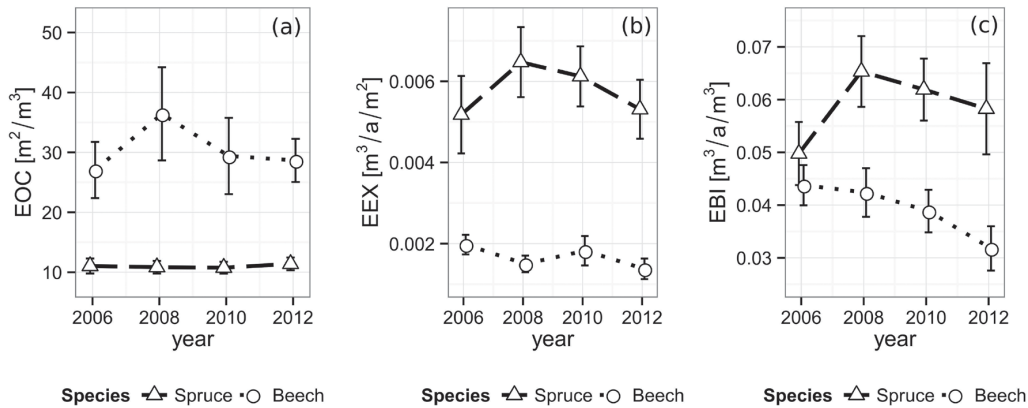
Fig. 5. Development of (a) efficiency of space occupation (*EOC*), (b) efficiency of space exploitation (*EEX*) and (c) efficiency of biomass investment (*EBI*) for each species from 2006 until 2012. Vertical bars indicate the one-fold standard error.

of spruce seems to be unaffected by the gap's appearance, beech features a rather strong increase after the first observation period, followed by a decrease back to approximately the original level in the following years (Fig. 5).

Norway spruce shows a significantly higher efficiency of space exploitation than beech during all periods (all *p*-values ≤ 0.002), starting at 5.18×10^{-3} m^3 a^{-1} m^{-2} (Fig. 5). In contrast to the *EOC*, spruce's *EEX* rises to its peak of 6.48×10^{-3} m^3 a^{-1} m^{-2} during the period right after the cutting and from there on decreases back to approximately the original level over the following periods. The *EEX* development of beech seems to feature no significant direction with values alternating around 1.67×10^{-3} m^3 a^{-1} m^{-2} decreasing immediately after the gap creation, then rising and decreasing again in the following periods.

Consequently, while the efficiency of biomass investment starts at a similar level in 2006 (*EBI* spruce: 4.98×10^{-2} m^3 a^{-1} m^{-3}, *EBI* beech: 4.38×10^{-2} m^3 a^{-1} m^{-3}), spruce shows significantly higher values than beech with a maximum of 6.53×10^{-2} m^3 a^{-1} m^{-3} immediately after the cut and in the following periods ($p_{2008} = 0.009$, $p_{2010} = 0.003$, $p_{2012} = 0.008$, Fig. 5). Beech, in contrast, features a steadily decreasing *EBI* trend, starting at 4.38×10^{-2} m^3 a^{-1} m^{-3} and reaching a significantly lower value of 3.18×10^{-2} m^3 a^{-1} m^{-3} ($p = 0.046$) at the end of our observation. An overview of the space utilization results is given in Table 3.

Table 3. Space utilization parameters by species from 2006 to 2012.

Species	Year	$CPAG_{in}$ [m^2 m^{-2}]	SE	$CPAG_{out}$ [m^2 m^{-2}]	SE	EOC [m^2 m^{-3}]	SE	EEX [m^3 a^{-1} m^{-2}]	SE	EBI [m^3 a^{-1} m^{-3}]	SE
Norway spruce	2006	--	--	--	--	11.0	1.25	5.18×10^{-3}	9.54×10^{-4}	4.98×10^{-2}	5.98×10^{-3}
	2008	0.07	0.07	0.11	0.10	10.8	1.06	6.48×10^{-3}	8.63×10^{-4}	6.53×10^{-2}	6.71×10^{-3}
	2010	0.11	0.06	0.03	0.06	10.8	1.00	6.12×10^{-3}	7.41×10^{-4}	6.19×10^{-2}	5.87×10^{-3}
	2012	0.26	0.07	0.07	0.05	11.4	1.06	5.31×10^{-3}	7.27×10^{-4}	5.83×10^{-2}	8.64×10^{-3}
European beech	2006	--	--	--	--	27.1	4.69	1.98×10^{-3}	2.41×10^{-4}	4.38×10^{-2}	3.81×10^{-3}
	2008	1.24	0.42	0.48	0.28	36.4	7.77	1.50×10^{-3}	2.05×10^{-4}	4.24×10^{-2}	4.61×10^{-3}
	2010	-0.12	0.08	-0.24	0.06	29.4	6.37	1.83×10^{-3}	3.61×10^{-4}	3.89×10^{-2}	4.04×10^{-3}
	2012	0.06	0.05	0.20	0.11	28.7	3.59	1.38×10^{-3}	2.54×10^{-4}	3.18×10^{-2}	4.21×10^{-3}

$CPAG_{in}$ = CPA growth per unit CPA towards gap, $CPAG_{out}$ = CPA growth per unit CPA away from gap, EOC = efficiency of space occupation, EEX = efficiency of space exploitation, EBI = efficiency of biomass investment, SE = standard error.

11
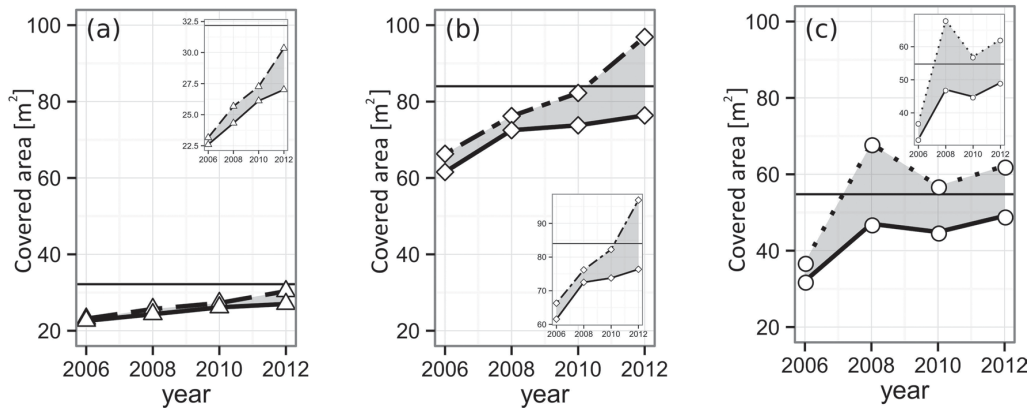
Fig. 6. Layering development of the analyzed (a) spruce, (b) mixed and (c) beech gaps from 2006 until 2012. The solid lines indicate the area of the leaf-cover as a whole. The dashed lines show the sum of all individual tree *CPA*s forming the respective gap. The difference (gray area) indicates crown overlap, i.e. multi-layering. The black horizontal lines mark the area of the gap polygon, i.e. the highest possible area of the single-layered cover.

3.3 Whole-gap development

The α-shape derived gap areas of all three gaps closed during the course of our observation (Fig. 6, Table 4). The pure spruce gap, starting with a single-layer gap projection area (*GPA*) of 22.6 m^2, increased its *GPA* steadily up to 27.0 m^2 in 2012. By definition, the maximum *GPA* is given by the gap polygon area (A_{poly}, pure spruce = 32.2 m^2), meaning at the end of our observation 84.0% of the available, single layered space was occupied (70.2% at the beginning). The larger European beech gap (A_{poly}, pure beech = 54.8 m^2) grew its initial *GPA* of 32.0 m^2 in 2006 to 49.1 m^2 in 2012, translating to a relative single-layer closure development from 59% up to 90% at the end of the observation. The mixed-species gap (A_{poly}, mixed = 84.0 m^2), similarly to the pure spruce gap, features a steady *GPA* growth, encompassing values from 61.6 m^2 (2006) to 76.4 m^2 (2012). Accordingly, the mixed-species relative single-layer area during the whole time-span grew from 73.3% to 90.9%.

Table 4. Descriptive data of the gap-level development from 2006–2012.

Gap	Year	A_{poly} [m^2]	*GPA* [m^2]	Rel. closed	$\sum CPA_{in}$ [m^2]	*ML* [m^2]	*RML*
Norway spruce	2006	32.2	22.6	0.70	23.15	0.55	0.02
	2008	32.2	24.3	0.76	25.68	1.36	0.06
	2010	32.2	26.1	0.81	27.27	1.15	0.04
	2012	32.2	27.0	0.84	30.35	3.33	0.12
European beech	2006	54.8	32.0	0.59	36.97	4.93	0.15
	2008	54.8	47.0	0.86	68.02	21.00	0.44
	2010	54.8	44.9	0.82	56.00	12.10	0.27
	2012	54.8	49.1	0.90	62.16	13.06	0.27
Mixed	2006	84.0	61.6	0.73	66.31	4.75	0.08
	2008	84.0	72.5	0.86	76.19	3.68	0.05
	2010	84.0	73.8	0.88	82.24	8.46	0.11
	2012	84.0	76.4	0.91	96.91	20.54	0.27

A_{poly} = area of gap polygon, *GPA* = gap projection area, $\sum CPA_{in}$ = sum of all crown sections reaching into the gap polygon, *ML* = multi-layered area, *RML* = *ML* in relation to *GPA*.

12

The multi-layering area *ML* of all three gaps increased. However, it is less distinct in the case of the pure spruce gap, reaching its maximum relative *ML* (*RML)* of 12.3% in 2012. The pure beech as well as the mixed-species gap both reached a *RML* of 27.0% until the end of the study. Yet, the European beech gap features a higher level during the middle of the observation period (beech: 21.0% and 12.1% vs mixed: 3.7% and 8.5%).

4   Discussion

One of the more intriguing results of our study is that the type of gap (mixed or pure) had no significant impact on the observed reactions of both species. The mechanisms of intra- and inter-specific competition are important drivers within the feedback loop of stand structure and functioning (Hari 1985; Pretzsch 2009), and in former studies have shown a significant impact on crown shape, size and inner structure (Bayer et al. 2013). It is likely that in our case, the sheer abundance of free above-ground resources overshadowed mixing effects between the two species until most of the gap space was occupied. Our results however, show marked differences in the behavior of the two studied species independent of the type of gap (mixed vs pure). In fact, both species display rather opposing reactions.

4.1 Lateral expansion and interlocking

Spruce's *DBH* growth immediately increases within the first period after gap emergence, then stays at high level with slight downtrend. Significant shifts in the allocation of exploited resources during the study could not be observed (Fig. 3). We observed that the efficiency of space occupation does not significantly change during the observation period, while the efficiencies of space exploitation and biomass investment rise during the first two years after gap emergence. This strongly suggests that spruce utilized the additionally available above-ground resources primarily for increased *DBH* growth without significant morphological adaptations to the altered environment. Norway spruce's crowns feature rather slow but steady lateral expansion, seemingly almost unaffected by gap emergence. The expected asymmetry of lateral growth (towards gap vs the rest of the stand), while existent (Fig. 4), develops only slowly over time so that it is only significant during the last period. This was not unexpected, since conifers tend to feature low growth towards light (Muth and Bazzaz 2002). Seidel et al. 2016 found similar results comparing Douglas-fir (*Pseudotsuga menziesii* (Mirb.) Franco) growing at the border to gaps and under normal spacing, where significant differences in lateral crown extension between both groups could not be observed and the major differences lied in lower crown base height as well as a lower height of maximum crown projection of the gap trees. Both significant changes in crown basal height as well the maximum height could not be observed in our study. This however is likely a result of the shorter timespan from 2006 until 2012 in comparison to Seidel et al. 2016 as well as the smaller gap sizes involved and, as a consequence thereof, rather fast closure of our gaps.

For European beech in contrast to spruce, during the first two years after gap emergence, we observed fast lateral crown expansion followed by a sharp decrease in crown size. Unfortunately, the decrease could, based on our data, not be attributed to a particular event with certainty. It seems likely however, that the observed lateral crown retreat was caused by one or several weather events, especially storms which resulted in mechanical damage. Another conceivable cause for the observed crown retreat could, as a result of the rapid initial crown expansion and the resulting increase in competition, be mechanical abrasion between crowns which may be one of the substantial drivers of above-ground competition (Franco 1986; Hajek et al. 2015). Even though the gaps are free

13

space, their size allows contact of trees even on opposite sides of the gap given strong enough winds. The high plasticity of European beech and the resulting strong morphological reaction to the emergence of gaps is also reflected in the allocation ratios (Fig. 3) which show a strong bias towards lateral crown expansion during the first two years, whereby the expansion itself is biased towards the gap space. Also, beech's efficiency of space occupation, while generally on a higher level than spruce, rises after gap cutting and then comes down to before-gap levels. The efficiency of space exploitation and biomass investment, are below the values of spruce and in the case of *EEX* show no clear trend over time and a downtrend in the case of *EBI*. Concluding the individual tree dynamics with the rapid closing observed in the whole gap development, European beech seems to strongly react to the new gap space, utilizing the new above-ground resources in favor of fast space occupation and its associated competitive effects, initially even to the cost of reduced *DBH* and biomass growth.

Multi-layering of crowns existed in all three gaps from the beginning and increased over time. Thereby, the gap comprised of pure spruce displayed the least tendency towards multi-layering, beech the highest and the mixed gap lied in between. This as well showed the much higher crown plasticity of European beech resulting in the development and the ability to maintain overlapping crowns (Pretzsch and Schütze 2005). All in all, our observations fit rather well in the context of former studies on allometry and growing space efficiency of spruce and beech (Pretzsch and Schütze 2005; Dieler and Pretzsch 2013; Bayer et al. 2013)

4.2 Ecological implications

In crowded plant communities larger individuals often claim a disproportionate share of contested resources and supress their less competitive neighbours, leading to size-asymmetric competition (Schwinning and Weiner 1998; Weiner and Damgaard 2006). In temperate forests, where light is often the primary limit to tree growth, the existence of taller trees with a higher potential for light interception often cause such size-asymmetric competition (Wichmann 2002).

Space serves as an important abstraction for above-ground resources, because the actual distribution and availability of resources within the canopy space, light for example, are hard to measure. Some authors argue that space may even be considered a resource itself (Grams and Lüttge 2011). Abundance, shape and size of gaps within the canopy therefore play a key role in the mechanisms of stand dynamics. The relevance of gaps, their emergence and dynamics for competition and stand development and productivity may be stressed by the following estimation. A 3% annual rate of tree loss due to mortality or thinning means a gap area of 300 m^2 per hectare and year. Over a rotation period of 100 years, the transient gap area caused by this drop out process amounts to about 30 000 m^2, i.e. 3.0 ha (Pretzsch 2014). Growing space is repeatedly contested by neighbouring trees, occupied, released due to mortality and thinning and recaptured by the most competitive individuals (Bauhus 2009).

After, when planted several thousand or, when naturally regenerated even millions of individual trees contributed to the process of competitive space capturing and recapturing, about 50 to 100 trees per ha are left within a mature stand. These ever-emerging gaps are occupied faster and more completely by species featuring high crown plasticity. Especially in more or less mono-layer stands this ongoing mortality and subsequent closure by crown extension causes a continuous opening up of the canopy.

Crown size and accordingly gap size increases with tree age, and as larger gaps need more time to be recaptured by neighbours and older trees' lateral shoot growth is rather slow the crown re-coverage becomes more sluggish with increasing stand age. The ongoing gap dynamics is probably the main reason why even in un-thinned mono-layered pure stands 5–15% of the stand

14

area remains uncovered by crowns (Wiedemann 1951). In temperate forests, where individual tree growth is mainly light limited, gaps are faster closed by crown extension above ground than by tree root extension below-ground (Bauhus 2009). Those species with higher crown plasticity can achieve more additional canopy space by faster and more extensive gap occupation equivalent with additional resource capture and competitive strength. Especially gaps caused abruptly by thinning favour those species with quick and wide extension capacity. Additional growing space due to mortality emerges more continuously and is gradually occupied by neighbours already in advance of tree death.

Among the most important factors for the competitive strength of a tree species are its capability of long-term adaptation, for example by genotypic variation and its ability to quickly acclimate to changing environments, which itself is dependent on genetic predisposition. In comparison to Norway spruce, European beech displays superior competitive strength under a majority of Central European site conditions. A key aspect of its success lies in its high crown plasticity and adaptability which is often demonstrated by variations of branch angles, ramification or differing branch curvature for example (Bayer et al. 2013).

4.3 Impacts of forest function and services

The competitive strength of European beech (Fischer 1995) in Central Europe's natural forest systems is strongly driven by its ability to morphologically adapt to its surroundings (Dieler and Pretzsch 2013; Bayer et al. 2013) and the fast occupation of available growing space it demonstrated in this study. Thereby, not only is beech able to secure space and its resources for itself but also to deny competitors access to the same resources and to hold back competitors from the understory (Pretzsch and Schütze 2009). Fast crown expansion and its associated faster and more complete exploitation of growing space may be favourable in concerning future growth and yield, however larger crowns have negative economic effects, namely on tree value, as well. Lower height of the crown base, knottiness, stem-bending and irregularities of tree-ring width for example, are often more prevalent in more complex stands (Macdonald et al. 2010; Pretzsch and Rais 2016).

The size and structure of crowns and gaps and their development over time also determine a major part of habitat formation. In fact, the plant community and its structure frequently define the majority of a habitat's physical environment which plays a key role in the distribution and interaction of animal species (Lawton 1983; McCoy and Bell 1991). Plant species diversity or structural complexity are often positively correlated with animal species diversity (Tews et al. 2004). In contrast to trees growing within the stand interior under more regular spacing, trees growing at the border to gaps develop different crown shapes. Especially species featuring high crown plasticity are likely to, among other traits, develop more asymmetric crown shapes, longer branches and, given a big enough gap and time, lower crown base heights during the process of space occupation. The resulting variety provides a larger set of different habitat structures and may enable certain animal species, which would otherwise not be able, to inhabit a stand (North et al. 1999; Hinsley et al. 2009; Müller et al. 2012).

4.4 Methodological considerations

The application of two- and three-dimensional α-shapes of TLS point clouds facilitates the quantification of volume, surface and projection area of individual tree crowns as well as tree groups and gaps on a more detailed level than classical dendrometrical methods under reasonable efforts. To some extent, inhomogeneous point densities, occlusion and noise within the TLS data compromise the quality of raw point clouds within forest stands. The upper canopy regions are usually clearly

15

more affected than the lower ones. Due to multiple scan positions per measurement including one at the gap center and the use of the respective device's last-pulse mode, we minimized these issues. Three dimensional measurements, for example crown volume calculations, can still be affected. Two-dimensional data, in our case the projections of the originally three-dimensional point clouds onto the xy-plane are hardly compromised because higher crown parts are for the most part occluded by lower crown parts of the same tree and therefore still represented within the respective alpha shapes.

We used two different scanners. The older scanner (Riegl LMS-Z360) was used for the first two measurement dates (2006 and 2008). Its predecessor model (Riegl LMS-Z420i) was used for the later scans of 2010 and 2012. Both devices are high precision instruments. Potential differences in accuracy would be in the order of magnitude of millimeters (Table 1) and therefore should not have had any significant impact on our results. The biggest issue of a study relying so heavily on α-shapes is the choice of proper α-values. We optimized our choice of α by picking the smallest member of a series of alpha values which still yielded α-shapes in compliance with the expected behavior of the relationship between α-value, surface and volume. Thus recreating the most detailed representation of the respective individual tree.

Real TLS time-series and actual observations of structural development over several years are still very rare in forest research and cannot quickly be produced. Unfortunately, we had only three gaps under observation from the beginning, resulting in a rather small sample size. Future experiments are going to include a larger number of gaps as well as different sites, species and species combinations.

5   Conclusions

In compliance with former studies (Bayer et al. 2013; Seidel et al. 2016), we found terrestrial laser scanning to be a suitable tool to accurately measure, and as a consequence thereof, better understand forest structures. Gaps and their dynamics are a major factor in the manifestation of a stand's light regime, competition and the architecture of individual trees. Thus, wood quality, growth, habitat and biodiversity among others are heavily influenced by gap dynamics.

The importance of forest gaps and their dynamics gain even more relevance as knowledge about the value of spatial variability of forest stands increases and forest management strategies more and more involve transitions towards more heterogeneous mixed-species stands where sil-viculturally generated gaps play a key role. Next to direct economic and ecological impacts, gap dynamics and especially the quickness of closure of gaps are a major concern in protective forest stands. Depending on the circumstances, hydrologic balance, soil protection and preservation, as well as mechanical stabilization within for example the scope of landslide prevention in montane regions, are often major elements of management plans. To enhance knowledge about gap dynamics and the process of a stand's reestablishment of economical, ecological and protective functions after disturbances is therefore crucial for sound management decisions.

Analyzing a larger number of forest gaps encompassing a variety of stand structures and species compositions are subjects for further research. Thereby, the utilization of state of the art hardware such as the latest TLS devices as well as advancements and the development of more sophisticated data interpretation methodologies show great potential to yield more comprehensive insights and constitute a valuable contribution towards a more complete understanding of forest gaps and their dynamics.

Acknowledgements

References

Assmann E. (1970). The principles of forest yield study. Pergamon Press, Oxford, New York.

Bauhus J. (2009). Rooting patterns of old-growth forests: is aboveground structural and functional diversity mirrored belowground? In: Wirth C., Gleixner G., Heimann M. (eds.). Old-growth forests: function, fate and value. Springer Berlin Heidelberg, Berlin, Heidelberg. p. 211–229. https://doi.org/10.1007/978-3-540-92706-8_10.

Bayer D., Seifert S., Pretzsch H. (2013). Structural crown properties of Norway spruce (*Picea abies* [L.] Karst.) and European beech (*Fagus sylvatica* [L.]) in mixed versus pure stands revealed by terrestrial laser scanning. Trees 27(4): 1035–1047. https://doi.org/10.1007/s00468-013-0854-4.

BayFORKLIM (1996). Klimaatlas Bayern. Fachbuchhandlung Kanzler, München, Germany.

Bucksch A., Lindenbergh R., Menenti M. (2010). SkelTre – Robust skeleton extraction from imperfect point clouds. Visual Computer 26(10): 1283–1300. https://doi.org/10.1007/s00371-010-0520-4.

Buddle C.M., Langor D.W., Pohl G.R., Spence J.R. (2006). Arthropod responses to harvesting and wildfire: implications for emulation of natural disturbance in forest management. Biological Conservation 128(3): 346–357. https://doi.org/10.1016/j.biocon.2005.10.002.

Burschel P., Huss J. (1997). Grundriss des Waldbaus. Parey, Berlin.

Côté J.-F., Fournier R.A., Egli R. (2011). An architectural model of trees to estimate forest structural attributes using terrestrial LiDAR. Environmental Modelling & Software 26(6): 761–777. https://doi.org/10.1016/j.envsoft.2010.12.008.

Dieler J., Pretzsch H. (2013). Morphological plasticity of European beech (*Fagus sylvatica* L.) in pure and mixed-species stands. Forest Ecology and Management 295: 97–108. https://doi.org/10.1016/j.foreco.2012.12.049.

Drössler L., Feldmann E., Glatthorn J, Annighöfer P., Kucbel S., Tabaku V. (2016). What happens after the gap? – Size distributions of patches with homogeneously sized trees in natural and managed beech forests in Europe. Open Journal of Forestry 6(3): 177–190. https://doi.org/10.4236/ojf.2016.63015.

Edelsbrunner H., Mücke E.P. (1994). Three-dimensional alpha shapes. ACM Transactions on Graphics 13(1): 43–72. https://doi.org/10.1145/174462.156635.

Edelsbrunner H., Kirkpatrick D.G., Seidel R. (1983). On the shape of a set of points in the plane. IEEE Transactions on Information Theory 29(4): 551–559. https://doi.org/10.1109/TIT.1983.1056714.

Fischer A. (1995). Forstliche Vegetationskunde. Pareys Studientexte 82. Blackwell Wissenschaft, Berlin, Wien.

Franco M. (1986). The influences of neighbours on the growth of modular organisms with an example from trees. Philosophical Transactions of the Royal Society B: Biological Sciences 313(1159): 209–225. https://doi.org/10.1098/rstb.1986.0034.

17

Goetz S.J., Steinberg D., Betts M.G., Holmes R.T., Doran P.J., Dubayah R., Hofton M. (2010). Lidar remote sensing variables predict breeding habitat of a Neotropical migrant bird. Ecology 91(6): 1569–1576. https://doi.org/10.1890/09-1670.1.

Grams T.E.E., Lüttge U. (2011). Space as a resource. In: Lüttge E.U., Beyschlag W., Büdel B., Francis D. (eds.). Progress in Botany 72. Springer Berlin Heidelberg, Berlin, Heidelberg. p. 349–370.

Hackenberg J., Spiecker H., Calders K., Disney M., Raumonen P. (2015). SimpleTree – an efficient open source tool to build tree models from TLS clouds. Forests 6(11): 4245–4294. https://doi.org/10.3390/f6114245.

Hajek P., Seidel D., Leuschner C. (2015). Mechanical abrasion, and not competition for light, is the dominant canopy interaction in a temperate mixed forest. Forest Ecology and Management 348: 108–116. https://doi.org/10.1016/j.foreco.2015.03.019.

Hari P. (1985). Theoretical aspects of eco-physiological research. In: Tigerstedt P.M.A., Puttonen P., Koski V. (eds.). Crop physiology of forest trees. Helsinki Univercity Press, Helsinki. p. 21–30.

Hilker T., van Leeuwen M., Coops N., Wulder M.A., Newnham G.J., Jupp D.L.B., Culvenor D.S. (2010). Comparing canopy metrics derived from terrestrial and airborne laser scanning in a Douglas-fir dominated forest stand. Trees 24(5): 819–832. https://doi.org/10.1007/s00468-010-0452-7.

Hinsley S., Hill R., Fuller R., Rothery P. (2009). Bird species distributions across woodland canopy structure gradients. Community Ecology 10(1): 99–110. https://doi.org/10.1556/ComEc.10.2009.1.12.

Kuuluvainen T., Grenfell R. (2012). Natural disturbance emulation in boreal forest ecosystem management – theories, strategies, and a comparison with conventional even-aged management. Canadian Journal of Forest Research 42(7): 1185–1203. https://doi.org/10.1139/x2012-064.

Lawton J.H. (1983). Plant architecture and the diversity of phytophagous insects. Annual Review of Entomology 28: 23–39. https://doi.org/10.1146/annurev.en.28.010183.000323.

Lertzman K.P., Sutherland G.D., Inselberg A., Saunders S.C. (1996). Canopy gaps and the landscape mosaic in a coastal temperate rain forest. Ecology 77(4): 1254–1270. https://doi.org/10.2307/2265594.

Macdonald E., Gardiner B., Mason W. (2010). The effects of transformation of even-aged stands to continuous cover forestry on conifer log quality and wood properties in the UK. Forestry 83(1): 1–16. https://doi.org/10.1093/forestry/cpp023.

Mandelbrot B. (1967). How long is the coast of Britain? Statistical self-similarity and fractional dimension. Science 156(3775): 636–638. https://doi.org/10.1126/science.156.3775.636.

Matyssek R., Schnyder H., Elstner E.F., Munch J.C., Pretzsch H., Sandermann H. (2002). Growth and parasite defence in plants; the balance between resource sequestration and retention: in lieu of a guest editorial. Plant Biology 4(2): 133–136. https://doi.org/10.1055/s-2002-25742.

McCoy E.D., Bell S.S. (1991). Habitat structure: the evolution and diversification of a complex topic. In: Bell S.S., McCoy E.D., Mushinsky H.R. (eds.). Habitat structure: the physical arrangement of objects in space. Springer Netherlands, Dordrecht. p. 3–27. https://doi.org/10.1007/978-94-011-3076-9_1.

Metz J., Seidel D., Schall P., Scheffer D., Schulze E.-D., Ammera C. (2013). Crown modeling by terrestrial laser scanning as an approach to assess the effect of aboveground intra- and inter-specific competition on tree growth. Forest Ecology and Management 310: 275–288. https://doi.org/10.1016/j.foreco.2013.08.014.

Mueller-Dombois D. (1991). The mosaic theory and the spatial dynamics of natural dieback and regeneration in Pacific forests. In: Remmert H. (ed.). The mosaic-cycle concept of ecosystems. Springer Berlin / Heidelberg. p. 46–60. https://doi.org/10.1007/978-3-642-75650-4_3.

18

Müller J., Mehr M., Bässler C., Fenton M.B., Hothorn T., Pretzsch H., Klemmt H.-J., Brandl R. (2012). Aggregative response in bats: prey abundance versus habitat. Oecologia 169(3): 673–684. https://doi.org/10.1007/s00442-011-2247-y.

Muth C.C., Bazzaz F.A. (2002). Tree canopy displacement at forest gap edges. Canadian Journal of Forest Research 32(2): 247–254. https://doi.org/10.1139/x01-196.

North M.P., Franklin J.F., Carey A.B., Forsman E.D., Hamer T. (1999). Forest stand structure of the northern spotted owl's foraging habitat. Forest Science 45(4): 520–527.

Pretzsch H. (1992). Modellierung der Kronenkonkurrenz von Fichte und Buche in Rein- und Mischbeständen. AFJZ 163: 203–213.

Pretzsch H. (2009). Forest dynamics, growth and yield – from measurement to model. Springer, Berlin, Heidelberg.

Pretzsch H. (2006). Species-specific allometric scaling under self-thinning: evidence from long-term plots in forest stands. Oecologia 146(4): 572–583. https://doi.org/10.1007/s00442-005-0126-0.

Pretzsch H. (2014). Canopy space filling and tree crown morphology in mixed-species stands compared with monocultures. Forest Ecology and Management 327: 251–264. https://doi.org/10.1016/j.foreco.2014.04.027.

Pretzsch H., Schütze G. (2005). Crown allometry and growing space efficiency of Norway spruce (*Picea abies* [L.] Karst.) and European beech (*Fagus sylvatica* L.) in pure and mixed stands. Plant Biology 7: 628–639. https://doi.org/10.1055/s-2005-865965.

Pretzsch H., Schütze G. (2009). Transgressive overyielding in mixed compared with pure stands of Norway spruce and European beech in Central Europe: evidence on stand level and explanation on individual tree level. European Journal of Forest Research 128(2): 183–204. https://doi.org/10.1007/s10342-008-0215-9.

Pretzsch H., Rais A. (2016). Wood quality in complex forests versus even-aged monocultures: review and perspectives. Wood Science and Technology 50(4): 845–880. https://doi.org/10.1007/s00226-016-0827-z.

Pretzsch H., Block J., Dieler J., Gauer J., Göttlein A., Moshammer R., Schuck J., Weis W., Wunn U. (2014). Nährstoffentzüge durch die Holz- und Biomassenutzung in Wäldern. Teil 1: Schätzfunktionen für Biomasse und Nährelemente und ihre Anwendung in Szenariorechnungen. Allgemeine Forst- und Jagdzeitung 185(11/12): 261–285.

Pretzsch H., Biber P., Uhl E., Dauber E. (2015). Long-term stand dynamics of managed spruce-fir-beech mountain forests in Central Europe: structure, productivity and regeneration success. Forestry 88(4): 407–428. https://doi.org/10.1093/forestry/cpv013.

Puettmann K.J., Coates K.D., Messier C.C. (2012). A critique of silviculture: managing for complexity. Island Press.

Purves D.W., Lichstein J.W., Pacala S.W. (2007). Crown plasticity and competition for canopy space: a new spatially implicit model parameterized for 250 North American tree species. PLoS ONE 2(9): e870. https://doi.org/10.1371/journal.pone.0000870.

Quine C.P., Gardiner B.A. (2007). Understanding how the interaction of wind and trees results in wind- throw, stem breakage, and canopy gap formation. Elsevier, Amsterdam.

Remmert H. (1991). The mosaic-cycle concept of ecosystems – an overview. Springer, Berlin, Heidelberg. https://doi.org/10.1007/978-3-642-75650-4_1.

Röhle H., Huber W. (1985). Untersuchungen zur Methode der Ablotung von Kronenradien und der Berechnung von Kronengrundflächen. Forstarchiv 56: 238–243.

Schwinning S., Weiner J. (1998). Mechanisms determining the degree of size asymmetry in competition among plants. Oecologia 113(4): 447–455. https://doi.org/10.1007/s004420050397.

Seidel D., Leuschner C., Müller A., Krause B. (2011). Crown plasticity in mixed forests – quantifying asymmetry as a measure of competition using terrestrial laser scanning. Forest Ecology

19

and Management 261(11): 2123–2132. https://doi.org/10.1016/j.foreco.2011.03.008.

Seidel D., Hoffmann N., Ehbrecht M., Juchheim J., Ammer C. (2015). How neighborhood affects tree diameter increment – new insights from terrestrial laser scanning and some methodical considerations. Forest Ecology and Management 336: 119–128. https://doi.org/10.1016/j.foreco.2014.10.020.

Seidel D., Ruzicka K.J., Puettmann K. (2016). Canopy gaps affect the shape of Douglas-fir crowns in the western Cascades, Oregon. Forest Ecology and Management 363: 31–38. https://doi.org/10.1016/j.foreco.2015.12.024.

Tews J., Brose U., Grimm V., Tielborger K., Wichmann M.C., Schwager M. (2004). Animal species diversity driven by habitat heterogeneity/diversity: the importance of keystone structures. Journal of Biogeography 31: 79–92. https://doi.org/10.1046/j.0305-0270.2003.00994.x.

van der Meer P.J., Bongers F. (1996). Formation and closure of canopy gaps in the rain forest at Nouragues, French Guiana. Vegetatio 126(2): 167–179. https://doi.org/10.1007/BF00045602.

Weiner J., Damgaard C. (2006). Size-asymmetric competition and size-asymmetric growth in a spatially explicit zone-of-influence model of plant competition. Ecological Research 21(5): 707–712. https://doi.org/10.1007/s11284-006-0178-6.

Wichmann L. (2002). Modelling the effects of competition between individual trees in forest stands. Royal Veterinary University Copenhagen.

Wiedemann E. (1951). Ertragskundliche und waldbauliche Grundlagen der Forstwirtschaft. JD Sauerländer's Verlag, Frankfurt am Main.

Total of 56 references.

Bayer et al. 2017

Structural response of black locust (*Robinia pseudoacacia* L.) and small-leaved lime (*Tilia cordata* Mill.) to varying urban environments analyzed by terrestrial laser scanning. Implications for ecological functions and services

Dominik Bayer *†, Astrid Moser*, Thomas Rötzer*, Hans Pretzsch*

Abstract

Structure and morphology of urban trees are hardly quantified so far, especially in regard to variations caused by altering urban environments. However, structure and functions of trees are heavily interwoven. In fact, knowledge about structural attributes is essential for a better understanding of urban ecosystem functions and services. In order to scrutinize spatially explicit and detailed structural attributes under varying urban environments, we acquired terrestrial laser scans and applied the according methodological approaches to the common urban tree species black locust (*Robinia pseudoacacia* L.) and small-leaved lime (*Tilia cordata* Mill.). We analyzed 52 small-leaved limes and 41 black locust trees within the city of Munich. Species as well as growing location had a significant effect on the height-diameter relation. We also found greater crown volumes for small-leaved lime. Black locust however, displayed more crown projection area and likely more shade efficient crown shapes at similar volumes. Stem inclination of black locust was found to be higher in parks than in street canyons with town squares lying in between. Furthermore, black locust displayed heavy crown center displacements in park areas, likely caused by competition with neighbors. The angles of main branches did not differ significantly between both species nor between the growing location. Branch angles, branch bending, the length of the branches as well as species and growing location had a significant effect on vertical crown center position, i.e. general crown shape. Surface complexity of lime is lower than of black locust, with its lowest manifestation in parks. Fractal-like crown surface structures, increasing surface roughness and complexity, were found to be more pronounced for black locust than for small-leaved lime. Thereby, black locust featured the highest crown surface complexity in parks, the lowest in street canyons. The results suggest that studies on spatially explicit tree structures may contribute to more target oriented tree plantings and thus, more effective exploitation of ecosystem services and benefits.

Keywords: TLS; LiDAR; crown plasticity; tree morphology; skeletonization; crown surface; space filling; urban ecosystems; allometry

---

*Chair for Forest Growth and Yield Science, Center of Life and Food Sciences Weihenstephan, Technische Universität München, Hans-Carl-von-Carlowitz-Platz 2, 85354 Freising, Germany.

†Email: dominik.bayer@lrz.tu-muenchen.de

1

1 Introduction

Within urban landscapes, many environmental challenges are important for human health and well-being but costly to mitigate (Livesley et al., 2016). Given enough understanding, urban planers might exploit ecosystem services and functions in order to address these challenges. Consequently, trees are a key aspect in urban green space planning. Besides aesthetic considerations, structural traits, for example size, shape and density, surface complexity and transparency of tree crowns are among the most important drivers of their ecological features and benefits (Bolund and Hunhammar, 1999; Gómez-Baggethun and Barton, 2013). Urban trees are not only important for pedestrian comfort by providing aesthetic benefits, rain-cover, shade and wind-flow mitigation (Mochida and Lun, 2008; Mochida et al., 2008) but can also help to save energy on larger scales due to air cleaning, cooling (Rahman et al., 2017), wind buffering and shading (McPherson et al., 1997; Rosenfeld et al., 1998). Potential noise reduction (Aylor, 1972; Kragh, 1981; Fang and Ling, 2003), temperature management (Akbari et al., 2001; Akbari, 2005; Bolund and Hunhammar, 1999; Hardin and Jensen, 2007), waterflow regulation and water runoff mitigation (Higgens et al., 1997; Villarreal and Bengtsson, 2005; Pataki et al., 2011), wind-flow (Mochida and Lun, 2008; Mochida et al., 2008), air purification (Nowak, 1994, 1996; Escobedo and Nowak, 2009) and habitat functionality (Hinsley et al., 2009; Goetz et al., 2010; Tews et al., 2004; Müller et al., 2012) are directly related to tree structure as well.

As awareness of the potential benefits of urban trees grows, a better understanding how and under what circumstances services can be expected, designed, planned and optimally exploited becomes increasingly relevant. In order to select the right tree species for planting in an urban location, to ensure tree health and provided benefits, knowledge about the growth of the respective tree species and its structural development from planting to maturity is essential (Peper et al., 2014). However, even for the most common urban tree species, research about tree structure, morphology and growth is scarce. Even more so, if the variation of these traits at different tree ages (Kjelgren and Clark, 1992; Rust, 2014) and under varying urban environments such as streets, public squares, parking sites, etc. is considered. Because urban site conditions are totally different from forest site conditions (Nowak et al., 1990), knowledge from forest research cannot be applied. Moreover, even existing data of urban trees cannot simply be transferred to other cities and different climates because of distinct maintenance practices and differing durations of growing seasons (Peper et al., 2001a,b).

Taking tree age and varying urban environment into account, Moser et al. (2015) for example, studied the growth patterns and services of the two common but physiologically contrasting tree

2

species *Tilia cordata* and *Robinia pseudoacacia* to uncover growth relationships and the development of provided benefits over age in three typical urban site categories (street canyons, public squares and parks). Nonetheless, tree growth and structure are usually described and modeled using classical dendrometrical measurements such as diameter at breast height (*dbh*) and tree height and thus, are rather limited in detail and resolution. However, advanced, spatially explicit measurement techniques have emerged during the last decades.

Terrestrial laser scanning (TLS) provides high resolution three dimensional data. In archaeology, architecture, geology and several other fields, TLS is already extensively used and may be considered common practice (Vosselmann and Maas, 2010). In forest research, recent TLS-based methodologies have begun to outgrow pure methodological development (e.g. Côté et al., 2011; Hackenberg et al., 2015; Olivier et al., 2016; Olivier and Robert, 2017; Kelbe et al., 2017). More and more, results based on TLS data contributes to the understanding of forest (e.g. Bayer et al., 2013; Seidel et al., 2016; Liang et al., 2016) and in some cases urban ecosystems (e.g. Jones et al., 2016). As one of the first studies, Bayer et al. (2013) used terrestrial laser scanning beyond the scope of pure methodology to gain more detailed knowledge about the structure of trees and the resulting implications for a forest stand's functioning.

In order to quantify structural attributes of small-leaved lime and black locust in urban environments, we scanned 52 small-leaved lime and 41 black locust trees within the city of Munich growing at streets canyons, public places and parks. Based on this, we investigate (i) if the structure of black locust and small-leaved lime can be comprehensively described and quantified within urban environments by terrestrial laser scanning, (ii) if the structure differs between black locust and small-leaved lime growing under urban conditions, (iii) if there are structural differences within tree species, depending on the surroundings (street, place, park). Lastly, we discuss, (iv) implications of found structural attributes for functions and urban ecosystem services.

2 Material and Methods

2.1 Study Area and Sample Trees

The sample trees (Tab. 1) are located within the city of Munich (48°09' N, 11°35' E, 519 m above sea level) in southern Germany. On long-term (1961-1990), the annual precipitation amounts to 959 mm, while the mean temperature averages at 9.1°C (DWD, 2015).

Within the municipal area of Munich, 750.000 trees have been planted according to tree inventories. For our study, 42 *T. cordata* and 41 *R. pseudoacacia* trees have been measured by a Riegl

3

LMS-Z420i terrestrial laser scanner (Tab. 1). Besides the TLS scans, stem diameter data at the height of 1.3 m (*dbh*) has been collected using standard diameter measurement tapes. We chose the tree species *Tilia cordata* and *Robinia pseudoacacia* for our study because they are among the most common urban trees in Munich (Pauleit et al., 2002) and represent considerably different ecological features (Moser et al., 2015, 2016). The overall tree selection was based on visual impression so that damaged, low-forked and pruned trees have not been included. Depending on their respective surroundings, each measured tree was classified as park tree (Pa), street tree (St) or tree growing at town squares (Ts). Park trees were defined as growing in a green space without surrounding buildings. Street trees were defined when planted within a street canyon and trees at town squares were classified when growing free-standing in smaller, mostly paved places.

2.2 TLS Scan Acquisition

A Riegl LMS-Z420i TLS-System was used for the tree scanning. The device works based on the time-of-flight principle. A short near-infrared laser impulse is emitted towards a specified direction. Once a target is hit, a part of the light is reflected back towards the device's sensor. The time between the emission and the return of the impulse in combination with the speed of light in air yield the distance to the target. The specified azimuth and inclination are recorded with a precision of 0.002°. Combining each measured distance and direction of a large number of consecutive measurements yields the spherical coordinates representing a precise three dimensional image of the scanned region.

A typical problem with laser scanning of tree crowns is, that objects behind other targets cannot be measured (Hilker et al., 2010). While the sight on tree crowns in urban areas is usually much less prone to being blocked by neighboring trees and other objects than it is in forests, self-occlusion can still be detrimental to the overall data quality of individual trees (Bayer et al., 2013; Olivier et al., 2016). To overcome this, we combined the point-clouds of scans from opposing sides of each sample tree and used the a distance measurement mode called last-pulse. Hereby, not the first but the last echo of the laser pulse is recorded, favoring deeper penetration of the crown while still yielding an accurate representation of the crown's periphery. Furthermore, we acquired scans of our sample trees under leaved and leafless conditions in order to provide the best suited data basis for specific target parameters. We used leafless scans for the measurement of skeletal structure and leaved scans for crown shapes and inner density distribution, for example.

The TLS-device's manufacturer's software RiSCAN Pro has been used for the preprocessing of the point clouds. By exclusion of everything not being part of the respective tree's point-cloud -

4

such as buildings, vehicles, and ground for example - each individual tree's TLS data was isolated.

Our sample tree data was then exported and converted into various formats for further processing.

2.3 Skeletonization

In order to quantify the inner crown structure of the sample trees, we used a specific software developed by Bayer et al. (2013). Hereby, the tree's skeletal structure is recorded semi-manually by three-dimensionally visualizing the point-cloud. Then, the user interactively defines the course of the stem axis and individual branches by successively assigning segments of a given branch or stem through a dedicated graphical user-interface. Since the acquired skeleton contains information about the hierarchical structure of a tree's inner crown, information on attributes such as stem inclination, branch angle, branch shape, branch length and the crooking of branches can be derived. In the scope of this study, we concentrated on the stem and the primary branches.

The smallest possible angle φ between a vector $\vec{z}$, which is aligned towards the earth's center of gravity, and a vector $\vec{s}$ between the branch or stem base and a point in a freely definable measurement distance d is given by the scalar product of both vectors. $\vec{s}$ is defined by the intersection between a hypothetical sphere with $r = d$ around the branch base b and the branch segment that penetrates the sphere and therefore fulfills $|\vec{p}_1| < r < |\vec{p}_2|$, where p_1 is the position vector of the beginning and p_2 of the end of the segment.

$$\cos(\varphi_b) = \frac{\vec{s} * \vec{z}}{|\vec{s}| * |\vec{z}|}, \tag{1}$$

$$\vec{s} = \vec{p}_1 + \frac{-t_2 + \sqrt{t_2^2 - 4t_1 t_3}}{2t_1}(\vec{p}_2 - \vec{p}_1) \tag{2}$$

with

$$t_1 = (x_{p2} - x_{p1})^2 + (y_{p2} - y_{p1})^2 + (z_{p2} - z_{p1})^2$$

$$t_2 = 2((x_{p2} - x_{p1})(x_{p1} - b_x) + (y_{p2} - y_{p1})(y_{p1} - b_y) + (z_{p2} - z_{p1})(z_{p1} - b_z))$$

$$t_3 = b_x^2 + b_y^2 + b_z^2 + x_{p1} + y_{p1} + z_{p1} - 2(b_x x_{p1} + b_y y_{p1} + b_z z_{p1}) - r^2$$

The branch length l_b is defined as the sum of lengths of all branch segments belonging to the respective branch. Thus, the curvature of the branch is taken into account by l_b. Following this, the crooking of the measured branches was determined by the quotient of l_b and the Euclidean distance between branch base b and the end of the branch e.

$$l_b = \sum_{i=1}^{n} |\vec{ss}_i - \vec{se}_i| \tag{3}$$

5

$$crook = \frac{l_b}{|\vec{b} - \vec{e}|} \tag{4}$$

2.4 Alpha shape calculations

In order to describe the volume and surface properties of the scanned trees, we applied general-izations of the convex hull of a given point-set based on Delauny-triangulation. These so-called α-shapes (Edelsbrunner et al., 1983; Edelsbrunner and Mücke, 1994) are adjustable concerning the level of detail in which they represent their respective point-clouds by altering their α-value. Since the shape is built from mostly irregular tetrahedrons, the volume V of an α-shape is the sum of all tetrahedrons included within it.

$$V = \sum_{i=1}^{n} \sqrt{\frac{1}{288} * det \begin{pmatrix} 0 & u_i^2 & v_i^2 & w_i^2 & 1 \\ u_i^2 & 0 & W_i^2 & V_i^2 & 1 \\ v_i^2 & W_i^2 & 0 & U_i^2 & 1 \\ w_i^2 & V_i^2 & U_i^2 & 0 & 1 \\ 1 & 1 & 1 & 1 & 0 \end{pmatrix}} \tag{5}$$

During the α-shape generation, a normal vector $\vec{N}_i$ is generated for each triangle on the shape's boundary. Its magnitude is proportional to the area A_i of the triangle's surface.

$$|\vec{N}_i| \sim A_i \tag{6}$$

Therefore, the sum of magnitudes of all $\vec{N}_i$, scaled by a factor C according to the measurement unit equals the total surface S of a given α-shape.

$$S = \sum_{i=1}^{n} |\vec{N}_i| * C \tag{7}$$

To further analyze the crown surface and describe its structural complexity, we calculated a series of α-shapes. With smaller α-values, i. e. smaller measurement scales, the measured value for volume decreases. This means that within a series of α-shape calculations with α ranging from small to large, we get a non-linear relationship between α-value and volume of the point cloud's shape (Fig. 1). After linearization of the curve (Eq. 8), differences in the slopes of β_1 show how strongly the surface complexity of an individual tree influences the respective measured α-shapes' values. The benefit of this method lies in the characteristic that the rate of change β_1 is independent of individual tree size and gives an estimation of the fractal properties and structural complexity

6

of the crown's surface.

$$ln(V) = \beta_0 + \beta_1 * \frac{1}{\alpha} \tag{8}$$

Furthermore, α-shape series solve another issue with α-shape application in general. Depending on the quality of the point cloud and its resolution, it can be hard to determine the smallest sensible α-value. Too large values yield coarse hulls and lead to the loss of many details. Choosing α-values which are too small however, may result in an incomplete reconstruction of the point-cloud if the distance between boundary points on the surface cannot be covered by the α-shape's application radius. Due to the fractal properties of surfaces, as long as the quality and resolution of the TLS point cloud is suited for the used α-values, decreasing α-values must result in increasing measured surfaces (Mandelbrot, 1967, 1983). The smallest α-value of a series still fulfilling this law can be considered as the smallest sensible α-value.

2.5 Voxel space calculations

For further analysis of structural parameters such as vertical and horizontal crow center displacement as well as point density distributions, we arranged the trees' individual growing spaces into voxels of 0.5 m edge length. This allows for the analysis of point distributions and densities in regard to the spatial arrangement within the TLS point cloud. However, voxel representations of TLS clouds are less suited for the small scale analysis of structural attributes, like crown surface roughness for example. After that, we determined the three-dimensional center of the crown. Determining the center of a crown's point cloud can be problematic. As a result of self occlusion within the crown, the point distribution within the crown is not uniform. Hence, averaging or applying ordinary least square - methods over a crown's points set would lead to heavily skewed results. In fact, radial variations of the point density are among the parameters we are interested in. To overcome this, we treated all voxels equally and independently of the number of points contained within them. It is then possible to calculate the crown's center of mass c_m like that of a system of equal particles using only the crown's shape without the influence of the point distribution. This means each voxel fulfills the following condition

$$\sum_{i=1}^{n} m_i(\vec{v}_i - \vec{c}_m) = 0, \tag{9}$$

which leads to

$$\vec{c_m} = \frac{1}{M} \sum_{i=1}^{n} m_i \vec{v}_i, \tag{10}$$

7

where M represents the total hypothetical mass of the system, m_i is the mass of an individual particle, which may be arbitrarily defined, e.g. as 1 in our case since all voxels are considered equal and v_i defines the position of a given position vector of an individual voxel.

The horizontal crown center displacement CD_h was defined as the Euclidean distance between projections of the stem base b and the crown's center c_m onto the xy-plane of the coordinate system (Eq. 11). Vertically, the crown center position CD_v was defined by the relation of the center's height and the overall tree height (Eq. 12).

$$CD_h = |\vec{b}_{xy} - \vec{c}_{xy}| \tag{11}$$

$$CD_v = \frac{c_{m_z}}{h} \tag{12}$$

In order to define the spherical, three-dimensional crown radius r_c, we calculated the 95% quantile of all voxel distances d from the crown center $\vec{c_m}$ (Eq. 13). Following the calculation of the three-dimensional crown center and the crown radius, we estimated the point density distribution within the crown volume. This was done in a similar fashion, however instead of calculating quantiles of voxel distances, we calculated quantiles (10%, 20%, 30%,..., 90%) of their point content. Then, the mean voxel distance from the crown center of voxels falling into a point density quantile has been determined, resulting in an estimation of the radial distribution of point densities.

$$d = \frac{1}{n} \sum_{i=1}^{n} |\vec{v}_i - \vec{c}_m| \tag{13}$$

$$r_\rho = \frac{1}{n} \sum_{i=1}^{n} |\vec{\rho}_i - \vec{c}_m| \tag{14}$$

$$r_{\rho rel} = \frac{r_\rho}{r_{crown}} \tag{15}$$

3 Results

All parameters included in the following models are statistically significant if not stated otherwise. The categorical variables species and growing location are dummy coded as 0 and 1 in order to represent the respective group's statistical difference to the reference group. Where appropriate, after the initial model testing, post-hoc tests such as pairwise Tukey's HSD have been conducted in order to analyze differences between groups, for example growing locations.

8

3.1 Tree Stem dimensions

The basic descriptive size parameters diameter at breast height *dbh*, height *h*, slenderness ratio *h/d*, crown projection area *CPA*, crown volume *V* and crown surface area *S* are given in Tab. 2. The allometric relationship between *dbh* and height significantly depends on species as well as growing location (Adj. $R^2 = 0.71$, $p < 0.001$, Eq. 16). *T. cordata* features lower *h* values than *R. pseudoacacia* over the majority of the measured *dbh* spectrum. However, the height increase per *dbh* ($+0.32 * ln(dbh)$) is significantly more pronounced for *T. cordata*.

$$ln(\hat{h}) = 1.79 + ln(dbh) * (0.29 + 0.32 * Tilia) - 1.18 * Tilia - 0.22 * Ts - 0.27 * St \qquad (16)$$

T. cordata and *R. pseudoacacia* both show strong relations between α-shape derived ($\alpha = 0.5$) crown size parameters and *dbh* as well as height. However, their specific allometries differ significantly (e.g. Fig. 2). Given comparable height and *dbh*, *T. cordata* develops significantly higher crown volumes (Adj. $R^2 = 0.70$, $p < 0.001$, Eq. 17).

$$ln(\hat{V}) = -0.18 + 1.09 * ln(dbh) + (1.67 * ln(h) - 2.50) * Tilia \qquad (17)$$

Besides *dbh* and *h*, the measured crown length l_c significantly depend on species as well as growing location (Adj. $R^2 = 0.92$, $p < 0.001$, Eq. 18)

$$\hat{l}_c = -4.26 + 0.78 * h + dbh * (0.05 + Tilia * (-0.09 * Ts - 0.10 * St)) + 2.37 * Ts + 2.24 * St \quad (18)$$

Since both, *CPA* and crown volume *V* are crown size parameters, a highly significant relation between them exists. However, with comparable crown volume, *R. pseudoacacia* is able to cover more area on the ground ($R^2 = 0.92$, $p < 0.001$, Eq. 19).

$$ln(\hat{V}) = ln(CPA) * (1.23 * Robinia + 1.30 * Tilia) \qquad (19)$$

3.2 Crown Surface properties

A series of α-shape volumes revealed the specific relationship between measurement unit and measured volume. The coefficient β_1 of the relation serves as a proxy for the fractal properties of the measured point clouds and its surface complexity independently of tree size (Eq. 8). For *R. pseudoacacia*, our series of α-shape volumes showed significant differences between all three growing locations in relation between measured volume and chosen α-values (Fig. 3, Tab. 3). In

9

the case of *T. cordata*, there is no statistical difference between the trees in the parks and at the town squares. However, trees growing in a street environment showed a significantly different coefficient from park and town square trees.

$$ln(\hat{V}) = 5.77 - (0.26 - 0.15 * Ts) * Tilia + 0.13 * Ts - 0.31 * St - (0.47 + 0.18 * Tilia)\frac{1}{\alpha} \quad (20)$$

Overall, *R. pseudoacacia* featured steeper slopes, suggesting more structural complexity within the crown periphery. While *R. pseudoacacia* park trees featured the steepest slope among growing locations, *T. cordata* park trees display the least slope of the measured groups. The high R^2 values demonstrated the robustness of the underlying assumptions for the laws of the dependency of volume and surface on the chosen α-value.

3.3 Crown Volume Properties

Tab. 4 gives an overview of the descriptive statistics of the skeletal structure parameters as well as crown displacements. The horizontal displacement CD_h of the crown center (Fig. 4) did not significantly change for *T. cordata* depending on its growing location. *R. pseudoacacia* however, showed a significant disparity between individuals growing in park areas (2.82 m) in comparison to both streets (0.72 m, $p < 0.001$) and town squares (0.95 m, $p < 0.001$) as well as all *T. cordata* groups (0.66 m - 0.87 m, all $p < 0.001$). Obviously, stem inclination φ_s and tree height h influence the horizontal crown displacement CD_h. Yet, in an overall model for *R. pseudoacacia* ,

$$\hat{CD_h} = 0.075 * \varphi_s + 0.06 * h - 1.13 * Ts - 1.27 * St, \quad (21)$$

the growing location park still yielded significantly different results from both other locations (Eq. 21, Adj. $R^2 = 0.69$, $p < 0.001$). This suggests, besides the strong effects of stem inclination and tree height, that the competition with surrounding trees itself lead to significantly distinct crown shapes of *R. pseudoacacia*. The vertical crown center displacement CD_v (Fig. 4) is not dependent on *bdh* and *h*. However, within an overall model, branch angle φ_b, branch length l_b, species and growing location are significant factors (Eq. 22, Adj. $R^2 = 0.44$, $p < 0.001$).

$$\hat{CD_v} = 0.930 + 0.002 * \varphi_b - 0.590 * crook - 0.011 * l_b - 0.080 * Tilia - 0.064 * Pa - 0.045 * St \quad (22)$$

Similarly to the horizontal crown center displacement, there was no significant difference among the growing locations of *T. cordata*. Yet, it seems plausible that a larger sample size might have

10

yielded a distinct difference between town square and the park growing locations. *R. pseudoacacia*'s park groups differed significantly from both town square trees and street trees ($p = 0.025$).

The stem inclination (Fig. 5) of *R. pseudoacacia* featured a significant difference between the growing location park and street ($p = 0.038$). Between growing locations of *T. cordata* as well as between both species, there were no further significant differences. The branch crook was significantly related to CPA, φ_b, and species ($R^2 = 0.27$, $p < 0.001$). Branch angles φ_b as well as branch length l_b had a significant impact on crown volume (Eq. 23, Adj. $R^2 = 0.63$, $p < 0.001$). No distinct differences between species or growing locations could be found.

$$ln(\hat{V}) = 5.17 - 0.019 * \varphi_b + 0.371 * ln(l_b) \tag{23}$$

In regard to the mean distances of voxels belonging to an individual tree crown's point density quantile in relation to the spherical crown radius (Fig. 6), species had no significant impact. Within the *T. cordata* group, growing location as well had no significant effect on the relation between density quantile and its mean relative distance from the crown's center. For *R. pseudoacacia* however, growing location plays a significant role in the density quantile-distance relation (Eq. 24, Adj. $R^2 = 0.57$, $p < 0.001$).

$$\hat{r}_{\rho rel} = 0.817 - 0.303 * \rho_i + 0.026 * Pl + 0.030 * St \tag{24}$$

4 Discussion

4.1 Influence of Structure on Functions and Services

In cities, green spaces provide an important cornerstone of social and cultural values (Chan et al., 2012). Moral, spiritual and aesthetic values are often influenced by the urban environment (Chiesura, 2004; Tyrväinen et al., 2005; Chan et al., 2012). Sense of community, place value, physical and mental health, social cohesion and environmental education values as well as a multitude of recreational opportunities make urban green spaces a major factor for the overall quality of life in cities (Gómez-Baggethun and Barton, 2013; Livesley et al., 2016). Contributions to these values through ecosystem services of urban trees, such as temperature regulation, shading, wind and rainfall sheltering, air purification, noise reduction, animal sighting and aesthetics, are related to tree structure.

11

Temperature Regulation and Shading

Our results revealed larger crown volumes for small leaved lime than for black locust at comparable tree size. With similar crown volume, black locust displayed higher crown projection areas and a higher crown center in comparison to small leaved lime. Small-leaved lime however, is known to have denser crowns and therefore promotes a stronger shading effect. Furthermore, the higher amount of leaf area of urban small-laved limes within the crown results in a stronger average cooling effect through evapotranspiration than it is the case with black locust (Moser et al., 2015; Rahman et al., 2017). For both species, the growing location had no significant effect on crown volume and crown projection area.

The combination of urban heat island effect, summer heat waves and global warming can have serious detrimental effects on the urban environment, human health and well-being (Hamin and Gurran, 2009; McGeehin and Mirabelli, 2001). Urban trees affect local temperatures by providing humidity and shade (Bolund and Hunhammar, 1999; Hardin and Jensen, 2007) as well as cooling through transpiration (Rahman et al., 2017), thus help to mitigate the urban heat-island-effect (Akbari et al., 2001). Ground temperatures may be considerably reduced depending on crown size, shape and leaf area index (Napolia et al., 2016; Kong et al., 2016). Urban green spaces regulate local temperatures by absorbing heat through evapotranspiration (Hardin and Jensen, 2007) and might be the most impactful and cost-efficient approach to mitigate future challenges (Norton et al., 2015). Canopy structure, i. e. the stand or group openness or spacing of individual trees and crown structures alter the wind resistance. Consequently, leaf area index, branching patterns or crown surface complexity affect the evapotranspirative potential of trees (Ringgaard et al., 2012; Sjöman et al., 2016). Ballinas and Barradas (2016) suggest, that increasing tree cover alone cannot mitigate the urban heat island effect adequately. Hence, the choice of appropriate tree species based on their respective ecology and structure is crucial.

Windflow

Based on our results, small-leaved lime might be more effective for the speed reduction of strong or cold winds than black locust. Small leave-lime's larger crown size in combination with its lower crown center (see Fig. 4) and therefore potentially better sheltering at lower heights such as pedestrian levels might be a sensible choice, especially at wind exposed urban locations like town squares. The growing location of small-leaved lime did not significantly affect the relative crown center height. However, a larger sample size might have yielded the lowest crown centers at town squares and the highest in parks. Black locust displayed the lowest crown centers in street

12

canyons and at town squares where sheltering at low, i.e. pedestrian levels, is most beneficial. The differences for black locust were significant between parks and street canyons.

Wind speed is one of the most important factors for pedestrian comfort. Besides buildings, urban trees are among the largest objects within cities. Therefore, in the turbulent wind-flowfield of street canyons, trees can be considered stationary subgrid-scale obstacles (Mochida and Lun, 2008; Mochida et al., 2008). Crown size and shape which are strongly dependent on tree structure and tree dimension as well as air permeability, which itself is dependent on inner crown structure such as branching attributes, are major factors determining wind resistance (see Fig., 4 Roodbaraky et al., 1994; Stathopoulos, 2006). Wind speeds have been found to be considerably lower on the leeward side of urban trees, and negatively correlated with branch density (Sjöman et al., 2016). During winter months in particular, urban trees are able to contribute to the overall well-being of pedestrians by providing shelter from cold winds.

Waterflow Regulation and Runoff Mitigation

The finding that small-leaved lime features larger crown volumes than black locust suggests that its potential for interception of rain is higher. Also, the mean leaf are index of small-leaved limes under urban conditions was found to be higher than black locust's (Moser et al., 2015), which further promotes interception. However, in the case of space restrictions, black locust with its ability to cover more projected area on the ground under comparable crown volume and generally smaller crowns than small-leaved lime might be a better choice for rain interception and sheltering.

The high proportion of impermeable surfaces in urbanized landscapes increases the risk of storm water runoff and flash flooding by reducing the capacity for water uptake of the soil (Villarreal and Bengtsson, 2005; Walsh et al., 2012). These floodings might become increasingly problematic in regard to climate change and expected increases in the frequency of extreme rainfall events (Wissmar et al., 2004). Waterstreams in urban areas often suffer from considerably higher heavy metal, nitrate, phosphate, sulfate, carbon pollution than it is the case in comparably undeveloped catchments (Bernhardt et al., 2008; Kaushal and Belt, 2012). Through interception of rainfall, tree crowns decelerate flooding effects (Bolund and Hunhammar, 1999; Pataki et al., 2011). The amount of intercepted rain is heavily dependent on tree structure attributes such as crown shape and size, leaf area index and even structural details like leaf angles (Xiao et al., 2000).

Air Purification

Black locust with its more complex crown surfaces and more complex leaf morphology, may be more efficient filtering air pollutants than small-leaved lime. Considering the differences we found

13

in surface complexity, black locust might have the highest potential for air purification in parks, followed by town squares and the least potential in street canyons. High LAI values likely inhibit the particle filtering capabilities of tree crowns by reducing the inner crown wind speed and suppressing the turbulent deposition of atmospheric particles through impaction (Hofman et al., 2014), further increasing the purification potential of black locust in relation to small leaved lime. Small-leaved lime displayed the least crown surface complexity in parks. Yet, in parks the effect individual crown attributes might be overshadowed by the abundance of trees.

Particulate air pollution is considered a serious health problem causing several respiratory and vascular illnesses in urban areas (e.g. Bind et al., 2016). Particle trapping efficiency of trees has been found to be dependent on structural attributes. Finer, more complex and thoroughly distributed foliage for example, results in stronger filtering effects (Beckett et al., 2000a,b). Furthermore, atmospheric pollutants such as O_3, SO_2, NO_2 and CO are considerably cleared away as well (Nowak, 1994; Escobedo and Nowak, 2009; Calfapietra et al., 2016).

Noise Reduction

Urban noise, such as produced by traffic, construction, air- and railtraffic and other human activities, has non-trivial negative effects on human health and well-being (e.g. Fyhri and Klæboe, 2009; Welch et al., 2013). Sound waves included in noise pollution are absorbed, deviated, reflected and refracted by trees (Aylor, 1972; Kragh, 1981; Ishii, 1994; Fang and Ling, 2003). The specific spatial arrangement of trees as well as their individual structural attributes can have considerable effects on noise levels and frequencies (Martínez-Sala et al., 2006). Crown density, size and the spatial arrangement of branches determine a tree's structural suitability as effective acoustic elements of the urban landscape. However, in order to assess the noise reduction and alteration by different urban tree species, especially under varying growing environments, further research is essential (Pathak et al., 2011).

Biodiversity

Since our results for black locust suggest more complex crown structures compared to small-leaved lime, it may provide a wider range of habitats. The generally higher crown surface complexity in relation to small-leaved lime result in a higher abundance of concavities and gaps in the periphery of black locust crown which can be the decisive factor whether a tree is an appropriate habitat for certain species (e.g. Müller et al., 2012; Blakey et al., 2017). Furthermore, black locust displayed its highest crown surface complexities and crown displacements in parks, where biodiversity and the according animal sighting may enhance the desired recreational value.

14

Structural complexity and habitat diversity plays a big role for biodervisity (MacArthur and MacArthur, 1961; Bazzaz, 1975). Trees are, even in urban environments, among the dominating habitat-structure forming aspects of an ecosystem. Structural richness and variation of the habitat forming plants is often associated with animal species diversity (Tews et al., 2004). Differences in branch angles or crown surface for example might be the deciding factor wether a tree may serve as an appropriate habitat for certain bird species. Pena et al. (2017) found that street trees are able to mitigate negative effects of urbanization on certain bird species. High numbers of birds or butterflies (Melles et al., 2003; Blair, 1996; Blair and Launer, 1997), for instance, may contribute to the recreational value of urban green spaces.

Ecosystem Disservices

In contrast to the numerous benefits, some ecosystem functions of urban trees have effects which are mostly perceived as detrimental to human well-being (Lyytimäki and Sipilä, 2009). These detrimental effects are often neglected when assessing the effects of urban trees on their environment. Disservices are often directly related to tree structure, for example in the case of pavement damage by rooting activities or the blocking of views (Lyytimäki et al., 2008). Corrosion of buildings caused by bird excrements or animal digging may be related to habitat-forming structural tree attributes enhancing biodiversity (De Stefano and Deblinger, 2005; Lyytimäki and Sipilä, 2009) and can indirectly be related to tree structures. Abundance of animals like rats, pigeons, wasps and mosquitoes are perceived as pests by a majority of people and may function as disease transmitters. Furthermore, several health issues are related to allergenic pollen release (Dales et al., 2008; Cariñanos and Casares-Porcel, 2011). Hereby, wind-pollinated species were found to display higher allergenicity values (Cariñanos et al., 2016). Structural attributes determining wind interaction such as crown permeability and leaf area density as well as surface complexity might influence pollination of individual trees.

4.2 Using TLS to uncover tree structures

Terrestrial laser scanning has been proven to yield valuable insights to tree structure and its implications for forest trees (e.g. Bayer et al., 2013; Seidel et al., 2016). Compared to forest trees, urban trees are methodologically a considerably easier subject for TLS devices, since occlusion by competing neighbor trees is seldom and if existent less substantial than in mature and comparably dense forest stands (Hilker et al., 2010; Jones et al., 2016). The calculation of voxel-based crown center positions effectively circumvents several problems in regards to point density gradients

15

within TLS data. Furthermore, voxel representations of point clouds allow spatially explicit analysis of point densities which may serve as a proxy for foliage distribution, for example. Point cloud volume and borders can be better represented and analyzed by α-shapes.

While TLS methodologies for structural analysis of trees become more and more advanced (e.g. Hackenberg et al., 2015; Liang et al., 2016) many studies focus on the automated retrieval of parameters such as dbh, height, stem- and crown volume or tree mapping (Moskal and Zheng, 2012; Holopainen et al., 2013). However, terrestrial laser scanning holds a lot of potential in terms of novel parameters such as the α-shape based approximation of the crown's fractal-like periphery complexity as used in this study. However, measurements of the inner density distribution of crowns remains problematic, especially with single target devices like the one used in this study (Li et al., 2016; Kong et al., 2016). After combination of several scan positions and careful consideration of each scan's scanner positioning, self occlusion still produces point density gradients within the measured point clouds. Therefore, our results regarding the radial point density distribution within the crown display a gradient and are best interpreted concerning deviations around a regression line for example. Recent, and even more so future advancements in the field of multi-target and full-waveform TLS sensors in combination with further methodological refinements might yield reliable and robust point density distributions. As such, better estimations of biomass and leaf area density distributions can be expected in the coming years.

5 Conclusions

In order to provide a better basis for the understanding, analysis and quantitative design of urban green spaces and to optimize aesthetics as well as other ecosystem functions and services, knowledge about tree morphology under different urban environments is essential. Two of the most common tree species, black locust and small-leaved lime have been analyzed by terrestrial laser scanning. The combination of voxel based, α-shape based, and skeleton based evaluation of structural tree attributes yields novel insights into tree structure and holds great potential, especially in regard to future methodological advancements. Significant structural differences not only between species but also varying urban environments have been found. To what extent our results can be applied to other cities is subject for further research. Considering the differences in local climates between different cities, it is conceivable, that for example structural attributes of a species significantly differ under otherwise comparable circumstances. While many studies acknowledge the importance of tree structure for specific ecosystem services, a lot more research about the structure of urban trees and the resulting implications for their respective ecosystem functions and

16

services is required. Terrestrial laser scanning may, especially in regard to increasing sophisticated methodological capabilities, provide a tool to deliver higher detailed empirical measurements of the 3D structure of trees. It may therefore serve as a basis for a better understanding, modeling and evaluation of ecosystem functions and services within urban environments.

17

References

Akbari, H. (2005). Energy Saving Potentials and Air Quality Benefits of Urban Heat Island Mitigation. *Sol Energy*, pages 1–19.

Akbari, H., Pomerantz, M., and Taha, H. (2001). Cool surfaces and shade trees to reduce energy use and improve air quality in urban areas. *Sol Energy*, 70(3):295–310.

Aylor, D. (1972). Noise reduction by vegetation and ground. *J Acoust Soc Am*, 51:197–205.

Ballinas, M. and Barradas, V. (2016). The urban tree as a tool to mitigate the urban heat island in mexico city: A simple phenomenological model. *J Environ Qual*, 45:157–166.

Bayer, D., Seifert, S., and Pretzsch, H. (2013). Structural crown properties of Norway spruce (Picea abies [L.] Karst.) and European beech (Fagus sylvatica [L.]) in mixed versus pure stands revealed by terrestrial laser scanning. *Trees*, 27:1035–1047.

Bazzaz, F. (1975). Plant species diversity in old-field successional ecosystems in southern illinois. *Ecology*, 56:485–488.

Beckett, K., Smith, P. F., and Taylor, G. (2000a). Effective Tree Species for Local Air-Quality Management. *Journal of Arboriculture*, 26:12–19.

Beckett, K. P., Freer-Smith, P. H., and Taylor, G. (2000b). Particulate pollution capture by urban trees: Effect of species and windspeed. *Global Change Biol.*, 6(8):995–1003.

Bernhardt, E., Band, L., Walsh, C., and Berke, P. (2008). Understanding, managing, and minimizing urban impacts on surface water nitrogen loading. *Ann. N. Y. Acad. Sci.*, 1(134):61–96.

Bind, M.-A., Peters, A., Koutrakis, P., Coull, B., Vokonas, P., and Schwartz, J. (2016). Quantile regression analysis of the distributional effects of air pollution on blood pressure, heart rate variability, blood lipids, and biomarkers of inflammation in elderly american men: The normative aging study. *Environ Health Perspect*, 124(8):1189–1198.

Blair, R. B. (1996). Land use and avian species diversity along an urban gradient. *Ecol Appl*, 6:500–519.

Blair, R. B. and Launer, A. E. (1997). Butterfly diversity and human land use: Species assemblages along an urban grandient. *Biol Conserv*, 80(1):113–125.

Blakey, R. V., Law, B. S., Kingsford, R. T., and Stoklosa, J. (2017). Terrestrial laser scanning reveals below-canopy bat trait relationships with forest structure. *Remote Sensing of Environment*, 198:40 – 51.

Bolund, P. and Hunhammar, S. (1999). Ecosystem services in urban areas. *Ecol Econ*, 29(2):293–301.

Calfapietra, C., Morani, A., Sgrigna, G., Giovanni, S. D., Muzzini, V., Pallozzi, E., Guidolotti, G., Nowak, D., and Fares, S. (2016). Removal of ozone by urban and peri-urban forests: Evidence from laboratory, field, and modeling approaches. *J Environ Qual*, 45:224–233.

Cariñanos, P., Adinolfi, C., de la Guardia, C. D., Linares, C. D., and Casares-Porcel, M. (2016). Characterization of allergen emission sources in urban areas. *J. Environ. Qual.*, 45:244–252.

Cariñanos, P. and Casares-Porcel, M. (2011). Urban green zones and related pollen allergy: A review. some guidelines for designing spaces with low allergy impact. *Landscape and Urban Planning*, 101(3):205 – 214.

Chan, K., Satterfield, T., and Goldstein, J. (2012). Rethinking ecosystem services to better address and navigate cultural values. *Ecol Econ*, 74:8–18.

Chiesura, A. (2004). The role of urban parks for the sustainable city. *Landscape Urban Plann*, 68:129–138.

18

Côté, J.-F., Fournier, R. A., and Egli, R. (2011). An architectural model of trees to estimate forest structural attributes using terrestrial LiDAR. *Environ Modell Softw*, 26(6):761–777.

Dales, R, E., S, C., S, J., and F, C. (2008). Tree pollen and hospitalization for asthma in urban canada. *Int Arch Allergy Immunol*, 146:241–247.

De Stefano, S. and Deblinger, R. (2005). Wildlife as valuable natural resources vs intolerable pests: a suburban wildlife management mode. *Urban Ecosystems*, 8:131–137.

DWD (2015). Deutscher wetterdienst.

Edelsbrunner, H., Kirkpatrick, D. G., and Seidel, R. (1983). On the shape of a set of points in the plane. *IEEE T Inform Theory*, 29:551–559.

Edelsbrunner, H. and Mücke, E. P. (1994). Three-Dimensional Alpha Shapes. *ACM Trans. Graphics*, 13(1):43–72.

Escobedo, F. and Nowak, D. (2009). Spatial heterogeneity and air pollution removal by an urban forest. *Landscape Urban Plann*, 90:102–110.

Fang, C.-F. and Ling, D.-L. (2003). Investigation of the noise reduction provided by tree belts. *Landscape Urban Plann*, 63:187–195.

Fyhri, A. and Klæboe, R. (2009). Road traffic noise, sensitivity, annoyance and self-reported health—a structural equation model exercise. *Environ Int*, 35(1):91 – 97.

Goetz, S. J., Steinberg, D., Betts, M. G., Holmes, R. T., Doran, P. J., Dubayah, R., and Hofton, M. (2010). Lidar remote sensing variables predict breeding habitat of a Neotropical migrant bird. *Ecology*, 91(6):1569–1576.

Gómez-Baggethun, E. and Barton, D. N. (2013). Classifying and valuing ecosystem services for urban planning. *Ecol Econ*, 86:235–245.

Hackenberg, J., Spiecker, H., Calders, K., Disney, M., and Raumonen, P. (2015). SimpleTree —An Efficient Open Source Tool to Build Tree Models from TLS Clouds. *Forests*, 6(11):4245–4294.

Hamin, E. and Gurran, N. (2009). Urban form and climate change: Balancing adaptation and mitigation in the u.s. and australia. *Habitat Int.*, 33:238–245.

Hardin, P. J. and Jensen, R. R. (2007). The effect of urban leaf area on summertime urban surface kinetic temperatures: A terre haute case study. *Urban Forestry & Urban Greening*, 6(2):63 – 72.

Higgens, S., Turpie, J., Costanza, R., Cowling, R., Le Maitre, D., Marais, C., and Midgley, G. (1997). An ecological simulation model of mountain fynbos ecosystems: dynamics, valuation and management. *Ecol Econ*, 22:155–169.

Hilker, T., van Leeuwen, M., Coops, N., Wulder, M., Newnham, G., Jupp, D., and Culvenor, D. (2010). Comparing canopy metrics derived from terrestrial and airborne laser scanning in a Douglas-fir dominated forest stand. *Trees*, 24(5):819–832.

Hinsley, S. A., Hill, R. a. R. A., Fuller, R., Bellamy, P. E., and Rothery, P. (2009). Bird species distributions across woodland canopy structure gradients. *Community Ecology*, 10(1):99–110.

Hofman, J., Bartholomeus, H., Calders, K., Wittenberghe, S. V., Wuyts, K., and Samson, R. (2014). On the relation between tree crown morphology and particulate matter deposition on urban tree leaves: A ground-based lidar approach. *Atmospheric Environment*, 99:130 – 139.

Holopainen, M., Kankare, V., Vastaranta, M., Liang, X., Lin, Y., Vaaja, M., Yu, X., Hyyppä, J., Hyyppä, H., Kaartinen, H., Kukko, A., Tanhuanpää, T., and Alho, P. (2013). Tree mapping using airborne, terrestrial and mobile laser scanning – a case study in a heterogeneous urban forest. *Urban Forestry & Urban Greening*, 12(4):546 – 553.

19

Ishii, M. (1994). Measurement of road traffic noise reduced by the employment of low physical barriers and potted vegetation. *inter noise*, 29–31:595–597.

Jones, T., Marzen, L., and Chappelka, A. (2016). Mapping, modeling, and estimating tree measurements of urban tree canopy structure using terrestrial lidar scanning. *Papers in Applied Geography*, 2(2):236–242.

Kaushal, S. and Belt, K. (2012). The urban watershed continuum: Evolving spatial and temporal dimensions. *Urban Ecosyst.*, 15(409–435).

Kelbe, D., van Aardt, J., Romanczyk, P., van Leeuwen, M., and Cawse-Nicholson, K. (2017). Multiview marker-free registration of forest terrestrial laser scanner data with embedded confidence metrics. *IEEE Trans. Geosci. Remote Sens.*, 55(2):729–741.

Kjelgren, R. K. and Clark, J. R. (1992). Microclimates and tree growth in three urban spaces. *Journal of Environmental Horticulture*, 10(3):139–145.

Kong, F., Yan, W., Zheng, G., Yin, H., Cavan, G., Zhan, W., Zhang, N., and Cheng, L. (2016). Retrieval of three-dimensional tree canopy and shade using terrestrial laser scanning (tls) data to analyze the cooling effect of vegetation. *Agricultural and Forest Meteorology*, 217:22 – 34.

Kragh, J. (1981). Road traffic noise attenuation by belts of trees. *J Sound Vib*, 74:235–241.

Li, Y., Guo, Q., Tao, S., Zheng, G., Zhao, K., Xue, B., and Su, Y. (2016). Derivation, validation, and sensitivity analysis of terrestrial laser scanning-based leaf area index. *Canadian Journal of Remote Sensing*, 42(6):719–729.

Liang, X., Kankare, V., Hyyppä, J., Wang, Y., Kukko, A., Haggrén, H., Yu, X., Kaartinen, H., Jaakkola, A., Guan, F., et al. (2016). Terrestrial laser scanning in forest inventories. *ISPRS Journal of Photogrammetry and Remote Sensing*, 115:63–77.

Livesley, S. J., McPherson, E. G., and Calfapietra, C. (2016). The urban forest and ecosystem services: Impacts on urban water, heat, and pollution cycles at the tree, street, and city scale. *J Environ Qual*, 45:119–124.

Lyytimäki, J., Kjerulf Petersen, L., Normander, B., and Bezák, P. (2008). Nature as nuisance? ecosystem services and disservices to urban lifestyle. *Environnemental Sciences*, 5:161–172.

Lyytimäki, J. and Sipilä, M. (2009). Hopping on one leg—the challenge of ecosystem disservices for urban green management. *Urban Forestry & Urban Greening*, 8:309–315.

MacArthur, R. and MacArthur, J. (1961). On bird species diversity. *Ecology*, 42:594–598.

Mandelbrot, B. (1967). How Long Is the Coast of Britain? Statistical Self-Similarity and Fractional Dimension. *Science*, 156:636–638.

Mandelbrot, B. (1983). *The Fractal Geometry of Nature*. W.H. Freeman and Co.

Martínez-Sala, R., Rubio, C., García-Raffi, L. M., Sánchez-Pérez, J. V., Sánchez-Pérez, E. A., and Llinares, J. (2006). Control of noise by trees arranged like sonic crystals. *J Sound Vib*, 291(1):100 – 106.

McGeehin, M. and Mirabelli, M. (2001). The potential impacts of climate variability and change on temperature-related morbidity and mortality in the united states. *Environ Health Perspect*, 109:185–189.

McPherson, E. G., Nowak, D., Heisler, G., Grimmpnd, S., Souch, C., Grant, R., and Rowntree, R. (1997). Quantifying urban forest structure, function, and value: the Chicago urban forest project. *Urban Ecosystems*, 1:49–61.

Melles, S., Glenn, S., and Martin, K. (2003). Urban bird diversity and landscape complexity: species–environment associations along a multiscale habitat gradient. *Conservation Ecology*, 7(1).

20

Müller, J., Mehr, M., Bässler, C., Fenton, M. B., Hothorn, T., Pretzsch, H., Klemmt, H.-J., and Brandl, R. (2012). Aggregative response in bats: Prey abundance versus habitat. *Oecologia*, 169(3):673–684.

Mochida, A. and Lun, I. Y. (2008). Prediction of wind environment and thermal comfort at pedestrian level in urban area. *J Wind Eng Ind Aerodyn*, 96(10-11):1498–1527.

Mochida, A., Tabata, Y., Iwata, T., and Yoshino, H. (2008). Examining tree canopy models for CFD prediction of wind environment at pedestrian level. *J Wind Eng Ind Aerodyn*, 96(10-11):1667–1677.

Moser, A., Rötzer, T., Pauleit, S., and Pretzsch, H. (2015). Structure and ecosystem services of small-leaved lime (Tilia cordata Mill.) and black locust (Robinia pseudoacacia L.) in urban environments. *Urban Forestry & Urban Greening*, 14(4):1110–1121.

Moser, A., Rötzer, T., Pauleit, S., and Pretzsch, H. (2016). The Urban Environment Can Modify Drought Stress of Small-Leaved Lime (Tilia cordata Mill.) and Black Locust (Robinia pseudoacacia L.). *Forests*, 7(3):71.

Moskal, L. M. and Zheng, G. (2012). Retrieving forest inventory variables with terrestrial laser scanning (TLS) in urban heterogeneous forest. *Remote Sensing*, 4(1):1–20.

Napolia, M., Massetti, L., Brandaniac, G., Petralliac, M., and Orlandiniac, S. (2016). Modeling tree shade effect on urban ground surface temperature. *J Environ Qual*, 45:146–156.

Norton, B., Coutts, A., Livesley, S., Harris, R., Hunter, A., and Williams, N. (2015). Planning for cooler cities: A framework to prioritise green infrastructure to mitigate high temperatures in urban landscapes. *Landsc. Urban Plan.*, 134:127–138.

Nowak, D. (1994). *Air pollution removal by Chicago's urban forest. In McPherson, E.G., Nowak, D.J., Rowntree, R.A.(eds): Chicago's urban forest ecosystem: results of the Chicago Urban Forest Climate Project. Gen. Tech. Rep. NE-186*. U.S. Department of Agriculture, Forest Service, Northeastern Forest Experiment Station, Radnor PA.

Nowak, D. J. (1996). Estimating leaf area and leaf biomass of open-grown deciduous urban trees. *Forest Science*, 42(Walton):504–507.

Nowak, D. J., McBride, J. R., and Beatty, R. A. (1990). Newly planted street tree growth and mortality. *Journal of Arboriculture*, 16(5):124–130.

Olivier, M. D. and Robert, S. (2017). A method to quantify canopy changes using multi-temporal terrestrial lidar data: Tree response to surrounding gaps. *Agricultural and Forest Meteorology*, 237:184–195.

Olivier, M. D., Robert, S., and Fournier, R. A. (2016). Response of sugar maple (acer saccharum, marsh.) tree crown structure to competition in pure versus mixed stands. *Forest Ecology and Management*, 374:20–32.

Pataki, D., Carreiro, M., Cherrier, J., Grulke, N., Jennings, V., Pincetl, S., Pouyat, R., Whitlow, T., and Zipperer, W. (2011). Coupling biogeochemical cycles in urban environments: ecosystem services, green solutions, and misconceptions. *Front Ecol Environ*, 9:27–36.

Pathak, V., Tripathi, B., and Mishra, V. (2011). Evaluation of anticipated performance index of some tree species for green belt development to mitigate traffic generated noise. *Urban Forestry & Urban Greening*, 10(1):61 – 66.

Pauleit, S., Jones, N., Garcia-Martin, G., Garcia-Valdecantos, J. L., Rivière, L. M., Vidal-Beaudet, L., Bodson, M., and Randrup, T. B. (2002). Tree establishment practice in towns and cities – results from a european survey. *Urban Forestry & Urban Greening*, 1:83 – 96.

Pena, J. C. d. C., Martello, F., Ribeiro, M. C., Armitage, R. A., Young, R. J., and Rodrigues, M. (2017). Street trees reduce the negative effects of urbanization on birds. *PLoS One*, 12(3):1–19.

21

638 Peper, P., McPherson, E., and Mori, S. (2001a). Equations for predicting diameter, height, crown
639   width, and leaf area of san joaquin valley street trees. *Journal of Arboriculture*, 27:306–317.

640 Peper, P., McPherson, E., and Mori, S. (2001b). Predictive equations for dimensions and leaf area of
641   coastal southern california street trees. *Journal of Arboriculture*, 27:169–180.

642 Peper, P. J., Alzate, C. P., McNeil, J. W., and Hashemi, J. (2014). Allometric equations for urban
643   ash trees (fraxinus spp.) in oakville, southern ontario, Canada. *Urban Forestry & Urban Greening*,
644   13(1):175–183.

645 Rahman, M. A., Moser, A., Rötzer, T., and Pauleit, S. (2017). Microclimatic differences and their
646   influence on transpirational cooling of tilia cordata in two contrasting street canyons in munich,
647   germany. *Agric For Meteorol*, 232:443 – 456.

648 Ringgaard, R., Herbst, M., and Friborg, T. (2012). Partitioning of forest evapotranspiration: The
649   impact of edge effects and canopy structure. *Agric For Meteorol*, 166:86 – 97.

650 Roodbaraky, H., Baker, C., Dawson, A., and Wright, C. (1994). Experimental observations of the
651   aerodynamic characteristics of urban trees. *J Wind Eng Ind Aerodyn*, 52:171 – 184.

652 Rosenfeld, A. H., Akbari, H., Romm, J. J., and Pomerantz, M. (1998). Cool communities: strategies
653   for heat island mitigation and smog reduction. *Energy Build*, 28(1):51–62.

654 Rust, S. (2014). Analysis of regional variation of height growth and slenderness in populations of
655   six urban tree species using a quantile regression approach. *Urban Forestry & Urban Greening*,
656   13(2):336 – 343.

657 Seidel, D., Ehbrecht, M., and Puettmann, K. (2016). Assessing different components of three-
658   dimensional forest structure with single-scan terrestrial laser scanning: A case study. *For Ecol
659   Manage*, 381:196 – 208.

660 Sjöman, J. D., Hirons, A., and Sjöman, H. (2016). Branch area index of solitary trees: Understanding
661   its significance in regulating ecosystem services. *J Environ Qual*, 45:175–187.

662 Stathopoulos, T. (2006). Pedestrian level winds and outdoor human comfort. *Urban Trees*, 94(11):769–
663   780.

664 Tews, J., Brose, U., Grimm, V., Tielbörger, K., Wichmann, M. C., Schwager, M., and Jeltsch, F. (2004).
665   Animal species diversity driven by habitat heterogeneity/diversity: the importance of keystone
666   structures. *J Biogeogr*, 31(1):79–92.

667 Tyrväinen, L., Pauleit, S., Seeland, K., and de Vries, S. (2005). Benefits and uses of urban forests
668   and trees. In Konijnendijk, C., Nilsson, K., Randrup, T. and Schipperijn, J. (eds). *Urban Forests
669   and Trees, Springer*.

670 Villarreal, E. L. and Bengtsson, L. (2005). Response of a sedum green-roof to individual rain events.
671   *Ecol Eng*, 25(1):1–7.

672 Vosselmann, G. and Maas, H.-G. (2010). *Airborne and terrestrial laser scanning*. Whittles Publishing.

673 Walsh, C., Fletcher, T., and Burns, M. (2012). Urban stormwater runoff: A new class of environmen-
674   tal flow problem. *PLoS One*, 7:doi:10.1371/journal.pone.0045814.

675 Welch, D., Shepherd, K. N. D., McBride, D., and Marsh, S. (2013). Road traffic noise and health-
676   related quality of life: A cross-sectional study. *Noise and Health*, 65:224–230.

677 Wissmar, R., Timm, R., and Logsdon, M. (2004). Effects of changing forest and impervious land
678   covers on discharge characteristics of watersheds. *Environ Manage*, 34:91–98.

679 Xiao, Q., McPherson, E. G., L., U. S., and Grismer, M. (2000). A new approach to modeling tree
680   rainfall interception. *Jopurnal of Geophysical Research*, 105:29,173–29,188.
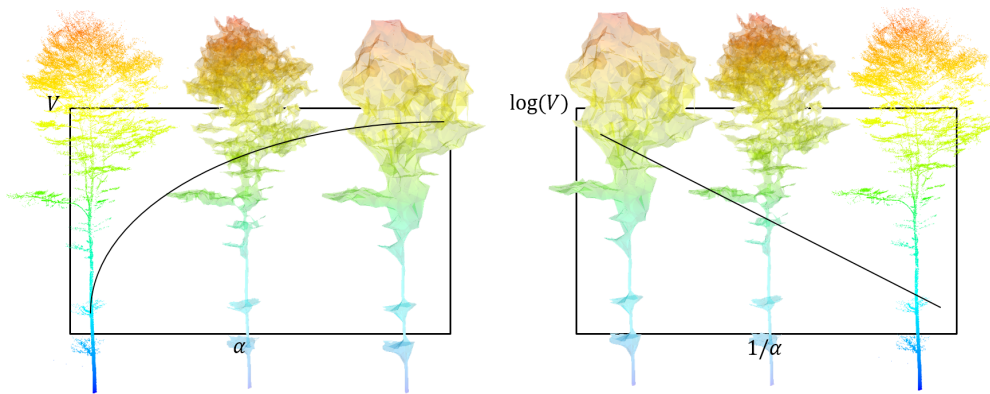
22

Figures

Figure 1: Schematic illustration of crown surface complexity estimation using a linearized α-shape volume series. **(l)** Repeated α-shape calculations of the same point cloud with varying α-values yield a non-linear relation between measured volume and α. **(r)** After the $1/\alpha$-transformation, the coefficients measure the rate of volume decrease by measurement scale (α-value). Differences in these rates are caused by differences in crown surface complexity on various scales. More negative slopes indicate higher structural complexity of the crown periphery.
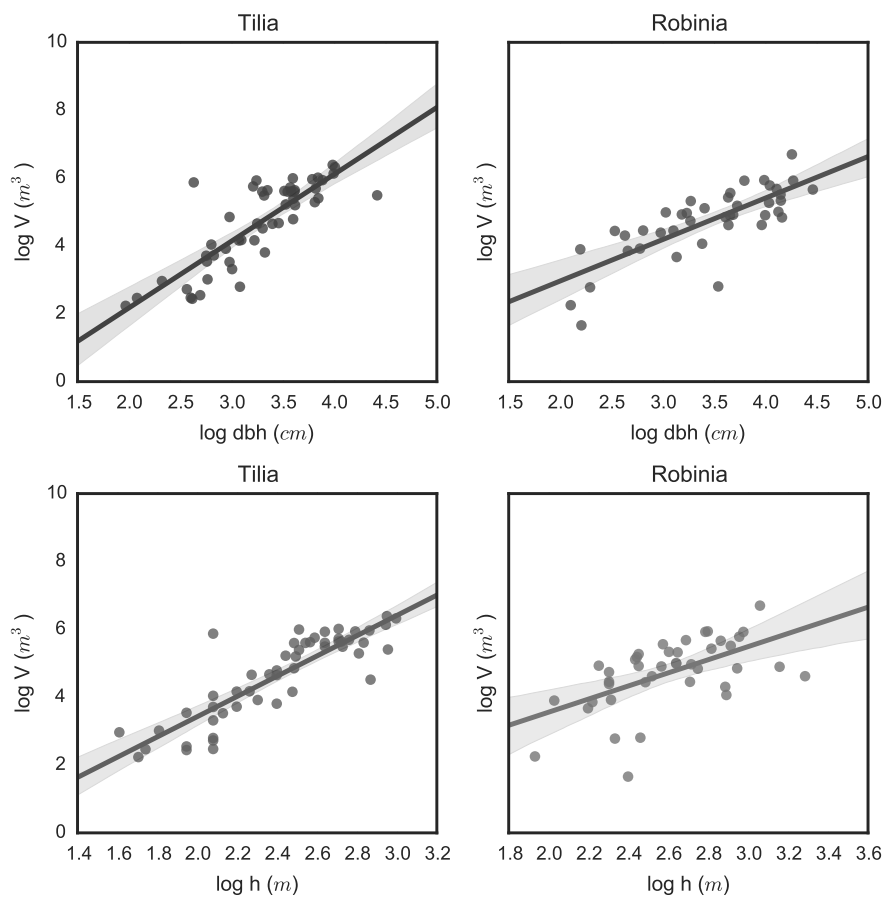
23

Figure 2: Allometric relations between *α*-shape derived crown volume and *dbh* (top row) as well as *h* (bottom row) for *T. cordata* (left column) and *R. pseudoacacia* (right column) (Eq. 17)
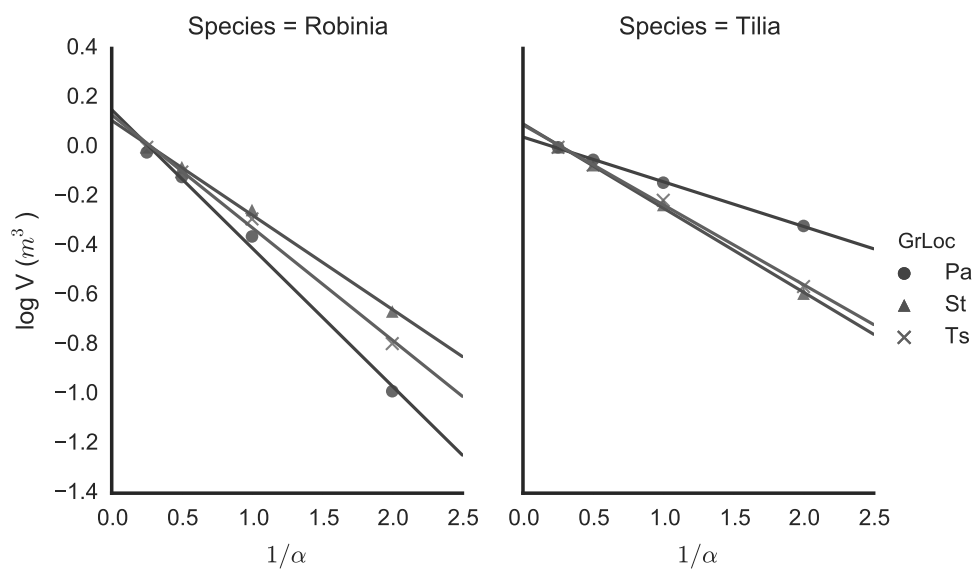
Figure 3: Crown surface roughness estimation for **(l)** *Robinia pseudoacacia* and **(r)** *Tilia cordata* and their respective growing locations using a linearized α-shape volume series. Due to the $1/\alpha$ transformation (Eq. 8), higher values on the x-axis mark smaller α-values, i.e. finer fitting shapes. Absolute $ln(V)$ values have been shifted to 0.0 for $\alpha = 0.25$ for better visualization and comparability of the differences between coefficients (β_1). Negative slopes suggest a higher fractal-like surface complexity of the crown.

25
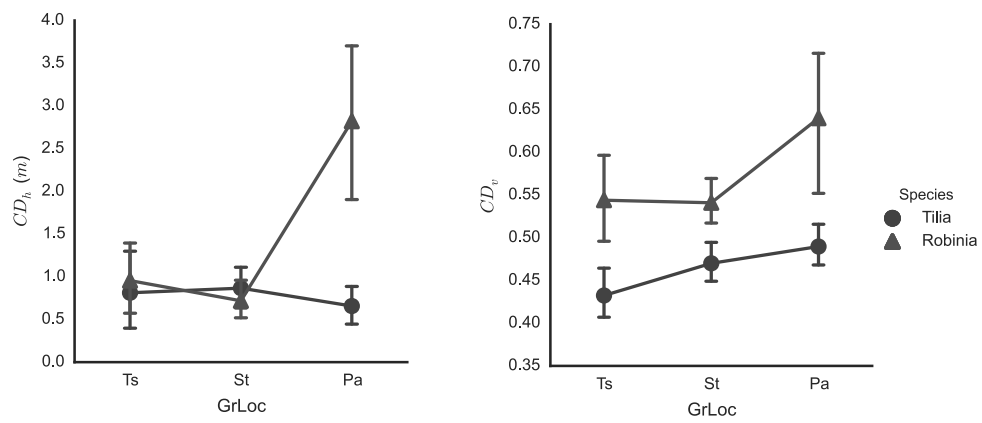
Figure 4: Horizontal crown center displacement (top) and relative vertical crown center position (bottom) by species and growing location. Bars mark the one-fold standard error

26
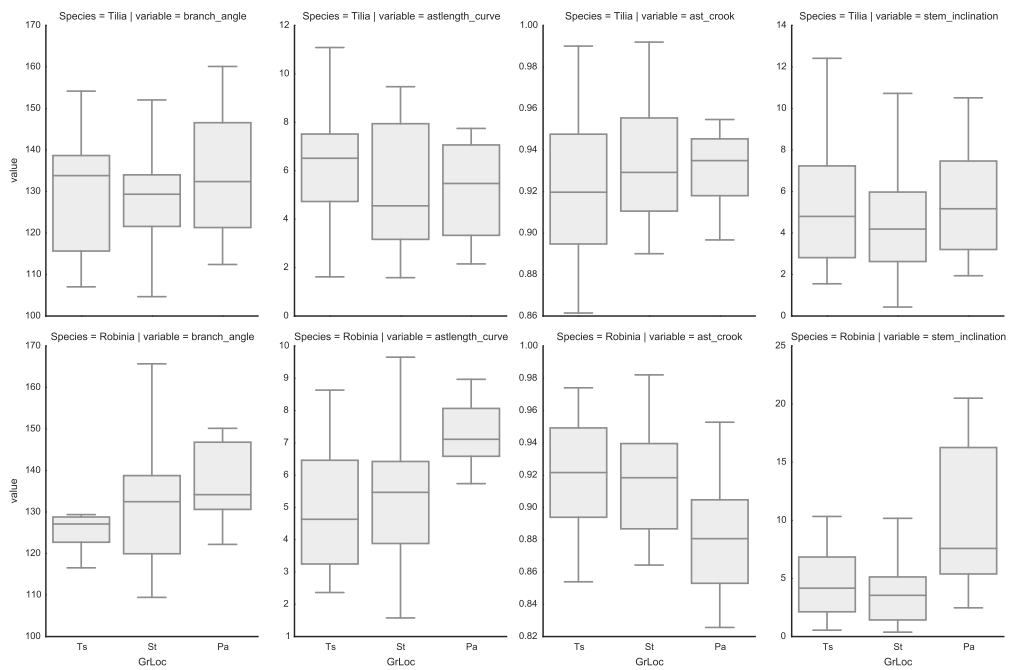
Figure 5: Skeleton parameters branch angle φ_b (measurement distance = straight branch length), stem inclination φ_s, l_b and branch bending *crook* by growing location and species (top: *Tilia cordata*, bottom *Robinia pseudoacacia*).

27
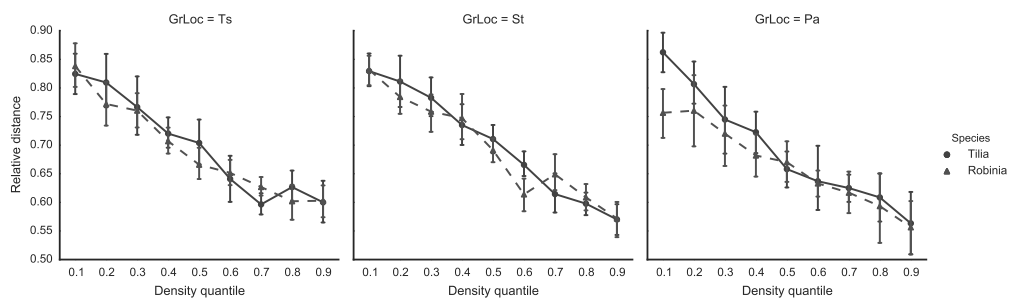
Figure 6: Exemplary radial mean distance of point density quantiles of voxels (10%, 20%, 30%,..., 90%) from crown center in relation to spherical crown radius of *Tilia cordata* and *Robina pseudoacacia* for **(l)** town squares, **(m)** street canyons and **(r)** parks.

28

Tables

Table 1: Overview of the scanned sample trees by species and growing location.

	N	*dbh* (*cm*)	*se*	*h* (*m*)	*se*
Tilia c.					
Park	8	26.7	3.2	12.5	1.2
Place	14	37.9	5.1	12.9	1.1
Street	30	26.5	2.3	11.2	0.7
Robinia p.					
Park	7	43.2	10.8	19.3	2.0
Place	11	37.8	4.5	14.3	1.0
Street	23	35.1	4.3	12.4	0.7

29

Table 2: Size parameters of *T. cordata* and *R. pseudoacacia* by growing location. Crown projection area *CPA*, volume *V* and Surface area *S* derived from two- (*CPA*) and three-dimensional (*V* and *S*) α-shapes ($\alpha = 0.5$)

	dbh (cm)	se	h (m)	se	h/d	se	CPA (m²)	se	V (m³)	se	S (m²)	se
T. cordata												
Park	26.7	3.2	12.5	1.2	0.48	0.03	45.1	7.5	214.6	46.3	548.0	109.7
Town square	37.9	5.1	12.9	1.1	0.39	0.04	57.0	8.8	216.7	36.7	860.2	154.2
Street	26.5	2.3	11.2	0.7	0.45	0.02	46.3	7.8	160.2	31.0	712.2	152.8
R. pseudoacacia												
Park	43.2	10.8	19.3	2.0	0.65	0.15	77.2	27.1	211.6	105.0	1226.3	583.1
Town square	37.8	4.5	14.3	1.0	0.42	0.04	60.0	9.0	196.9	40.0	912.6	184.3
Street	35.1	4.3	12.4	0.7	0.48	0.06	49.1	6.0	136.5	17.8	592.7	89.1

30

Table 3: Alpha shape logarithmic volume series model parameters for *Tilia cordata* (Adj. $R^2 = 0.96$, $p < 0.001$) and *Robinia pseudoacacia* (Adj. $R^2 = 0.97$, $p < 0.001$) as well as growing locations town square (*Ts*) and street canyon (*St*) in comparison to the reference growing location park.

	β_i	se	p	
T. cordata				
Intercept	5.51	0.038	0.000	***
Ts	-0.02	0.042	0.681	
St	-0.42	0.042	0.000	***
$1/\alpha$	-0.28	0.026	0.000	***
R. pseudoacacia				
Intercept	5.77	0.042	0.000	***
Ts	0.13	0.046	0.025	*
St	-0.31	0.046	0.000	***
$1/\alpha$	-0.47	0.028	0.000	***

31

Appendix

Abbreviations

Ts	Growing location: Town square
St	Growing location: Street canyon
Pa	Growing location: Park
Tilia	Dummy coded *Tilia cordata*
Robinia	Dummy coded *Robinia pseudoacacia*
CD_h	Crown center displacement
CD_v	Vertical crown position
V	Crown volume. Derived from α shapes.
CPA	Crown projection area. Derived from α shapes.
φ_b	Branch angle
φ_s	Stem inclination
l_b	Branch length
ρ	Point density quantile of voxel-arranged point cloud cloud

32

Table 4: Tree skeleton parameters. φ_s stem inclination, CD_h horizontal crown displacement, CD_v vertical crown displacement, φ_b branch angle from branch base to branch end, l_b branch length, *crook* relation between actual branch length and straight line from branch base to branch end.

	φ_s (°)	se	CD_h	se	CD_v	se	φ_b (°)	se	l_b (m)	se	crook	se
T. cordata												
Park	5.5	1.1	0.66	0.12	0.49	0.013	134.1	5.7	5.17	0.79	0.93	0.007
Place	7.7	2.6	0.81	0.24	0.43	0.015	132.1	5.0	5.96	0.71	0.93	0.011
Street	4.4	0.5	0.87	0.13	0.47	0.012	128.6	2.9	5.21	0.47	0.93	0.006
R. pseudoacacia												
Park	10.6	2.7	2.82	0.47	0.64	0.045	137.3	4.0	7.62	0.70	0.88	0.018
Place	4.7	1.0	0.95	0.22	0.54	0.026	128.9	4.5	4.89	0.62	0.92	0.012
Street	4.9	1.1	0.72	0.12	0.54	0.014	131.9	3.1	5.43	0.50	0.91	0.010

33